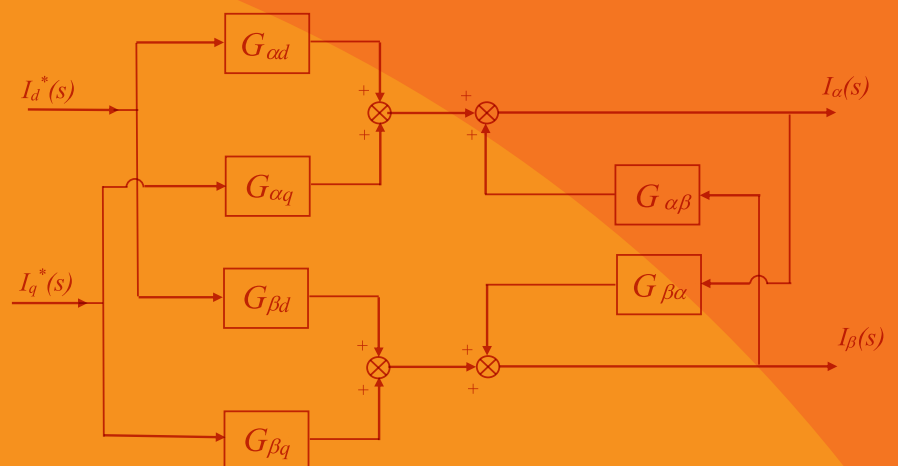
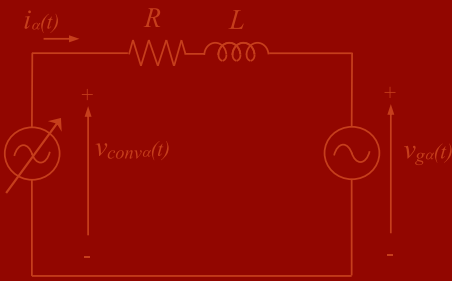




Mondragon
Unibertsitatea

Mathematical Model Equations in Stationary Reference Frame of Current Controls for Grid-Connected Converters

Gonzalo Abad, Ander de Marcos



Edita: Mondragon Unibertsitateko Zerbitzu Editoriala
Loramendi kalea, 4 - (23 p.k.)
20500 ARRASATE-MONDRAGON (Gipuzkoa)

Diseño y maquetación: AZK Taldea

ISBN: 978-84-09-15729-7

1ª Edición, 2019

El contenido de este libro está sujeto a la licencia Creative Commons de Atribución-No Comercial-Compartir Igual.

Atribución: el beneficiario de la licencia tiene el derecho de copiar, distribuir y comunicar públicamente la obra y hacer obras derivadas siempre y cuando reconozca y cite la obra de la forma especificada por el autor o el licenciante.

No comercial: no puede utilizarse con fines comerciales.

Compartir igual: si altera o transforma esta obra o genera una obra derivada, sólo puede distribuirla bajo una licencia idéntica a ésta.



Atribución-No Comercial-Compartir Igual
CC BY-NC-SA

Mathematical Model Equations
in
Stationary Reference Frame
of
Current Controls
for
Grid-Connected Converters

Authors:

Gonzalo Abad - Mondragon Unibertsitatea, Faculty of Engineering

Ander de Marcos - Mondragon Unibertsitatea, Faculty of Engineering



**Mondragon
Unibertsitatea**

**Goi Eskola
Politeknikoa
Faculty of
Engineering**

Electronics and Computing Department
Mondragon Unibertsitatea

Abstract: The grid-connected converter is a key element in many power electronic applications and technological devices which are commonly used nowadays. Wind turbines, photovoltaic generation, railway traction and grid-connected battery charges, are only some few examples of technological devices which incorporate grid-connected converters. In addition, one aspect within grid-connected converter is the current control. Current controls of grid-connected converters is one element of vital importance as well.

Thus, this book theorizes around two specific current controls of three phase grid-connected converters. Current control of three phase grid-connected converters, can be made in a stationary reference frame, or often called also as $\alpha\beta$ reference frame. Alternatively also and probably more extended in industry, current control can be made in a synchronous rotating reference frame, or often called also as dq reference frame.

Therefore, this book develops the mathematical equations describing the behavior of the controlled currents in a stationary reference frame ($\alpha\beta$) of three phase converters. These mathematical expressions in $\alpha\beta$ frame are derived, for the following well known and already well established current controls: current control with resonant controllers in stationary reference frame ($\alpha\beta$) and also, for current control with PI controllers in synchronous rotating reference frame (dq). Although these mathematical equations are already developed and quite commonly used for current controls in $\alpha\beta$ frame, it is not easy to find them for current controls in dq frame, if they exist.

Moreover, it is important to highlight that the mathematical equations derived in this book, are expressed in 's' domain after applying the Laplace transformation. This fact allows employing all the classic control theory tools, such as: pole-zero maps, frequency domain analysis, time domain responses to different inputs, etc... In addition, thanks to the knowledge of these mathematical equations in a common mathematical framework ($\alpha\beta$), it is possible to for instance: compare both current control methods at the same reference frame, easing comparative analyses.

Thus, after deriving the mathematical equations of the mentioned current controls, these equations are experimentally validated in a laboratory set-up. Finally, the last two chapters of the book introduce further analysis such as: effect of delays and performance of the current controls in weak grids. To conclude, the appendix summarizes the most important mathematical developments to derive some useful expressions.

Keywords: AC grids; analytical modeling; current control, grid-connected converter, pole-zero maps, frequency response, time domain dynamic response.

Contents

Chapter 1. Introduction	8
Chapter 2. Control of currents in stationary reference frame ($\alpha\beta$ control).....	11
2.1. <i>Mathematical model with an step input</i>	12
2.2. <i>Mathematical model with sinusoidal and cosenoidal input</i>	17
Chapter 3. Control of currents in rotating reference frame (dq control) with cancellation of coupling terms.....	23
3.1. <i>Mathematical model in dq</i>	24
3.2. <i>Mathematical model in $\alpha\beta$</i>	27
3.3. <i>Mathematical model in $\alpha\beta$ with an step input</i>	28
3.4. <i>Mathematical model in $\alpha\beta$ with sinusoidal and cosenoidal input</i>	35
3.5. <i>Bode Diagram</i>	40
Chapter 4. Control of currents in rotating reference frame (dq control) without cancellation of coupling terms	44
4.1. <i>Mathematical model in $\alpha\beta$ with a step input</i>	45
4.2. <i>Mathematical model in $\alpha\beta$ with sinusoidal and cosenoidal input</i>	52
4.3. <i>Bode Diagram</i>	58
Chapter 5. Comparison and analysis	61
Chapter 6. Experimental validation of the analytical models	68
Chapter 7. Inclusion of delay and filter at current measurement	73
7.1. <i>Control of currents in stationary reference frame ($\alpha\beta$) for step inputs</i>	73
7.2. <i>Control of currents in rotating reference frame (dq) with cancellation of coupling current terms for step inputs</i>	76
7.3. <i>Stability analysis of both controls: pole location for step inputs</i>	81

Chapter 8. Step response analysis in a weak grid	84
8.1. Control of currents in stationary reference frame ($\alpha\beta$ control) with a PLL tuned dynamically slow	85
8.2. Control of currents in synchronous rotating reference frame (dq control) with a PLL tuned dynamically slow	87
8.3. Control of currents in stationary reference frame ($\alpha\beta$ control) with a PLL tuned dynamically fast	89
Chapter 9. Conclusions	97
Appendix A. Step inputs in control at stationary reference frame ($\alpha\beta$)	99
Appendix B. Sine and cosine inputs in control at stationary reference frame ($\alpha\beta$)..	101
Appendix C. Step inputs in control at synchronously rotating frame (dq) with cancellation of coupling terms	103
Appendix D. Sine and cosine inputs in control at synchronously rotating frame (dq) with cancellation of coupling terms	110
Appendix E. Numerical conditions for simulations	114
Appendix F. Experimental platform	115
Appendix G. Space vectors	116
References	118

Chapter 1.

Introduction

When a historic evolution of different technologies is analyzed under detail, it is often seen that first, the more technical, rudimentary or manual technological devices are developed, while then, after the technological devices are well established and used by many people, a more scientific knowledge is applied to them for further improvements, understanding or even evolutions [1].

In the field of knowledge of control of power electronic converters connected to the grid or even in the field of knowledge of control of electric machines, it is possible to see an analogous behavior or tendency [1]. Since the first closed loop controls applied to electric machines were developed by pioneers K. Hasse and F. Blaschke in 1968–1972 [2], i.e. the so called ‘vector controls’, many authors have made a huge number of uncountable contributions or improvements to these original vector controls algorithms: theoretical analysis, analytical model equations describing its behavior, tuning methods of the regulators, discrete analytical models, improvements for compensation of delays, advanced estimators or observers to deal parameters uncertainties, sensorless controls, transient analysis, steady-state analysis, inclusion of active damping functionalities, etc... Many of the most representative of these improvements, or further studies for vector control techniques either applied to electric machine control or grid connected converters control, are already incorporated and covered in many specialized books such as: [2], [3], [4], [5], [6], [7], [8].

Thus, in the specific field of the grid-connected converters control, some of the most pioneering and important references addressing this issue in book formats are [9]-[10], although probably some leader companies also implemented previously, or in parallel, these type of grid connected converters. Since the first years of their existence, three phase grid-connected converters were controlled by means of vector control techniques [9]-[10]-[11], where the currents were controlled in a synchronous rotating frame (dq) by means of PI controllers. In this case, the controlled currents seen by the PI regulators at steady-state were dominantly constant (an amount of ripple is superposed due to the converter’s switching). Or alternatively also, resonant controllers were also used to control of grid connected converters [12]-[13], controlling the currents in abc or $\alpha\beta$ stationary reference frames (control 2 phases instead 3). Therefore, the current seen in this case by the resonant regulator was dominantly sinusoidal at steady state (an amount of ripple is superposed due to the converter’s switching) [7].

With this historical conditioning panorama, it can be affirmed that nowadays, either in industry or research, most of the current vector controls of three phase grid connected converters, are made by using PI controllers in synchronously rotating reference frame (dq)

or with resonant controllers in stationary reference frame ($\alpha\beta$) [8]. In addition, it can be observed that there is a clear and natural tendency to use mathematical models for analysis in stationary reference frame ($\alpha\beta$), obviously in controls with resonant controllers. While in controls with PI controllers, the mathematical models for analysis are more often developed in synchronous rotating reference frame (dq), even if the final resulting or real currents exchanged between the grid and the power electronic converter are actually sinusoidal [7].

Thus, what in this book is developed are the mathematical equations in stationary reference frame ($\alpha\beta$), for both controls: current control with resonant controllers in stationary reference frame ($\alpha\beta$) and also for current control with PI controllers in synchronous rotating reference frame (dq). Part of the mathematical equations developed in this book for the controls in $\alpha\beta$ frame are probably already derived [8], however, developments in this direction for controls in dq frame are less [13]. Thus, in this book a common and solid mathematical model for both controls is developed, allowing to dispense a powerful and global tool for further developments, studies or analyses. This common mathematical framework or mathematical model, allows for instance:

- Compare both control methods at the same reference frame, easing comparative analysis.
- To know mathematically the transient and steady state responses to different inputs, of both controls, in a common stationary reference frame ($\alpha\beta$).
- To understand the frequency analysis of both controls, in a common stationary reference frame ($\alpha\beta$).
- With this mathematical tool, it helps to do analysis of performance of both controls in a common stationary reference frame ($\alpha\beta$) such as: pole locations, modelling delays, modelling PLLs, modelling interactions with other power electronic converters connected in parallel in the vicinity of the grid, etc... [14]

Finally, summarizing the book is divided into the following chapters: chapter 2 develops the model equations of a control of currents in stationary reference frame ($\alpha\beta$). Then chapter 3, develops the model equations of a control of currents in synchronous rotating frame (dq) with cancellation of the coupling terms. Chapter 4, analyzes the same current control method but without cancelling the coupling terms. Note that control of currents in dq can be made with or without cancellation of coupling terms and therefore, a deep mathematical analysis of both options is carried out in the book. Then, a short comparison between the controls analyzed is presented in chapter 5, while in chapter 6, the experimental validation of the mathematical equations is provided. Finally, chapters 7 and 8, introduces further analysis such as: effect of delays and performance of the controls in weak grids. To conclude, several appendices summarize the most important mathematical developments to derive some useful expressions.

Therefore, in Figure 1 (a), a schematic is depicted of the converter connected to the three phase grid. As depicted, there may be many functionalities or applications where this converter can be used; reactive power compensators, active filters, wind turbines, etc... In all these cases in general, a current control is typically used, trying also to fulfill some standard or norms. At the AC side, a filter is necessary that for simplicity in this book, a purely inductive filter has been adopted with its corresponding parasitic resistance. Then at the DC side, depending on the application where this converter is used, there could be connected a battery pack, or another converter or even to nothing. Finally, commanding the current control, depending again on the application, there may be another control level,

generating the current references $i_d(t)$ and $i_q(t)$. For simplicity, this book is focused on the current control and no attention is paid to how the current references are generated, because it strongly depends on the application itself.

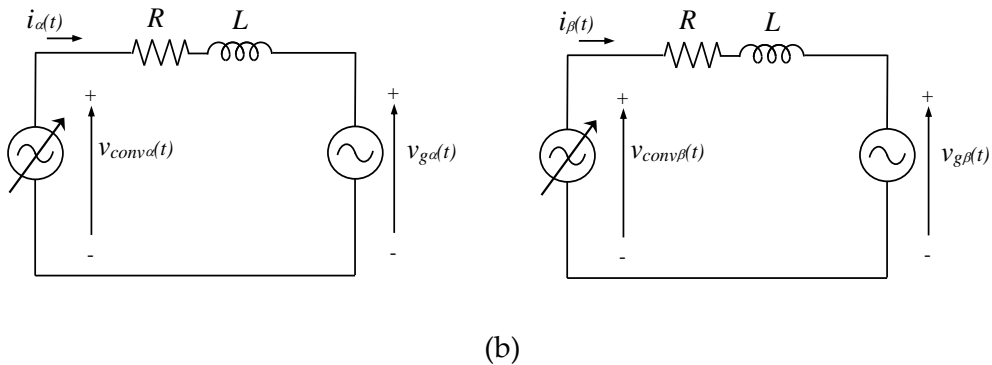
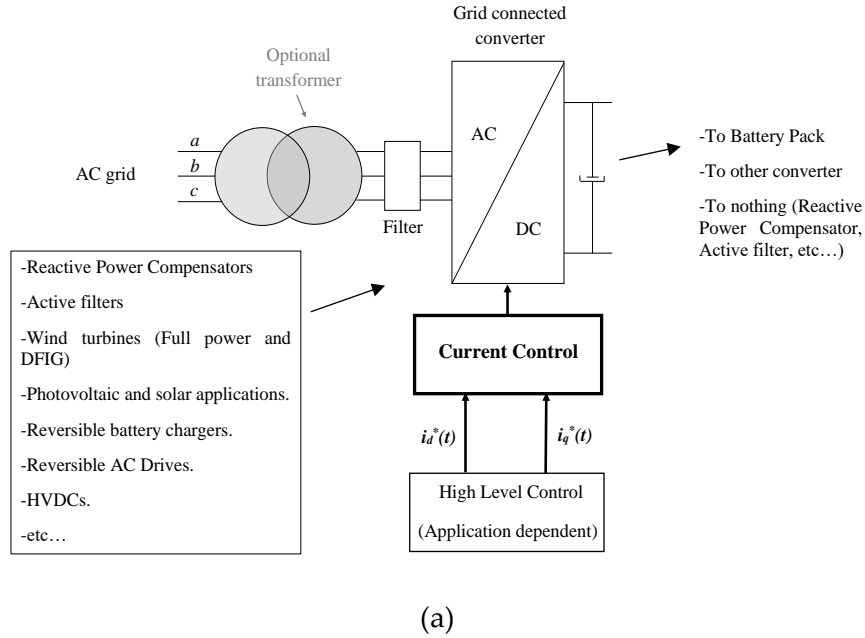


Figure 1. (a) Grid connected converter operating with current references in dq reference frame; $i_{ds}^*(t)$ and $i_{qs}^*(t)$, (b) Simplified equivalent electric circuit in $\alpha\beta$ reference frame.

After this, in Figure 1 (b), the $\alpha\beta$ equivalent power circuit is depicted [7]. Note that simply is composed by the grid voltage $v_{g\alpha}(t)$ and $v_{g\beta}(t)$ that in the first analysis of this book is supposed ideal (strong, with a neglectable series equivalent impedance). Then the equivalent impedance RL of the filter is also present, while finally the voltages created by the converter are also present. These voltages $v_{conv\alpha}(t)$ and $v_{conv\beta}(t)$ are automatically generated by the corresponding current control method employed. For simplicity in the analysis, this book derives all the mathematical expressions in a $\alpha\beta$ stationary reference frame. Note that the three components could be also used, abc , however the results and conclusions would be equivalent.

Chapter 2.

Control of currents in stationary reference frame ($\alpha\beta$ control)

The control block diagram is depicted in Figure 2, [13]. The current control is effectively implemented in stationary reference frame ($\alpha\beta$) by using two resonant controllers, called $PIR(t)$. A typical resonant controller configuration in 's' domain is [15]:

$$PIR(s) = k_p + \frac{k_i s}{s^2 + \omega^2} \quad (1)$$

Being k_p and k_i the gains of the regulator that must be tuned and ω the grid frequency at which the resonance of the regulator must be tuned.

As shown in previous chapter when contextualizing, in most of the applications the current references $i_d^*(t)$ and $i_q^*(t)$ are created in rotating reference frame (dq), therefore the rotational transformation is required together with the angle of the grid voltage [7]. Then, at the output of the regulators, often a feedforward term of the grid voltage is added (not strictly necessary, but recommendable as will be seen), obtaining thus the voltage references that will be applied by the VSC converter $v_{conv\alpha}(t)$ and $v_{conv\beta}(t)$.

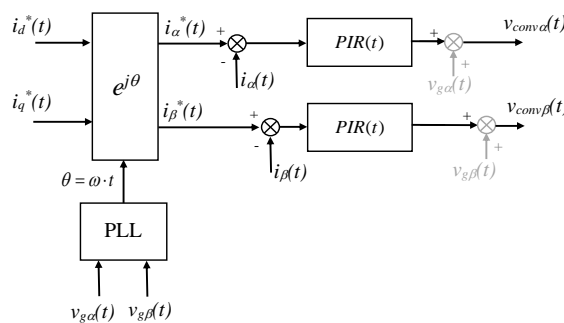


Figure 2. Current control block diagram in stationary reference frame ($\alpha\beta$) with two resonant controllers.

This control block diagram, can be represented as an equivalent 'black box' either in time domain and also in 's' domain, as shown in Figure 3.

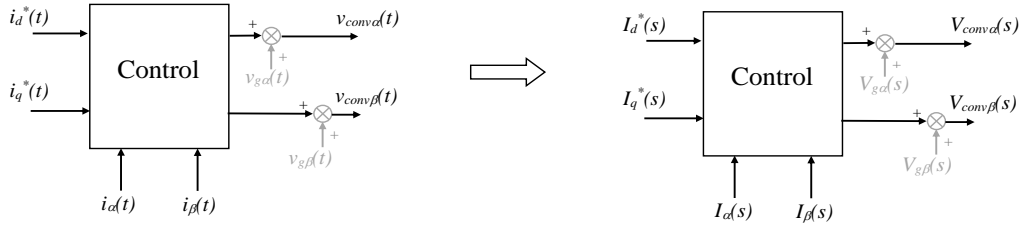


Figure 3. Current control blocks in time and 's' domains.

The α and β components of the converter voltages, considering the grid voltage feedforward terms, are mathematically represented in time domain as follows (' \otimes ' is the convolution product):

$$v_{conv\alpha}(t) = (i_d^*(t) \cdot \cos(\omega t) - i_q^*(t) \cdot \sin(\omega t)) \otimes PIR(t) - i_\alpha(t) \otimes PIR(t) + v_{g\alpha}(t) \quad (2)$$

$$v_{conv\beta}(t) = (i_d^*(t) \cdot \sin(\omega t) + i_q^*(t) \cdot \cos(\omega t)) \otimes PIR(t) - i_\beta(t) \otimes PIR(t) + v_{g\beta}(t) \quad (3)$$

Note that the harmonics created by the converter are neglected. This is only a first component harmonic model and the voltage harmonics generated by the specific converter topology employed, together with its corresponding modulation technique are assumed to be zero.

2.1. Mathematical model with an step input

Considering **step** inputs at at both $I_d^*(s)$ and $I_q^*(s)$ and assuming that the grid voltage is ideal, i.e., assuming no angle phase shift and ω constant, the previous time domain expressions can be transformed into the 's' domain as follows (see appendix A for detailed mathematical development) [13]:

$$\begin{aligned} V_{conv\alpha}(s) = & - \left(k_p + \frac{k_i s}{s^2 + \omega^2} \right) I_\alpha(s) + \left(\frac{k_p s^2}{s^2 + \omega^2} + \frac{k_i s^3}{(s^2 + \omega^2)^2} \right) I_d^*(s) \\ & - \left(\frac{k_p \omega s}{s^2 + \omega^2} + \frac{\omega k_i s^2}{(s^2 + \omega^2)^2} \right) I_q^*(s) + V_{g\alpha}(s) \end{aligned} \quad (4)$$

$$V_{conv\beta}(s) = -\left(k_p + \frac{k_i s}{s^2 + \omega^2}\right) I_\beta(s) + \left(\frac{k_p \omega s}{s^2 + \omega^2} + \frac{\omega k_i s^2}{(s^2 + \omega^2)^2}\right) I_d^*(s) + \left(\frac{k_p s^2}{s^2 + \omega^2} + \frac{k_i s^3}{(s^2 + \omega^2)^2}\right) I_q^*(s) + V_{g\beta}(s) \quad (5)$$

Being these expressions only valid for a step input at both $I_d^*(s)$ and $I_q^*(s)$:

$$I_d^*(s) = \frac{|I_d^*|}{s} \quad I_q^*(s) = \frac{|I_q^*|}{s} \quad (6)$$

The closed loop expression can be derived by using the electric circuit of Figure 1, where holds:

$$v_{conv\alpha}(t) - v_{g\alpha}(t) = R \cdot i_\alpha(t) + L \cdot \frac{di_\alpha(t)}{dt} \quad (7)$$

$$v_{conv\beta}(t) - v_{g\beta}(t) = R \cdot i_\beta(t) + L \cdot \frac{di_\beta(t)}{dt} \quad (8)$$

And therefore, the 's' domain equations of the power circuit are:

$$V_{conv\alpha}(s) - V_{g\alpha}(s) = I_\alpha(s) \cdot (R + Ls) \quad (9)$$

$$V_{conv\beta}(s) - V_{g\beta}(s) = I_\beta(s) \cdot (R + Ls) \quad (10)$$

Combining these expressions with the voltage applied by the control in equations (4) and (5), the closed loop current expression yield (appendix A):

$$I_\alpha(s) = \left(k_p + \frac{k_i s}{s^2 + \omega^2}\right) \left(\frac{s^2}{A(s)}\right) I_d^*(s) - \left(k_p + \frac{k_i s}{s^2 + \omega^2}\right) \left(\frac{\omega s}{A(s)}\right) I_q^*(s) \quad (11)$$

$$I_\beta(s) = \left(k_p + \frac{k_i s}{s^2 + \omega^2}\right) \left(\frac{\omega s}{A(s)}\right) I_d^*(s) + \left(k_p + \frac{k_i s}{s^2 + \omega^2}\right) \left(\frac{s^2}{A(s)}\right) I_q^*(s) \quad (12)$$

Being:

$$A(s) = Ls^3 + (k_p + R)s^2 + (L\omega^2 + k_i)s + (k_p + R)\omega^2 \quad (13)$$

Therefore, the output currents $\alpha\beta$ can be compactly represented as follows:

$$I_\alpha(s) = G_{\alpha d}(s) \cdot I_d^*(s) + G_{\alpha q}(s) \cdot I_q^*(s) \quad (14)$$

$$I_\beta(s) = G_{\beta d}(s) \cdot I_d^*(s) + G_{\beta q}(s) \cdot I_q^*(s) \quad (15)$$

Being $G_{\alpha d}(s)$, $G_{\alpha q}(s)$, $G_{\beta d}(s)$, $G_{\beta q}(s)$, easily deduced from correspondence of equations (11) and (12). These last equations are graphically represented in Figure 4.

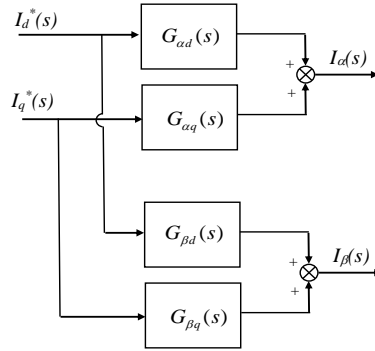


Figure 4. Equivalent block diagram of the $\alpha\beta$ control of the currents.

Note that if not voltage feedforward term would not have been used, the closed loop expressions would also depend on the grid voltage as follows:

$$I_\alpha(s) = \left(k_p + \frac{k_i s}{s^2 + \omega^2} \right) \left(\frac{s^2}{A(s)} \right) I_d^*(s) - \left(k_p + \frac{k_i s}{s^2 + \omega^2} \right) \left(\frac{\omega s}{A(s)} \right) I_q^*(s) - \left(\frac{s^2 + \omega^2}{A(s)} \right) V_{g\alpha}(s) \quad (16)$$

$$I_\beta(s) = \left(k_p + \frac{k_i s}{s^2 + \omega^2} \right) \left(\frac{\omega s}{A(s)} \right) I_d^*(s) + \left(k_p + \frac{k_i s}{s^2 + \omega^2} \right) \left(\frac{s^2}{A(s)} \right) I_q^*(s) - \left(\frac{s^2 + \omega^2}{A(s)} \right) V_{g\beta}(s) \quad (17)$$

Nevertheless, continuing with the analysis, from expression (11) and (12), substituting in both inputs a step (equation (6)), the output currents yields:

$$I_\alpha(s) = \left(\frac{k_p s^3 + k_i s^2 + k_p \omega^2 s}{(s^2 + \omega^2) A(s)} \right) | I_d^* | - \left(\frac{k_p \omega s^2 + k_i \omega s + k_p \omega^3}{(s^2 + \omega^2) A(s)} \right) | I_q^* | \quad (18)$$

$$I_\beta(s) = \left(\frac{k_p \omega s^2 + k_i \omega s + k_p \omega^3}{(s^2 + \omega^2) A(s)} \right) | I_d^* | + \left(\frac{k_p s^3 + k_i s^2 + k_p \omega^2 s}{(s^2 + \omega^2) A(s)} \right) | I_q^* | \quad (19)$$

Expanding the denominator:

$$I_\alpha(s) = \left(\frac{k_p s^3 + k_i s^2 + k_p \omega^2 s}{Ls^5 + (k_p + R)s^4 + (2L\omega^2 + k_i)s^3 + 2\omega^2(k_p + R)s^2 + (L\omega^2 + k_i)\omega^2 s + \omega^4(k_p + R)} \right) |I_d^*| \quad (20)$$

$$- \left(\frac{k_p \omega s^2 + k_i \omega s + k_p \omega^3}{Ls^5 + (k_p + R)s^4 + (2L\omega^2 + k_i)s^3 + 2\omega^2(k_p + R)s^2 + (L\omega^2 + k_i)\omega^2 s + \omega^4(k_p + R)} \right) |I_q^*|$$

$$I_\beta(s) = \left(\frac{k_p \omega s^2 + k_i \omega s + k_p \omega^3}{Ls^5 + (k_p + R)s^4 + (2L\omega^2 + k_i)s^3 + 2\omega^2(k_p + R)s^2 + (L\omega^2 + k_i)\omega^2 s + \omega^4(k_p + R)} \right) |I_d^*| \quad (21)$$

$$- \left(\frac{k_p s^3 + k_i s^2 + k_p \omega^2 s}{Ls^5 + (k_p + R)s^4 + (2L\omega^2 + k_i)s^3 + 2\omega^2(k_p + R)s^2 + (L\omega^2 + k_i)\omega^2 s + \omega^4(k_p + R)} \right) |I_q^*|$$

By using a partial fraction expansion and applying the inverse Laplace transform, the time domain expression of the output current can be obtained (only $i_\alpha(t)$ current is shown, $i_\beta(t)$ would present an equivalent form):

$$i_\alpha(t) = \left((B_0) \cdot e^{\sigma_0 t} + (2 \cdot B_1) \cdot e^{\sigma_1 t} \cdot \cos(\omega_{d1} \cdot t + \arg B_1) + (2 \cdot B_2) \cdot \cos(\omega \cdot t) \right) |I_d^*| \quad (22)$$

$$+ \left((B_3) \cdot e^{\sigma_3 t} + (2 \cdot B_4) \cdot e^{\sigma_4 t} \cdot \cos(\omega_{d4} \cdot t + \arg B_4) + (2 \cdot B_5) \cdot \cos(\omega \cdot t + \pi/2) \right) |I_q^*|$$

It is seen that the $i_\alpha(t)$ current time domain response to the input steps, is composed by the 'forced response' or 'steady state response', which are two cosine terms:

$$(|I_d^*| \cdot 2 \cdot B_2) \cdot \cos(\omega \cdot t) \quad (23)$$

$$(|I_q^*| \cdot 2 \cdot B_5) \cdot \cos(\omega \cdot t + \pi/2) \quad (24)$$

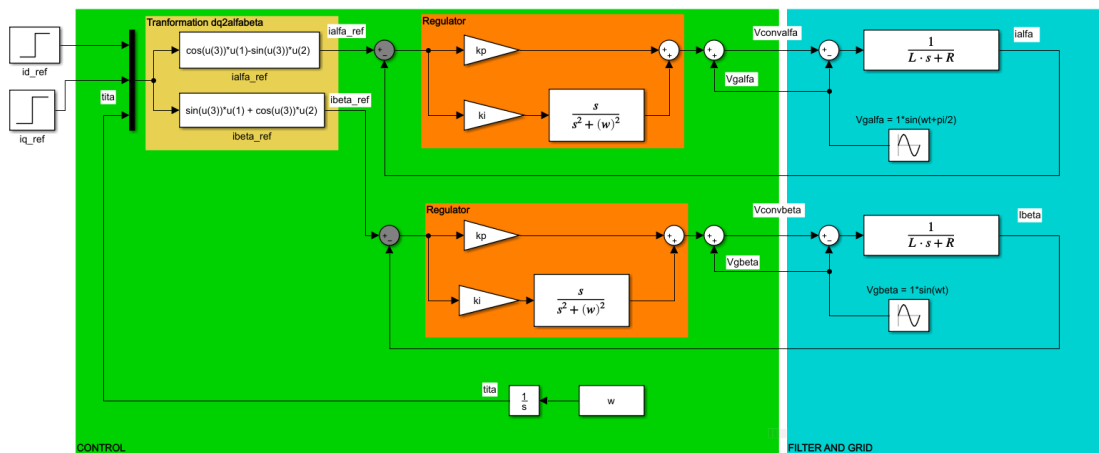
While the rest terms are pure exponentials or combinations of exponentials and cosine terms. All these terms are made zero at steady-state, if the system is stable, i.e., if all $\sigma_0, \sigma_1, \sigma_2, \sigma_3$ are negative. These terms are often called the 'natural response' and conformate the transient response of the system.

All the constants present in equation (22), B_0, σ, \dots can be easily numerically derived for instance using the 'residue' from Matlab Control Toolbox. Table I shows an example of numerical solution.

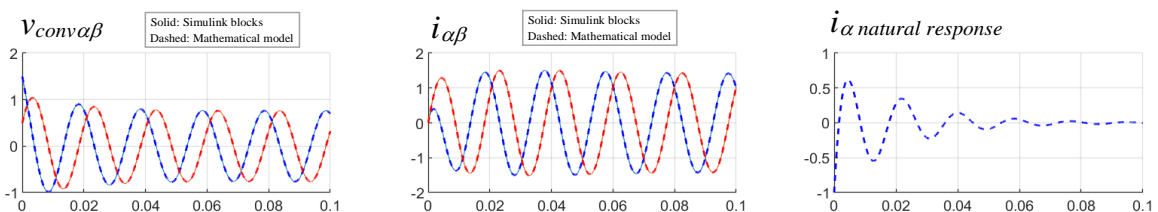
Table I. Numerical solution of expression (22) by using the the ‘residue’ function from Matlab Control Toolbox. Conditions of Appendix E.

d	q
$B_0 = -6.529590130061056e-01$ $\sigma_0 = -4.088851233797501e+02$	$B_3 = -5.016888903659279e-01$ $\sigma_3 = -4.088851233797501e+02$
$B_1 = 3.513965304953767e-01$ $\sigma_1 = -4.805743831012502e+01$ $\omega_{d1} = 3.458129312915602e+02$ $argB_1 = -2.087253535142668e+00$	$B_4 = 3.161931338686155e-01$ $\sigma_4 = -4.805743831012502e+01$ $\omega_{d4} = 3.458129312915602e+02$ $argB_4 = -6.545422830740641e-01$
$B_2 = 5.0000e-01$ $\omega = 3.14159e+02$	$B_5 = 5.0000e-01$ $\omega = 3.14159e+02$

Thus, the transient response is depicted in Figure 5. The time domain response provided by the mathematical model of expression (22) is superposed to the Simulink block diagram depicted in Figure 5. It is seen an exact correspondence of both time domain responses to the step inputs.



(a)



(b)

Figure 5. $\alpha\beta$ control of currents. (a) Simulink model for evaluating the Step response, of the $\alpha\beta$ control of the currents, (b) Time domain unit step response at both inputs $I_d^*(s)$ and $I_q^*(s)$. Conditions of Appendix E.

Finally, the poles and zeros of the expression (11) are also depicted in Figure 6. Note the correspondence with the poles and the constants of the time domain response of equations (22).

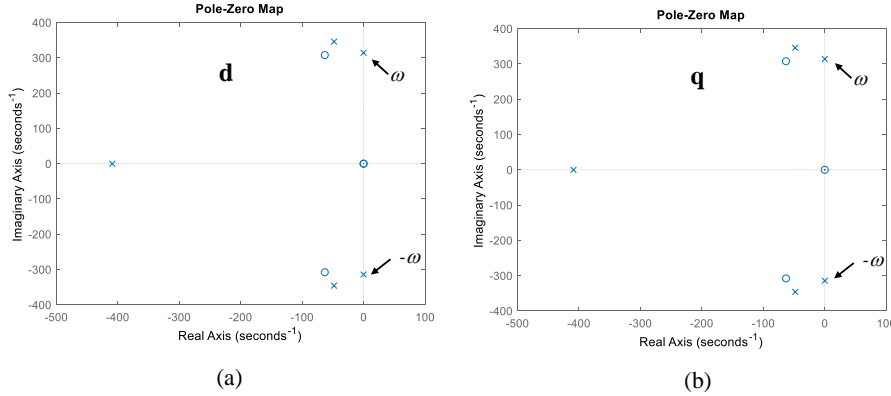


Figure 6. Poles for $I_\alpha(s)$ of expression (11), for the $\alpha\beta$ control of the currents and step inputs. Conditions of Appendix E.

Note that the poles and the zeros of equation (11) appear directly in the time domain expression (22). Thus, the real part of the poles are the σ constants of the exponential terms. Then, the imaginary part of the poles are directly the ω_d , of the cosine terms. While the phase shifts of the cosine terms ($\arg B_1, \arg B_2 \dots$) and the amplitudes ($B_1, B_2 \dots$) come from the combination of the poles and zeros.

In addition, although it is not covered in this book, ramp responses could be also evaluated as done in many classic control books [16]. However, in this book, sinusoidal input analysis is carried out in the following chapter.

2.2. Mathematical model with sinusoidal and cosenoidal input

Now considering **sine** and **cosine** inputs at $I_d^*(s)$ and $I_q^*(s)$ respectively and again assuming that the grid voltage is ideal, i.e., assuming no angle phase shift and ω constant, the time domain expressions (1) and (2) can be transformed into the 's' domain as follows (see appendix B for detailed mathematical development):

$$\begin{aligned}
 V_{conv\alpha}(s) = & \left(k_p + \frac{k_i s}{s^2 + \omega^2} \right) \left[-I_\alpha(s) + \left(\frac{1}{2} \right) \left(\frac{s^2 + \omega_1^2}{\omega_1} \right) \left(\frac{\omega_1 + \omega}{s^2 + (\omega_1 + \omega)^2} + \frac{\omega_1 - \omega}{s^2 + (\omega_1 - \omega)^2} \right) I_d^*(s) \right. \\
 & \left. - \left(\frac{1}{2} \right) \left(\frac{s^2 + \omega_1^2}{s} \right) \left(\frac{\omega_1 + \omega}{s^2 + (\omega_1 + \omega)^2} - \frac{\omega_1 - \omega}{s^2 + (\omega_1 - \omega)^2} \right) I_q^*(s) \right] + V_{g\alpha}(s)
 \end{aligned} \tag{25}$$

$$V_{conv\beta}(s) = \left(k_p + \frac{k_i s}{s^2 + \omega^2} \right) \left[-I_\beta(s) + \left(\frac{1}{2} \right) \left(\frac{s^2 + \omega_1^2}{\omega_1} \right) \left(\frac{s}{s^2 + (\omega_1 - \omega)^2} - \frac{s}{s^2 + (\omega_1 + \omega)^2} \right) I_d^*(s) \right. \\ \left. + \left(\frac{1}{2} \right) \left(\frac{s^2 + \omega_1^2}{s} \right) \left(\frac{s}{s^2 + (\omega_1 + \omega)^2} + \frac{s}{s^2 + (\omega_1 - \omega)^2} \right) I_q^*(s) \right] + V_{g\beta}(s) \quad (26)$$

Being these expressions only valid for a **sine** and **cosine** inputs at $I_d^*(s)$ and $I_q^*(s)$ respectively:

$$i_d^*(t) = |I_d^*| \cdot \sin(\omega_1 t) \quad \rightarrow \quad I_d^*(s) = \frac{\omega_1}{s^2 + \omega_1^2} |I_d^*| \quad (27)$$

$$i_q^*(t) = |I_q^*| \cdot \cos(\omega_1 t) \quad \rightarrow \quad I_q^*(s) = \frac{s}{s^2 + \omega_1^2} |I_q^*| \quad (28)$$

It has to be highlighted that sine and cosine inputs have been chosen for being as general as possible. Note that it could be also chosen at the inputs, for instance; sine and sine, or cosine and cosine, or cosine and sine. Then, combining these last two expressions in 's' domain, with the power circuit model equations (9) and (10), the closed loop expressions of the currents can be obtained:

$$I_\alpha(s) = \left(\left(\frac{k_p s^2 + k_i s + k_p \omega^2}{A(s)} \right) \left(\frac{1}{2} \right) \left(\frac{s^2 + \omega_1^2}{\omega_1} \right) \left(\frac{\omega_1 + \omega}{s^2 + (\omega_1 + \omega)^2} + \frac{\omega_1 - \omega}{s^2 + (\omega_1 - \omega)^2} \right) \right) I_d^*(s) \\ - \left(\left(\frac{k_p s^2 + k_i s + k_p \omega^2}{A(s)} \right) \left(\frac{1}{2} \right) \left(\frac{s^2 + \omega_1^2}{s} \right) \left(\frac{\omega_1 + \omega}{s^2 + (\omega_1 + \omega)^2} - \frac{\omega_1 - \omega}{s^2 + (\omega_1 - \omega)^2} \right) \right) I_q^*(s) \quad (29)$$

$$I_\beta(s) = \left(\left(\frac{k_p s^2 + k_i s + k_p \omega^2}{A(s)} \right) \left(\frac{1}{2} \right) \left(\frac{s^2 + \omega_1^2}{\omega_1} \right) \left(-\frac{s}{s^2 + (\omega_1 + \omega)^2} + \frac{s}{s^2 + (\omega_1 - \omega)^2} \right) \right) I_d^*(s) \\ + \left(\left(\frac{k_p s^2 + k_i s + k_p \omega^2}{A(s)} \right) \left(\frac{1}{2} \right) \left(\frac{s^2 + \omega_1^2}{s} \right) \left(\frac{s}{s^2 + (\omega_1 + \omega)^2} + \frac{s}{s^2 + (\omega_1 - \omega)^2} \right) \right) I_q^*(s) \quad (30)$$

Being these expressions only valid for a **sine** and **cosine** inputs at $I_d^*(s)$ and $I_q^*(s)$ respectively. As done in previous chapter, it is possible to define $G_{\alpha d_s}(s)$, $G_{\alpha q_s}(s)$, $G_{\beta d_s}(s)$, $G_{\beta q_s}(s)$ for previous two expressions, representing directly the transfer functions. Then, by substituting the **sine** and **cosine** inputs at $I_d^*(s)$ and $I_q^*(s)$, we obtain the output current expressions:

$$I_\alpha(s) = \left(\left(\frac{k_p s^2 + k_i s + k_p \omega^2}{A(s)} \right) \left(\frac{1}{2} \right) \left(\frac{\omega_1 + \omega}{s^2 + (\omega_1 + \omega)^2} + \frac{\omega_1 - \omega}{s^2 + (\omega_1 - \omega)^2} \right) \right) |I_d^*| \\ - \left(\left(\frac{k_p s^2 + k_i s + k_p \omega^2}{A(s)} \right) \left(\frac{1}{2} \right) \left(\frac{\omega_1 + \omega}{s^2 + (\omega_1 + \omega)^2} - \frac{\omega_1 - \omega}{s^2 + (\omega_1 - \omega)^2} \right) \right) |I_q^*| \quad (31)$$

$$I_{\beta}(s) = \left(\left(\frac{k_p s^2 + k_i s + k_p \omega^2}{A(s)} \right) \left(\frac{1}{2} \right) \left(-\frac{s}{s^2 + (\omega_1 + \omega)^2} + \frac{s}{s^2 + (\omega_1 - \omega)^2} \right) \right) |I_d^*| + \left(\left(\frac{k_p s^2 + k_i s + k_p \omega^2}{A(s)} \right) \left(\frac{1}{2} \right) \left(\frac{s}{s^2 + (\omega_1 + \omega)^2} + \frac{s}{s^2 + (\omega_1 - \omega)^2} \right) \right) |I_q^*| \quad (32)$$

Or expanding into two factors:

$$I_{\alpha}(s) = \left[\left(\frac{k_p s^2 + k_i s + k_p \omega^2}{A(s)} \right) \left(\frac{|I_d^*|}{2} - \frac{|I_q^*|}{2} \right) \right] \left(\frac{\omega_1 + \omega}{s^2 + (\omega_1 + \omega)^2} \right) + \left[\left(\frac{k_p s^2 + k_i s + k_p \omega^2}{A(s)} \right) \left(\frac{|I_d^*|}{2} + \frac{|I_q^*|}{2} \right) \right] \left(\frac{\omega_1 - \omega}{s^2 + (\omega_1 - \omega)^2} \right) \quad (33)$$

$$I_{\beta}(s) = \left[\left(\frac{k_p s^2 + k_i s + k_p \omega^2}{A(s)} \right) \left(\frac{1}{2} \right) \left(\frac{|I_q^*|}{2} - \frac{|I_d^*|}{2} \right) \right] \left(\frac{s}{s^2 + (\omega_1 + \omega)^2} \right) + \left[\left(\frac{k_p s^2 + k_i s + k_p \omega^2}{A(s)} \right) \left(\frac{1}{2} \right) \left(\frac{|I_q^*|}{2} + \frac{|I_d^*|}{2} \right) \right] \left(\frac{s}{s^2 + (\omega_1 - \omega)^2} \right) \quad (34)$$

Which is how the Bode diagram originally is defined in every classic book as for instance [16]. Since $A(s)$ is composed by poles with real negative parts, they present an exponential factor at the time domain response that is made zero at steady-state. Therefore, the output current $I_{\alpha}(s)$ at steady-state is composed by the addition of two sinusoidal terms of frequencies $\omega_1 + \omega$ and $\omega_1 - \omega$ and their amplitudes and phases, are calculated by substituting $s=j(\omega_1 + \omega)$ and $s=j(\omega_1 - \omega)$ and calculating the module and phases in (33). While the same occurs with $I_{\beta}(s)$ that is excited by cosine inputs, as we have chosen seeking a generalist analysis. By focusing only on $I_{\alpha}(s)$ current now, the steady-state two terms' amplitudes and phases, are calculated by substituting:

$$\begin{aligned} s = j(\omega_1 + \omega) &\rightarrow \left(\frac{k_p s^2 + k_i s + k_p \omega^2}{A(s)} \right) \left(\frac{|I_d^*|}{2} - \frac{|I_q^*|}{2} \right) \\ s = j(\omega_1 - \omega) &\rightarrow \left(\frac{k_p s^2 + k_i s + k_p \omega^2}{A(s)} \right) \left(\frac{|I_d^*|}{2} + \frac{|I_q^*|}{2} \right) \end{aligned} \quad (35)$$

Expanding considering $A(s)$:

$$\begin{aligned}
 s = j(\omega_1 + \omega) &\rightarrow \left(\frac{k_p s^2 + k_i s + k_p \omega^2}{Ls^3 + (k_p + R)s^2 + (L\omega^2 + k_i)s + (k_p + R)\omega^2} \right) \left(\frac{|I_d^*|}{2} - \frac{|I_q^*|}{2} \right) \\
 s = j(\omega_1 - \omega) &\rightarrow \left(\frac{k_p s^2 + k_i s + k_p \omega^2}{Ls^3 + (k_p + R)s^2 + (L\omega^2 + k_i)s + (k_p + R)\omega^2} \right) \left(\frac{|I_d^*|}{2} + \frac{|I_q^*|}{2} \right)
 \end{aligned} \quad (36)$$

What means that the two sinusoidal output currents, can be evaluated in terms of amplitude and phase by applying for instance 'Bode function' of previous expression (36) in a programs such as Matlab. Numerically, this means that for instance by choosing (note that the frequency at which the Bode is wanted to be evaluated is ω):

$$i_d^*(t) = |I_d^*| \cdot \sin(\omega t) \quad \rightarrow \quad i_d^*(t) = 1 \cdot \sin(250 \cdot 2 \cdot \pi \cdot t) \quad (37)$$

$$i_q^*(t) = 0 \quad \rightarrow \quad |I_q^*| = 0 \quad (38)$$

At the output current $i_\alpha(t)$, we obtain 0.187A at 200Hz and 0.127A at 300Hz, which corresponds with 14.5dB y -17.9dB and with obtained at Bode of previous expression (36) as noticed in next Figure 7.

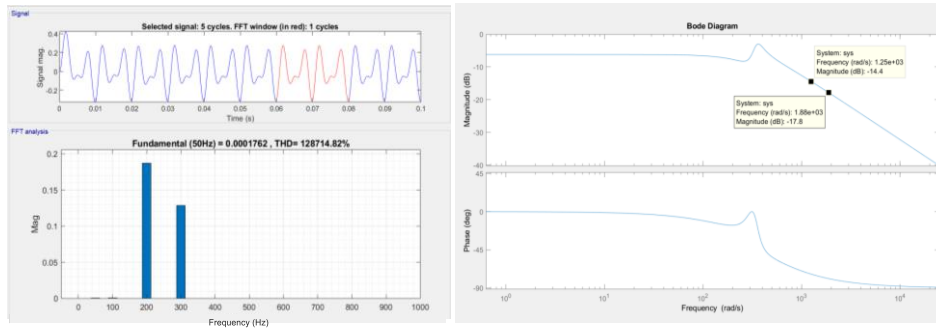


Figure 7. Time domain and Bode correspondence for the $\alpha\beta$ control of the currents. Conditions of Appendix E and: $i_d^*(t) = 1 \cdot \sin(250 \cdot 2 \cdot \pi \cdot t)$, $i_q^*(t) = 0$

On the other hand, by using a partial fraction expansion and applying the inverse Laplace transform, the time domain expression for sinus and cosines inputs of the output current can be obtained from expression (31) (only $i_\alpha(t)$ current is shown, $i_\beta(t)$ would present an equivalent form):

$$\begin{aligned}
 i_\alpha(t) = & \left((B_0) \cdot e^{\sigma_d t} + (2 \cdot B_1) \cdot e^{\sigma_d t} \cdot \cos(\omega_{d1} \cdot t + \arg B_1) + (2 \cdot B_2) \cdot \cos((\omega_1 + \omega) \cdot t + \arg B_2) + (2 \cdot B_3) \cdot \cos((\omega_1 - \omega) \cdot t + \arg B_3) \right) |I_d^*| \\
 & + \left((B_4) \cdot e^{\sigma_d t} + (2 \cdot B_5) \cdot e^{\sigma_d t} \cdot \cos(\omega_{d5} \cdot t + \arg B_5) + (2 \cdot B_6) \cdot \cos((\omega_1 + \omega) \cdot t + \arg B_6) + (2 \cdot B_7) \cdot \cos((\omega_1 - \omega) \cdot t + \arg B_7) \right) |I_q^*|
 \end{aligned} \quad (39)$$

All the constants present in this last equation, B_0, B_1 , etc... can be easily numerically derived for instance using the 'residue' from Matlab Control Toolbox. Table II shows an example of numerical solution.

Table II. Numerical solution of expression (39) by using the 'residue' function from Matlab Control Toolbox. Conditions of Appendix E.

d	q
$B_0 = 2.60333294897e-01$ $\sigma = -4.08885123379e+02$	$B_4 = 4.52013268064e-02$ $\sigma_4 = -4.08885123379e+02$
$B_1 = 2.69804207945e-02$ $argB_1 = 4.24146388400e-01$ $\sigma_1 = -4.80574383101e+01$ $\omega_{l1} = 3.45812931291e+02$	$B_5 = 5.958132362346896e-03$ $argB_5 = 4.52277565853e-01$ $\sigma_5 = -4.80574383101e+01$ $\omega_{l5} = 3.45812931291e+02$
$B_2 = 6.46561538423e-02$ $argB_2 = -2.94401826699e+00$ $\omega_{l+\omega} = 1.8849e+03$	$B_6 = 6.46561538423e-02$ $argB_6 = 1.97574386591e-01$ $\omega_{l+\omega} = 1.88495559215e+03$
$B_3 = 9.53533539998e-02$ $argB_3 = -2.85108949285e+00$ $\omega_{l-\omega} = 1.2566e+03$	$B_7 = 9.53533539998e-02$ $argB_7 = -2.85108949285e+00$ $\omega_{l-\omega} = 1.2566e+03$

Finally, the transient response to sinus and cosines inputs depicted in the following figure. The time domain response provided by the mathematical model of expression (39) is superposed to the Simulink block diagram depicted in previous Figure 5. It is seen an exact correspondence of both time domain responses to the sinus and cosines inputs. Note that at the time domain response, for the particular choice of inputs selected ($i_d^*(t) = 1 \cdot \sin(250 \cdot 2 \cdot \pi \cdot t)$, $i_q^*(t) = 0.5 \cdot \cos(250 \cdot 2 \cdot \pi \cdot t)$), the $(\omega_{l+\omega})$ terms is zero as can be deduced also in the resulting residuals of Table II.

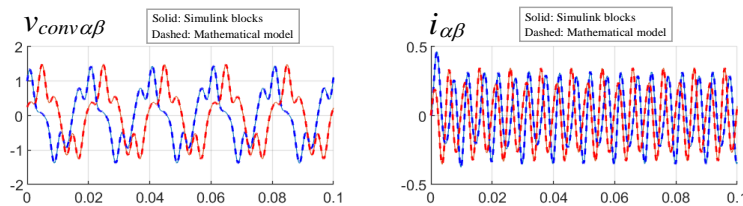


Figure 8. Time domain response for a sine and cosine input references of 250Hz at $I_d^*(s)$ (1 Amp) and $I_q^*(s)$ (0.5 Amp) respectively, for the $\alpha\beta$ control of the currents. Conditions of Appendix E.

Finally, the poles and zeros of transfer function of expression (29) are depicted in next figure. Note the correspondence with the poles and the constant terms of the time domain response.

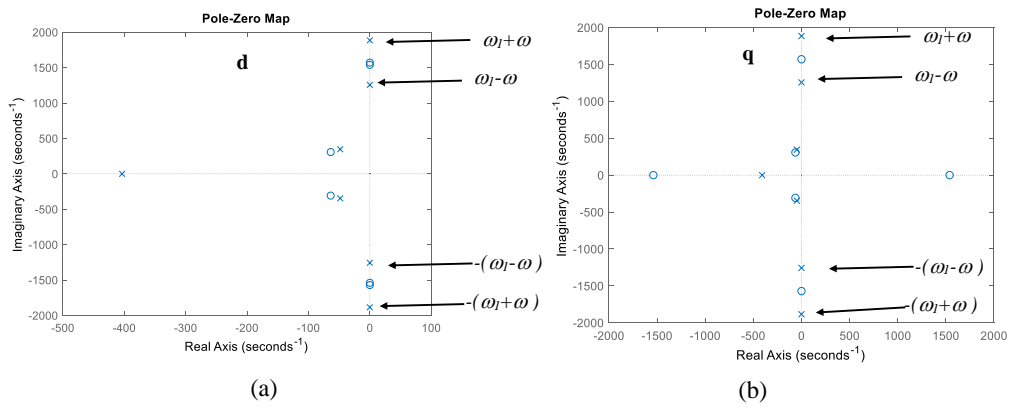


Figure 9. Poles of transfer function of expression (29), for the $\alpha\beta$ control of the currents with sinusoidal current references. Conditions of Appendix E.

Chapter 3.

Control of currents in rotating reference frame (dq control) with cancellation of coupling terms

The control block diagram [7] studied in this chapter is depicted in Figure 10. The current control is effectively implemented in rotating reference frame (dq) by using two PI controllers. A typical and ideal PI controller configuration in 's' domain is:

$$PI(s) = k_p + \frac{k_i}{s} \quad (40)$$

Being k_p and k_i the gains of the regulator that must be tuned. The rotating reference frame rotates at speed ω , the grid frequency. In most of the applications of three phase grid connected converters, the current references $i_d^*(t)$ and $i_q^*(t)$ are created in rotating reference frame (dq). Then, at the output of the regulators, a cancellation of coupling terms is adopted although is not strictly necessary [7]. After that, by using the rotational transformation the voltage references are transformed into the stationary reference frame ($\alpha\beta$), obtaining thus the voltage references that will be applied by the VSC converter $v_{conv\alpha}(t)$ and $v_{conv\beta}(t)$. Often a feedforward term of the grid voltage is added at the output [7].

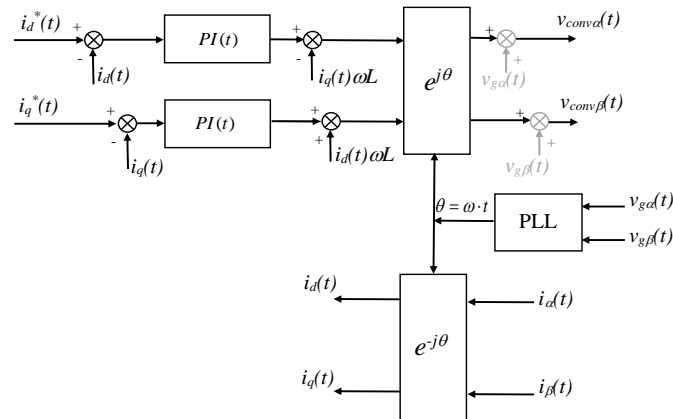


Figure 10. Current control block diagram in rotating reference frame (dq) with two PI controllers and cancellation of current coupling terms.

3.1. Mathematical model in dq

This model has been widely studied in specialized literature, such as for instance [6] – [7], so it will be shortly presented here. By using the equivalent electric circuit of Figure 11, the following expression can be derived:

$$v_{convd}(t) = R \cdot i_d(t) + L \cdot \frac{di_d(t)}{dt} + v_{gd}(t) - \omega \cdot L \cdot i_q(t) \quad (41)$$

$$v_{convq}(t) = R \cdot i_q(t) + L \cdot \frac{di_q(t)}{dt} + v_{gq}(t) + \omega \cdot L \cdot i_d(t) \quad (42)$$

Neglecting the transformations between reference frames, converter effect and some other non-dominant phenomena, the closed loop expression in dq reference frame, can be calculated from the union of the electric circuit equation and control represented in block diagram of Figure 10, which holds:

$$[i_d^*(t) - i_d(t)] \otimes PI(t) + v_{gd}(t) - \omega \cdot L \cdot i_q(t) = R \cdot i_d(t) + L \cdot \frac{di_d(t)}{dt} + v_{gd}(t) - \omega \cdot L \cdot i_q(t) \quad (43)$$

$$[i_q^*(t) - i_q(t)] \otimes PI(t) + v_{gq}(t) + \omega \cdot L \cdot i_d(t) = R \cdot i_q(t) + L \cdot \frac{di_q(t)}{dt} + v_{gq}(t) + \omega \cdot L \cdot i_d(t) \quad (44)$$

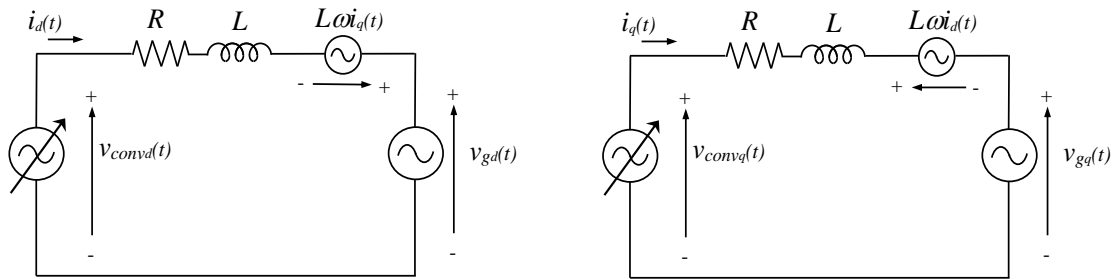


Figure 11. Equivalent electric circuit of grid connected converter, filter and grid operating with current control in dq reference frame.

In general, the d axis of the synchronously rotating frame is aligned with the grid voltage space vector, making therefore zero the q component of the grid voltage, $v_{gq}=0$. Eliminating the terms that can be cancelled in the equations, substituting the $PI(t)$ equations and applying the Laplace transform, the expressions yield:

$$[I_d^*(s) - I_d(s)] \cdot \left(k_p + \frac{k_i}{s} \right) = R \cdot I_d(s) + L \cdot s \cdot I_d(s) \quad (45)$$

$$[I_q^*(s) - I_q(s)] \cdot \left(k_p + \frac{k_i}{s} \right) = R \cdot I_q(s) + L \cdot s \cdot I_q(s) \quad (46)$$

Rearranging both equations, the transfer functions of each current control loop yields:

$$\frac{I_{ds}(s)}{I_{ds}^*(s)} = \frac{I_{qs}(s)}{I_{qs}^*(s)} = \frac{(k_p s + k_i)/L}{s^2 + \frac{(k_p + R)}{L}s + \frac{k_i}{L}} \quad (47)$$

With this, it is possible to associate the denominator to the canonic second order transfer function as follows:

$$\frac{I_{ds}(s)}{I_{ds}^*(s)} = \frac{I_{qs}(s)}{I_{qs}^*(s)} = \frac{(k_p s + k_i)/L}{s^2 + \frac{(k_p + R)}{L}s + \frac{k_i}{L}} = \frac{(k_p s + k_i)/L}{s^2 + 2\xi\omega_n s + \omega_n^2} \quad (48)$$

For a specified closed loop dynamic, it is possible to define the natural frequency ω_n and damping ξ ratio as desired, by choosing:

$$k_p = 2\xi\omega_n L - R \quad k_i = \omega_n^2 L \quad (49)$$

Thus, the poles and zeros of the closed loop transfer functions are represented in Figure 12 for a given numerical example:

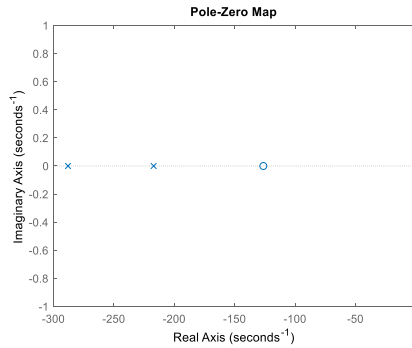


Figure 12. Poles of transfer functions $I_d(s)/I_d^*(s)$ and $I_q(s)/I_q^*(s)$ of expression (47), for control of currents in synchronous reference frame (dq) with current coupling cancellation. Conditions of Appendix E.

Thus, for a step input applied to both input current references $I_d^*(s)$ and $I_q^*(s)$:

$$I_d^*(s) = \frac{|I_d^*|}{s} \quad I_q^*(s) = \frac{|I_q^*|}{s} \quad (50)$$

the output currents yields:

$$I_d(s) = \frac{k_p / L}{s^2 + 2\xi\omega_n s + \omega_n^2} |I_d^*| + \frac{k_i / L}{s(s^2 + 2\xi\omega_n s + \omega_n^2)} |I_d^*| \quad (51)$$

$$I_q(s) = \frac{k_p / L}{s^2 + 2\xi\omega_n s + \omega_n^2} |I_q^*| + \frac{k_i / L}{s(s^2 + 2\xi\omega_n s + \omega_n^2)} |I_q^*| \quad (52)$$

Applying the inverse Laplace transform, the time domain current expressions are:

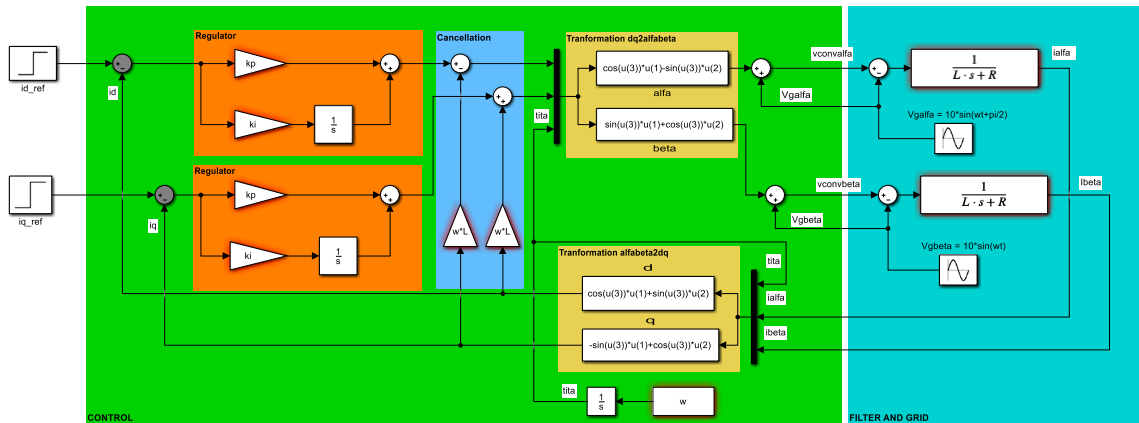
$$i_d(t) = |I_d^*| \frac{k_p / L}{\omega_n \sqrt{1-\zeta^2}} e^{-\zeta\omega_n t} \sin(\omega_n \sqrt{1-\zeta^2} t) + |I_d^*| \left(\frac{k_i}{L\omega_n^2} \right) - |I_d^*| \left(\frac{k_i}{L\omega_n^2} \right) \left(\frac{1}{\sqrt{1-\zeta^2}} e^{-\zeta\omega_n t} \sin \left(\omega_n \sqrt{1-\zeta^2} t + \tan^{-1} \left(\frac{\sqrt{1-\zeta^2}}{\zeta} \right) \right) \right) \quad (53)$$

$$i_q(t) = |I_q^*| \frac{k_p / L}{\omega_n \sqrt{1-\zeta^2}} e^{-\zeta\omega_n t} \sin(\omega_n \sqrt{1-\zeta^2} t) + |I_q^*| \left(\frac{k_i}{L\omega_n^2} \right) - |I_q^*| \left(\frac{k_i}{L\omega_n^2} \right) \left(\frac{1}{\sqrt{1-\zeta^2}} e^{-\zeta\omega_n t} \sin \left(\omega_n \sqrt{1-\zeta^2} t + \tan^{-1} \left(\frac{\sqrt{1-\zeta^2}}{\zeta} \right) \right) \right) \quad (54)$$

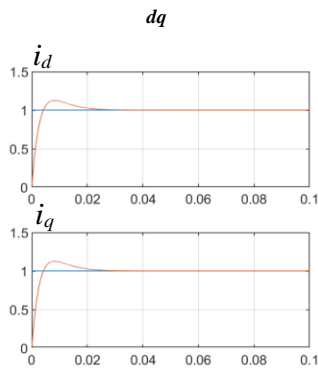
Once the exponential terms are damped and assuming that the expression (49) has been used, the steady-state expressions for the current yields:

$$i_d(t)_{t \rightarrow \infty} = |I_d^*| \quad \text{and} \quad i_q(t)_{t \rightarrow \infty} = |I_q^*| \quad (55)$$

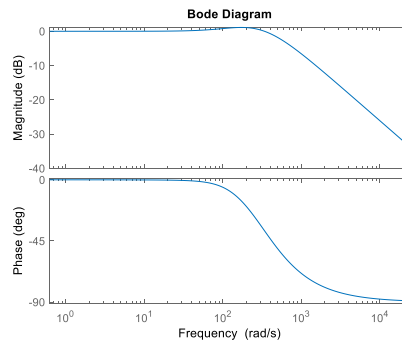
Thus, the step response in time domain is represented in the following figure. It is seen an exact match between the mathematical previously deduced equations (53-54) and the $i_d(t)$ and $i_q(t)$ currents provided by the control block diagram. In the figure, it is also represented the Bode diagram of the current transfer function (47).



(a)



(b)



(c)

Figure 13. (a) Block diagram of control in synchronous reference frame (dq) with current coupling cancellation, (b) time domain responses in dq reference frame, to a unit step input in $i_d^*(t)$ and $i_q^*(t)$, (c) Bode diagrams of $I_d(s)/I_d^*(s)$ and $I_q(s)/I_q^*(s)$. Conditions of Appendix E.

3.2. Mathematical model in $\alpha\beta$

This control block diagram, can be represented as an equivalent 'black box' either in time domain and also in 's' domain, as shown in Figure 14.

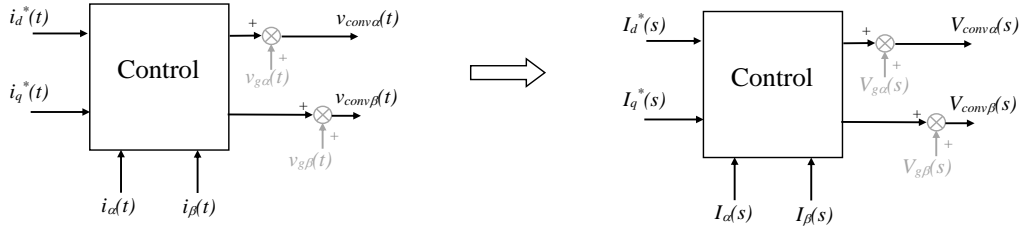


Figure 14. Current control blocks in time and 's' domains.

The α and β components of the converter voltages, considering the grid voltage feedforward terms, are mathematically represented in time domain as follows (Note that the harmonics created by the converter are neglected):

$$v_{conv\alpha}(t) = \left(\left[i_d^*(t) - i_d(t) \right] \otimes PI(t) \right) \cdot \cos(\omega t) - \left(\left[i_q^*(t) - i_q(t) \right] \otimes PI(t) \right) \cdot \sin(\omega t) - \omega \cdot L \cdot i_q(t) \cdot \cos(\omega t) - \omega \cdot L \cdot i_d(t) \cdot \sin(\omega t) + v_{g\alpha}(t) \quad (56)$$

$$v_{conv\beta}(t) = \left(\left[i_d^*(t) - i_d(t) \right] \otimes PI(t) \right) \cdot \sin(\omega t) - \left(\left[i_q^*(t) - i_q(t) \right] \otimes PI(t) \right) \cdot \cos(\omega t) - \omega \cdot L \cdot i_q(t) \cdot \sin(\omega t) + \omega \cdot L \cdot i_d(t) \cdot \cos(\omega t) + v_{g\beta}(t) \quad (57)$$

Which is equal to:

$$v_{conv\alpha}(t) = \left(\left[i_d^*(t) - (i_\alpha(t) \cdot \cos(\omega t) + i_\beta(t) \cdot \sin(\omega t)) \right] \otimes PI(t) \right) \cdot \cos(\omega t) - \left(\left[i_q^*(t) - (-i_\alpha(t) \cdot \sin(\omega t) + i_\beta(t) \cdot \cos(\omega t)) \right] \otimes PI(t) \right) \cdot \sin(\omega t) - \omega \cdot L \cdot i_q(t) \cdot \cos(\omega t) - \omega \cdot L \cdot i_d(t) \cdot \sin(\omega t) + v_{g\alpha}(t) \quad (58)$$

$$v_{conv\beta}(t) = \left(\left[i_d^*(t) - (i_\alpha(t) \cdot \cos(\omega t) + i_\beta(t) \cdot \sin(\omega t)) \right] \otimes PI(t) \right) \cdot \sin(\omega t) - \left(\left[i_q^*(t) - (-i_\alpha(t) \cdot \sin(\omega t) + i_\beta(t) \cdot \cos(\omega t)) \right] \otimes PI(t) \right) \cdot \cos(\omega t) - \omega \cdot L \cdot i_q(t) \cdot \sin(\omega t) + \omega \cdot L \cdot i_d(t) \cdot \cos(\omega t) + v_{g\beta}(t) \quad (59)$$

3.3. Mathematical model in $\alpha\beta$ with an step input

Considering **step** inputs at at both $I_d^*(s)$ and $I_q^*(s)$ and assuming that the grid voltage is ideal or purely sinusoidal and assuming no angle jumps and ω constant, the previous time domain expressions can be transformed into the 's' domain as follows (see appendix C for detailed mathematical development):

$$\begin{aligned}
 V_{conv\alpha}(s) = & -\left(k_p + \frac{k_i s}{s^2 + \omega^2}\right)I_\alpha(s) + \left(\frac{(-\omega L)s^2 + (k_i \omega - \omega^3 L)}{s^2 + \omega^2}\right)I_\beta(s) \\
 & + \left(\frac{k_p s^2}{s^2 + \omega^2} + \frac{k_i s(s^2 - \omega^2)}{(s^2 + \omega^2)^2}\right)I_d^*(s) - \left(\frac{k_p \omega s}{s^2 + \omega^2} - \frac{2\omega k_i s^2}{(s^2 + \omega^2)^2}\right)I_q^*(s) + V_{g\alpha}(s)
 \end{aligned} \tag{60}$$

$$\begin{aligned}
 V_{conv\beta}(s) = & -\left(\frac{(-\omega L)s^2 + (k_i \omega - \omega^3 L)}{s^2 + \omega^2}\right)I_\alpha(s) - \left(k_p + \frac{k_i s}{s^2 + \omega^2}\right)I_\beta(s) \\
 & + \left(\frac{k_p \omega s}{s^2 + \omega^2} - \frac{2\omega k_i s^2}{(s^2 + \omega^2)^2}\right)I_d^*(s) + \left(\frac{k_p s^2}{s^2 + \omega^2} + \frac{k_i s(s^2 - \omega^2)}{(s^2 + \omega^2)^2}\right)I_q^*(s) + V_{g\beta}(s)
 \end{aligned} \tag{61}$$

Being these expressions only valid for a step input at both $I_d^*(s)$ and $I_q^*(s)$:

$$I_d^*(s) = \frac{|I_d^*|}{s} \quad I_q^*(s) = \frac{|I_q^*|}{s} \tag{62}$$

As done in previous chapter, combining the last two control law expressions with the power circuit electric expressions, it is possible to derive the closed loop equation for both α and β currents:

$$I_\alpha(s) = \left(k_p s + \frac{k_i(s^2 - \omega^2)}{s^2 + \omega^2}\right)\left(\frac{s}{A(s)}\right)I_d^*(s) - \left(k_p + \frac{2k_i s}{s^2 + \omega^2}\right)\left(\frac{\omega s}{A(s)}\right)I_q^*(s) + \left(\frac{(-\omega L)s^2 + (k_i \omega - \omega^3 L)}{A(s)}\right)I_\beta(s) \tag{63}$$

$$I_\beta(s) = \left(k_p + \frac{2k_i s}{s^2 + \omega^2}\right)\left(\frac{\omega s}{A(s)}\right)I_d^*(s) + \left(k_p s + \frac{k_i(s^2 - \omega^2)}{s^2 + \omega^2}\right)\left(\frac{s}{A(s)}\right)I_q^*(s) - \left(\frac{(-\omega L)s^2 + (k_i \omega - \omega^3 L)}{A(s)}\right)I_\alpha(s) \tag{64}$$

Being again:

$$A(s) = Ls^3 + (k_p + R)s^2 + (L\omega^2 + k_i)s + (k_p + R)\omega^2 \tag{65}$$

Thus now substituting in both inputs a step, the output currents yields:

$$I_\alpha(s) = \left(\frac{k_p s^3 + k_i s^2 + k_p \omega^2 s - k_i \omega^2}{(s^2 + \omega^2)A(s)}\right)|I_d^*| - \left(\frac{k_p \omega s^2 + 2k_i \omega s + k_p \omega^3}{(s^2 + \omega^2)A(s)}\right)|I_q^*| + \left(\frac{(-\omega L)s^2 + (k_i \omega - \omega^3 L)}{A(s)}\right)I_\beta(s) \tag{66}$$

$$I_\beta(s) = \left(\frac{k_p \omega s^2 + 2k_i \omega s + k_p \omega^3}{(s^2 + \omega^2)A(s)}\right)|I_d^*| + \left(\frac{k_p s^3 + k_i s^2 + k_p \omega^2 s - k_i \omega^2}{(s^2 + \omega^2)A(s)}\right)|I_q^*| - \left(\frac{(-\omega L)s^2 + (k_i \omega - \omega^3 L)}{A(s)}\right)I_\alpha(s) \tag{67}$$

Which is equal to:

$$\begin{aligned}
 I_\alpha(s) = & \left(\frac{k_p s^3 + k_i s^2 + k_p \omega^2 s - k_i \omega^2}{Ls^5 + (k_p + R)s^4 + (2L\omega^2 + k_i)s^3 + 2\omega^2(k_p + R)s^2 + (L\omega^2 + k_i)\omega^2 s + \omega^4(k_p + R)} \right) |I_d^*| \\
 & - \left(\frac{k_p \omega s^2 + 2k_i \omega s + k_p \omega^3}{Ls^5 + (k_p + R)s^4 + (2L\omega^2 + k_i)s^3 + 2\omega^2(k_p + R)s^2 + (L\omega^2 + k_i)\omega^2 s + \omega^4(k_p + R)} \right) |I_q^*| \\
 & + \left(\frac{(-\omega L)s^2 + (k_i \omega - \omega^3 L)}{Ls^3 + (k_p + R)s^2 + (L\omega^2 + k_i)s + (k_p + R)\omega^2} \right) I_\beta(s)
 \end{aligned} \quad (68)$$

$$\begin{aligned}
 I_\beta(s) = & \left(\frac{k_p \omega s^2 + 2k_i \omega s + k_p \omega^3}{Ls^5 + (k_p + R)s^4 + (2L\omega^2 + k_i)s^3 + 2\omega^2(k_p + R)s^2 + (L\omega^2 + k_i)\omega^2 s + \omega^4(k_p + R)} \right) |I_d^*| \\
 & + \left(\frac{k_p s^3 + k_i s^2 + k_p \omega^2 s - k_i \omega^2}{Ls^5 + (k_p + R)s^4 + (2L\omega^2 + k_i)s^3 + 2\omega^2(k_p + R)s^2 + (L\omega^2 + k_i)\omega^2 s + \omega^4(k_p + R)} \right) |I_q^*| \\
 & - \left(\frac{(-\omega L)s^2 + (k_i \omega - \omega^3 L)}{Ls^3 + (k_p + R)s^2 + (L\omega^2 + k_i)s + (k_p + R)\omega^2} \right) I_\alpha(s)
 \end{aligned} \quad (69)$$

As can be noticed from the previous expressions, there is a coupling in α and β . What means that $I_\alpha(s)$ depends on $I_\beta(s)$ and vice versa. This coupling, can be represented graphically as in Figure 15.

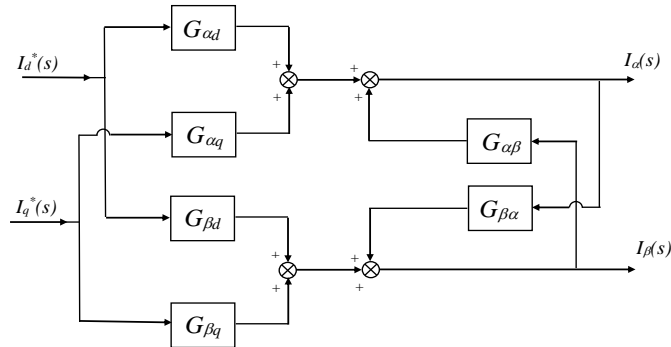


Figure 15. Block diagram of the control of currents in dq with cancellation of coupling terms.

With equations developed up to this point, we cannot derive decoupled expressions that connect the outputs ($I_\alpha(s)$ and $I_\beta(s)$) directly to the inputs ($I_d^*(s)$ and $I_q^*(s)$). In order to solve this problem, a further mathematical development must be carried out. Hence, by renaming the expressions (63) and (64) as follows:

$$I_\alpha(s) = G_{\alpha d}(s)I_d^*(s) + G_{\alpha q}(s)I_q^*(s) + G_{\alpha\beta}(s)I_\beta(s) \quad (70)$$

$$I_\beta(s) = G_{\beta d}(s)I_d^*(s) + G_{\beta q}(s)I_q^*(s) + G_{\beta\alpha}(s)I_\alpha(s) \quad (71)$$

If we combine both equations seeking to eliminate $I_\alpha(s)$ from the second equation and $I_\beta(s)$ from the first equation, the decoupled input-output transfer functions can be obtained easily:

$$I_\alpha(s) = \left(\frac{G_{\alpha d}(s) + G_{\beta d}(s)G_{\alpha\beta}(s)}{1 - G_{\alpha\beta}(s)G_{\beta\alpha}(s)} \right) I_d^*(s) + \left(\frac{G_{\alpha q}(s) + G_{\beta q}(s)G_{\alpha\beta}(s)}{1 - G_{\alpha\beta}(s)G_{\beta\alpha}(s)} \right) I_q^*(s) \quad (72)$$

$$I_\beta(s) = \left(\frac{G_{\beta d}(s) + G_{\alpha d}(s)G_{\beta\alpha}(s)}{1 - G_{\alpha\beta}(s)G_{\beta\alpha}(s)} \right) I_d^*(s) + \left(\frac{G_{\beta q}(s) + G_{\alpha q}(s)G_{\beta\alpha}(s)}{1 - G_{\alpha\beta}(s)G_{\beta\alpha}(s)} \right) I_q^*(s) \quad (73)$$

The decoupled transfer functions are graphically represented in block diagram in next figure:

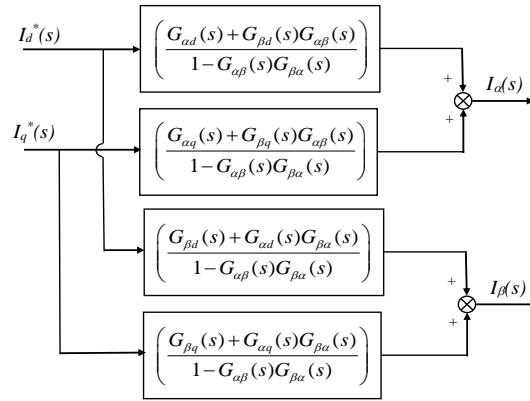


Figure 16. Equivalent block diagram of the control of currents in *dq* with cancellation of coupling terms.

Focusing on $I_\alpha(s)$ current and by solving these last expressions using a symbolic Toolbox from Matlab for instance, it is possible to obtain for d input current:

$$\frac{G_{\alpha d}(s) + G_{\beta d}(s)G_{\alpha\beta}(s)}{1 - G_{\alpha\beta}(s)G_{\beta\alpha}(s)} = \frac{g_{nd5} \cdot s^5 + g_{nd4} \cdot s^4 + g_{nd3} \cdot s^3 + g_{nd2} \cdot s^2 + g_{nd1} \cdot s}{g_6 \cdot s^6 + g_5 \cdot s^5 + g_4 \cdot s^4 + g_3 \cdot s^3 + g_2 \cdot s^2 + g_1 \cdot s + g_0} \quad (74)$$

Being each coefficient of the resulting transfer function:

$$\begin{aligned}
 g_{nd5} &= L \cdot k_p \\
 g_{nd4} &= k_p^2 + R \cdot k_p + L \cdot k_i \\
 g_{nd3} &= R \cdot k_i + 2 \cdot k_i \cdot k_p \\
 g_{nd2} &= k_i^2 - 3 \cdot L \cdot k_i \cdot \omega^2 + k_p^2 \cdot \omega^2 + R \cdot k_p \cdot \omega^2 \\
 g_{nd1} &= -L \cdot k_p \cdot \omega^4 - R \cdot k_i \cdot \omega^2 \\
 \\
 g_6 &= L^2 \\
 g_5 &= 2 \cdot L \cdot k_p + 2 \cdot L \cdot R \\
 g_4 &= 3 \cdot L^2 \cdot \omega^2 + 2 \cdot k_i \cdot L + R^2 + 2 \cdot R \cdot k_p + k_p^2 \\
 g_3 &= 2 \cdot R \cdot k_i + 2 \cdot k_i \cdot k_p + 4 \cdot L \cdot R \cdot \omega^2 + 4 \cdot L \cdot k_p \cdot \omega^2 \\
 g_2 &= 3 \cdot L^2 \cdot \omega^4 + 2 \cdot R^2 \cdot \omega^2 + 4 \cdot R \cdot k_p \cdot \omega^2 + k_i^2 + 2 \cdot k_p^2 \cdot \omega^2 \\
 g_1 &= 2 \cdot k_i \cdot k_p \cdot \omega^2 + 2 \cdot L \cdot R \cdot \omega^4 + 2 \cdot L \cdot k_p \cdot \omega^4 + 2 \cdot R \cdot k_i \cdot \omega^2 \\
 g_0 &= L^2 \cdot \omega^6 - 2 \cdot L \cdot k_i \cdot \omega^4 + R^2 \cdot \omega^4 + 2 \cdot R \cdot k_p \cdot \omega^4 + k_i^2 \cdot \omega^2 + k_p^2 \cdot \omega^4
 \end{aligned} \tag{75}$$

And for q input current:

$$\frac{G_{\alpha q}(s) + G_{\beta q}(s)G_{\alpha\beta}(s)}{1 - G_{\alpha\beta}(s)G_{\beta\alpha}(s)} = \frac{g_{nq4} \cdot s^4 + g_{nq3} \cdot s^3 + g_{nq2} \cdot s^2 + g_{nq1} \cdot s}{g_6 \cdot s^6 + g_5 \cdot s^5 + g_4 \cdot s^4 + g_3 \cdot s^3 + g_2 \cdot s^2 + g_1 \cdot s + g_0} \tag{76}$$

Being the denominator's coefficients, g_6, g_5, \dots equal to the previous expression. While the coefficients of the numerator are:

$$\begin{aligned}
 g_{nq4} &= -(2 \cdot L \cdot k_p) \cdot \omega \\
 g_{nq3} &= -(k_p^2 + R \cdot k_p + 3 \cdot L \cdot k_i) \cdot \omega \\
 g_{nq2} &= -(2 \cdot L \cdot k_p \cdot \omega^2 + 2 \cdot R \cdot k_i + 2 \cdot k_i \cdot k_p) \cdot \omega \\
 g_{nq1} &= -(k_i^2 + k_p^2 \cdot \omega^2 + R \cdot k_p \cdot \omega^2 - L \cdot k_i \cdot \omega^2) \cdot \omega
 \end{aligned} \tag{77}$$

Thus, in next Figure 17, the poles and zeros of the system are shown, after substituting the same numerical example used in previous chapter. It is seen that the real poles in synchronous reference frame (dq) that are located in this numerical example at -217 and -288, are directly translated to two complex conjugate pole pairs at the stationary reference frame ($\alpha\beta$), with same real parts (same σ of the exponential terms) and with imaginary parts $\omega_i=314.159\text{rd/s}$. Therefore, the time in which these poles are extinguished is equal (same σ of the exponential terms) in both stationary and synchronous rotating frames. Then, at the stationary reference frame ($\alpha\beta$) there is another conjugate imaginary poles, without real part and with imaginary part $\omega_i=314.159\text{rd/s}$, which are the components that create the steady-state current.

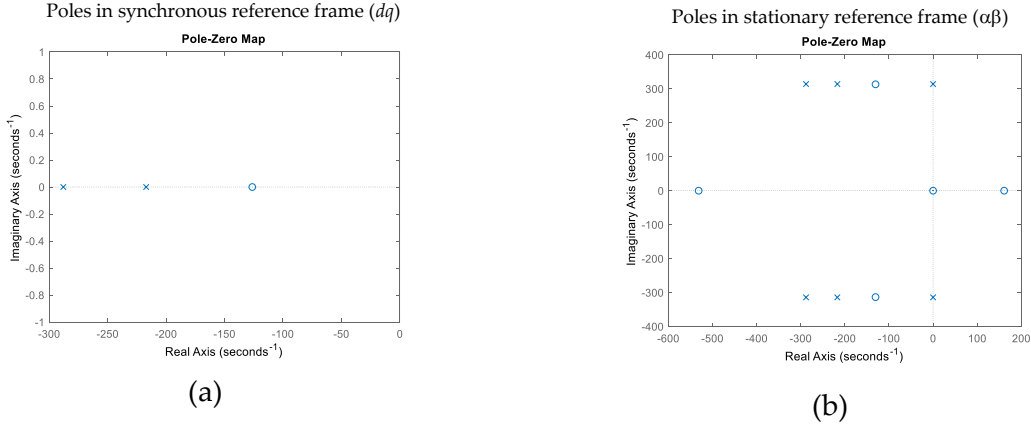


Figure 17. Control in dq with cancellation of coupling terms. (a) Poles in synchronous reference frame (dq) of $I_d(s)/I_d^*(s)$ and $I_q(s)/I_q^*(s)$ of expression (47), (b) Poles in stationary reference frame ($\alpha\beta$) of expression (72). Conditions of Appendix E.

After this, by substituting step inputs at at both $I_d^*(s)$ and $I_q^*(s)$, the output α current results in:

$$I_\alpha(s) = \left(\frac{G_{\alpha d}(s) + G_{\beta d}(s)G_{\alpha\beta}(s)}{1 - G_{\alpha\beta}(s)G_{\beta\alpha}(s)} \right) \frac{|I_d^*|}{s} + \left(\frac{G_{\alpha q}(s) + G_{\beta q}(s)G_{\alpha\beta}(s)}{1 - G_{\alpha\beta}(s)G_{\beta\alpha}(s)} \right) \frac{|I_q^*|}{s} \quad (78)$$

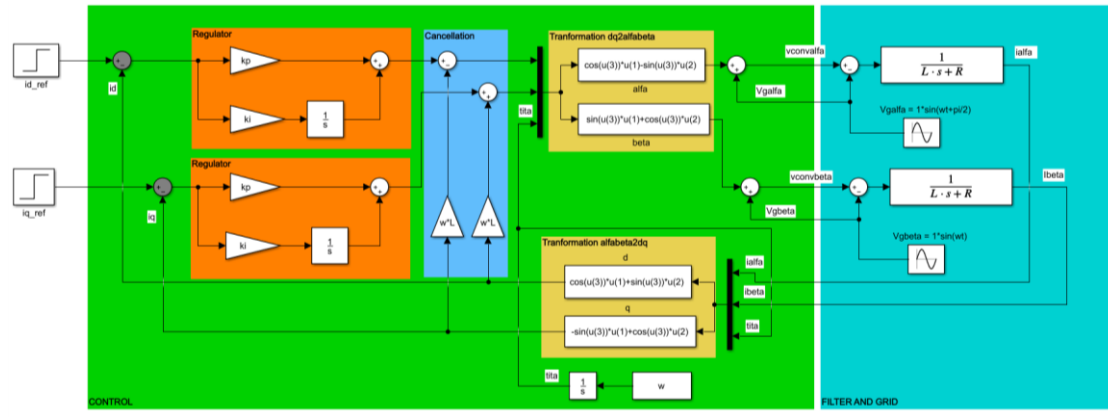
What is equal to:

$$I_\alpha(s) = \left(\frac{g_{nd5} \cdot s^4 + g_{nd4} \cdot s^3 + g_{nd3} \cdot s^2 + g_{nd2} \cdot s + g_{nd1}}{g_6 \cdot s^6 + g_5 \cdot s^5 + g_4 \cdot s^4 + g_3 \cdot s^3 + g_2 \cdot s^2 + g_1 \cdot s + g_0} \right) |I_d^*| + \left(\frac{g_{nq4} \cdot s^3 + g_{nq3} \cdot s^2 + g_{nq2} \cdot s^1 + g_{nq1}}{g_6 \cdot s^6 + g_5 \cdot s^5 + g_4 \cdot s^4 + g_3 \cdot s^3 + g_2 \cdot s^2 + g_1 \cdot s + g_0} \right) |I_q^*| \quad (79)$$

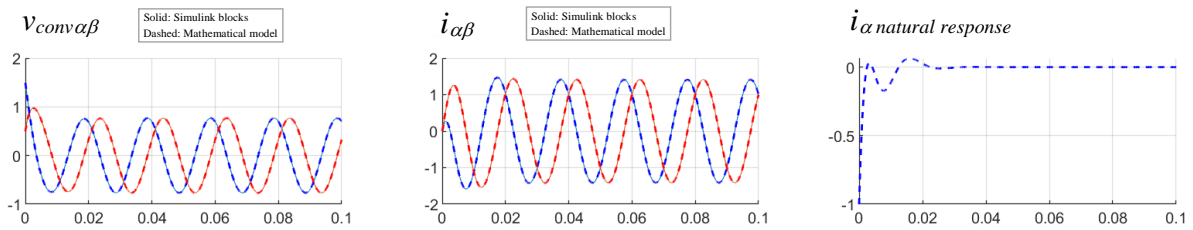
Note that the denominator is not altered compared to equation (74) and (76). By using a partial fraction expansion and applying the inverse Laplace transform, the time domain expression for step inputs of the output current can be obtained from previous equation (79). Being the time response of the complete final expressions (only $i_\alpha(t)$ current is shown, $i_\beta(t)$ would present an equivalent form):

$$i_\alpha(t) = \left((2 \cdot B_0) \cdot e^{\sigma_0 t} \cdot \cos(\omega_{d0} \cdot t + \arg B_0) + (2 \cdot B_1) \cdot e^{\sigma_1 t} \cdot \cos(\omega_{d1} \cdot t + \arg B_1) + (2 \cdot B_2) \cdot \cos(\omega \cdot t) \right) |I_d^*| + \left((2 \cdot B_3) \cdot e^{\sigma_3 t} \cdot \cos(\omega_{d3} \cdot t + \arg B_3) + (2 \cdot B_4) \cdot e^{\sigma_4 t} \cdot \cos(\omega_{d4} \cdot t + \arg B_4) + (2 \cdot B_5) \cdot \cos(\omega \cdot t + \pi/2) \right) |I_q^*| \quad (80)$$

As done in previous chapter, in Figure 18, the Simulink blocks and the derived mathematical expressions are compared, corroborating an exact match.



(a)



(b)

Figure 18. (a) Block diagram of control in synchronous reference frame (dq) with current coupling cancellation, (b) time domain responses in $\alpha\beta$ reference frame of control in dq frame with current coupling cancellation, to a unit step input in $i_d^*(t)$ and $i_q^*(t)$. Conditions of Appendix E.

Table III shows a numerical example of the constants obtained by Matlab by using the 'residue' function applied for equation (80).

Table III. Numerical solution of expression (80) by using the the 'residue' function from Matlab Control Toolbox. Conditions of Appendix E.

d	q
$B_0 = 1.960463118457156e+00$	$B_3 = 1.960463118457155e+00$
$argB_0 = 3.141592653589781e+00$	$argB_3 = -1.570796326794909e+00$
$\sigma = -2.879436171968935e+02$	$\sigma = -2.879436171968935e+02$
$wd_0 = 3.141592653589789e+02$	$wd_3 = 3.141592653589789e+02$
$B_1 = 1.460463118457152e+00$	$B_4 = 1.460463118457151e+00$
$argB_1 = -1.593711439601920e-14$	$argB_4 = 1.570796326794881e+00$
$\sigma_1 = -2.170563828031064e+02$	$\sigma_4 = -2.170563828031064e+02$
$\omega d_1 = 3.141592653589797e+02$	$\omega d_4 = 3.141592653589797e+02$
$B_2 = 4.999999999999999e-01$	$B_5 = 4.999999999999988e-01$
$\omega = 3.141592653589798e+02$	$\omega = 1.570796326794898e+00$

3.4. Mathematical model in $\alpha\beta$ with sinusoidal and cosenoidal input

Now considering **sine** and **cosine** inputs at $I_d^*(s)$ and $I_q^*(s)$ respectively and again assuming that the grid voltage is ideal and purely sinusoidal, i.e., assuming no angle phase shift and ω constant, the time domain expressions (58) and (59) can be transformed into the 's' domain as follows (see appendix D for detailed mathematical development):

$$\begin{aligned}
 V_{com\alpha}(s) = & -\left(k_p + \frac{k_i s}{s^2 + \omega^2}\right) I_\alpha(s) + \left(\frac{(-\omega L)s^2 + (k_i \omega - \omega^3 L)}{s^2 + \omega^2}\right) I_\beta(s) \\
 & + \left(\frac{k_p}{2}\right) \left(\frac{s^2 + \omega_1^2}{\omega_1}\right) \left(\frac{\omega_1 + \omega}{s^2 + (\omega_1 + \omega)^2} + \frac{\omega_1 - \omega}{s^2 + (\omega_1 - \omega)^2}\right) I_d^*(s) \\
 & - \left(\frac{k_i}{2}\right) \left(\frac{s^2 + \omega_1^2}{\omega_1^2}\right) \left(\frac{s}{s^2 + (\omega_1 + \omega)^2} + \frac{s}{s^2 + (\omega_1 - \omega)^2} + \frac{2s}{s^2 + \omega^2}\right) I_d^*(s) \\
 & - \left(\frac{k_p}{2}\right) \left(\frac{s^2 + \omega_1^2}{s}\right) \left(\frac{\omega_1 + \omega}{s^2 + (\omega_1 + \omega)^2} - \frac{\omega_1 - \omega}{s^2 + (\omega_1 - \omega)^2}\right) I_q^*(s) \\
 & - \left(\frac{k_i}{2\omega_1}\right) \left(\frac{s^2 + \omega_1^2}{s}\right) \left(\frac{s}{s^2 + (\omega_1 + \omega)^2} - \frac{s}{s^2 + (\omega_1 - \omega)^2}\right) I_q^*(s) + V_{g\alpha}(s)
 \end{aligned} \tag{81}$$

$$\begin{aligned}
 V_{com\beta}(s) = & -\left(k_p + \frac{k_i s}{s^2 + \omega^2}\right) I_\beta(s) - \left(\frac{(-\omega L)s^2 + (k_i \omega - \omega^3 L)}{s^2 + \omega^2}\right) I_\alpha(s) \\
 & - \left(\frac{k_i}{2}\right) \left(\frac{s^2 + \omega_1^2}{\omega_1^2}\right) \left(\frac{\omega_1 + \omega}{s^2 + (\omega_1 + \omega)^2} - \frac{\omega_1 - \omega}{s^2 + (\omega_1 - \omega)^2} - \frac{2\omega}{s^2 + \omega^2}\right) I_d^*(s) \\
 & + \left(\frac{k_p}{2}\right) \left(\frac{s^2 + \omega_1^2}{\omega_1}\right) \left(\frac{s}{s^2 + (\omega_1 - \omega)^2} - \frac{s}{s^2 + (\omega_1 + \omega)^2}\right) I_d^*(s) \\
 & + \left(\frac{k_i}{2\omega_1}\right) \left(\frac{s^2 + \omega_1^2}{s}\right) \left(\frac{\omega_1 + \omega}{s^2 + (\omega_1 + \omega)^2} + \frac{\omega_1 - \omega}{s^2 + (\omega_1 - \omega)^2}\right) I_q^*(s) \\
 & + \left(\frac{k_p}{2}\right) \left(\frac{s^2 + \omega_1^2}{s}\right) \left(\frac{s}{s^2 + (\omega_1 + \omega)^2} + \frac{s}{s^2 + (\omega_1 - \omega)^2}\right) I_q^*(s) + V_{g\beta}(s)
 \end{aligned} \tag{82}$$

Being these expressions only valid for a **sine** and **cosine** inputs at $I_d^*(s)$ and $I_q^*(s)$:

$$i_d^*(t) = |I_d^*| \cdot \sin(\omega_1 t) \quad \rightarrow \quad I_d^*(s) = \frac{\omega_1}{s^2 + \omega_1^2} |I_d^*| \tag{83}$$

$$i_q^*(t) = |I_q^*| \cdot \cos(\omega_1 t) \quad \rightarrow \quad I_q^*(s) = \frac{s}{s^2 + \omega_1^2} |I_q^*| \tag{84}$$

Then, combining these last two expressions in 's' domain, with the power circuit model equations, the closed loop expressions of the currents can be obtained:

$$I_\alpha(s) = \left(\frac{(s^2 + \omega^2) \cdot D_\alpha(s)}{A(s)}\right) I_d^*(s) - \left(\frac{(s^2 + \omega^2) \cdot Q_\alpha(s)}{A(s)}\right) I_q^*(s) + \left(\frac{(-\omega L)s^2 + (k_i \omega - \omega^3 L)}{A(s)}\right) I_\beta(s) \tag{85}$$

$$I_\beta(s) = \left(\frac{(s^2 + \omega^2) \cdot D_\beta(s)}{A(s)} \right) I_d^*(s) + \left(\frac{(s^2 + \omega^2) \cdot Q_\beta(s)}{A(s)} \right) I_q^*(s) - \left(\frac{(-\omega L)s^2 + (k_i \omega - \omega^3 L)}{A(s)} \right) I_\alpha(s) \quad (86)$$

With:

$$D_\alpha(s) = \left(\frac{s^2 + \omega_1^2}{\omega_1} \right) \left[\left(\frac{k_p}{2} \right) \left(\frac{\omega_1 + \omega}{s^2 + (\omega_1 + \omega)^2} + \frac{\omega_1 - \omega}{s^2 + (\omega_1 - \omega)^2} \right) - \left(\frac{k_i}{2\omega_1} \right) \left(\frac{s}{s^2 + (\omega_1 + \omega)^2} + \frac{s}{s^2 + (\omega_1 - \omega)^2} \right) + \left(\frac{k_i}{\omega_1} \right) \left(\frac{s}{s^2 + \omega^2} \right) \right] \quad (87)$$

$$Q_\alpha(s) = \left(\frac{k_p}{2} \right) \left(\frac{s^2 + \omega_1^2}{s} \right) \left(\frac{\omega_1 + \omega}{s^2 + (\omega_1 + \omega)^2} - \frac{\omega_1 - \omega}{s^2 + (\omega_1 - \omega)^2} \right) + \left(\frac{k_i}{2\omega_1} \right) \left(\frac{s^2 + \omega_1^2}{s} \right) \left(\frac{s}{s^2 + (\omega_1 - \omega)^2} - \frac{s}{s^2 + (\omega_1 + \omega)^2} \right) \quad (88)$$

And

$$D_\beta(s) = \left(\frac{s^2 + \omega_1^2}{\omega_1} \right) \left[\left(\frac{k_i}{\omega_1} \right) \left(\frac{\omega}{s^2 + \omega^2} \right) + \left(\frac{k_p}{2} \right) \left(-\frac{s}{s^2 + (\omega_1 + \omega)^2} + \frac{s}{s^2 + (\omega_1 - \omega)^2} \right) - \left(\frac{k_i}{2\omega_1} \right) \left(\frac{\omega_1 + \omega}{s^2 + (\omega_1 + \omega)^2} - \frac{\omega_1 - \omega}{s^2 + (\omega_1 - \omega)^2} \right) \right] \quad (89)$$

$$Q_\beta(s) = \left(\frac{s^2 + \omega_1^2}{s} \right) \left[\left(\frac{k_p}{2} \right) \left(\frac{s}{s^2 + (\omega_1 + \omega)^2} + \frac{s}{s^2 + (\omega_1 - \omega)^2} \right) + \left(\frac{k_i}{2\omega_1} \right) \left(\frac{\omega_1 + \omega}{s^2 + (\omega_1 + \omega)^2} + \frac{\omega_1 - \omega}{s^2 + (\omega_1 - \omega)^2} \right) \right] \quad (90)$$

Being again, these expressions only valid for a **sine** and **cosine** inputs at $I_d^*(s)$ and $I_q^*(s)$. By representing these expressions in a more compact form:

$$I_\alpha(s) = G_{\alpha d_s} I_d^*(s) + G_{\alpha q_s} I_q^*(s) + G_{\alpha \beta_s} I_\beta(s) \quad (91)$$

$$I_\beta(s) = G_{\beta d_s} I_d^*(s) + G_{\beta q_s} I_q^*(s) + G_{\beta \alpha_s} I_\alpha(s) \quad (92)$$

It is seen that there is again a coupling between two output currents that influence one in the other. Repeating again the same procedure applied in the previous chapter, the decoupled input-output transfer functions are obtained:

$$I_\alpha(s) = \left(\frac{G_{\alpha d_s}(s) + G_{\beta d_s}(s)G_{\alpha \beta_s}(s)}{1 - G_{\alpha \beta_s}(s)G_{\beta \alpha_s}(s)} \right) I_d^*(s) + \left(\frac{G_{\alpha q_s}(s) + G_{\beta q_s}(s)G_{\alpha \beta_s}(s)}{1 - G_{\alpha \beta_s}(s)G_{\beta \alpha_s}(s)} \right) I_q^*(s) \quad (93)$$

$$I_\beta(s) = \left(\frac{G_{\beta d_s}(s) + G_{\alpha d_s}(s)G_{\beta \alpha_s}(s)}{1 - G_{\alpha \beta_s}(s)G_{\beta \alpha_s}(s)} \right) I_d^*(s) + \left(\frac{G_{\beta q_s}(s) + G_{\alpha q_s}(s)G_{\beta \alpha_s}(s)}{1 - G_{\alpha \beta_s}(s)G_{\beta \alpha_s}(s)} \right) I_q^*(s) \quad (94)$$

The decoupled transfer functions are graphically represented in block diagrams in next figure:

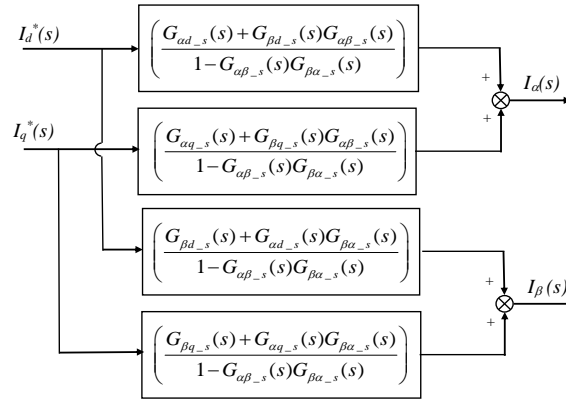


Figure 19. Equivalent block diagram of the currents control in dq with cancellation of current coupling.

By solving $I_\alpha(s)$ expressions using a symbolic Toolbox from Matlab for instance, it is possible to obtain for d input current:

$$\frac{G_{ad-s}(s) + G_{\beta d-s}(s)G_{\alpha\beta-s}(s)}{1 - G_{\alpha\beta-s}(s)G_{\beta\alpha-s}(s)} = \frac{g_{nd7} \cdot s^7 + g_{nd6} \cdot s^6 + g_{nd5} \cdot s^5 + g_{nd4} \cdot s^4 + g_{nd3} \cdot s^3 + g_{nd2} \cdot s^2 + g_{nd1} \cdot s + g_{nd0}}{g_8 \cdot s^8 + g_7 \cdot s^7 + g_7 \cdot s^7 + g_6 \cdot s^6 + g_5 \cdot s^5 + g_4 \cdot s^4 + g_3 \cdot s^3 + g_2 \cdot s^2 + g_1 \cdot s + g_0} \quad (95)$$

Being each coefficient of the numerator of the resulting transfer function:

$$\begin{aligned} g_{nd7} &= L \cdot k_p \\ g_{nd6} &= k_p^2 + R \cdot k_p + L \cdot k_i \\ g_{nd5} &= -2 \cdot L \cdot k_p \cdot \omega^2 + 2 \cdot L \cdot k_p \cdot \omega_1^2 + R \cdot k_i + 2 \cdot k_i \cdot k_p \\ g_{nd4} &= k_i^2 - 6 \cdot L \cdot k_i \cdot \omega^2 - 2 \cdot L \cdot k_i \cdot \omega_1^2 + 2 \cdot k_p^2 \cdot \omega_1^2 + 2 \cdot R \cdot k_p \cdot \omega_1^2 \\ g_{nd3} &= 4 \cdot k_i \cdot k_p \cdot \omega_1^2 - 2 \cdot k_i \cdot k_p \cdot \omega^2 + 3 \cdot L \cdot k_p \cdot \omega^4 + L \cdot k_p \cdot \omega_1^4 - 3 \cdot R \cdot k_i \cdot \omega^2 + 2 \cdot R \cdot k_i \cdot \omega_1^2 - L \cdot k_p \cdot \omega^2 \cdot \omega_1^2 \\ g_{nd2} &= -k_i^2 \cdot \omega^2 + 2 \cdot k_i^2 \cdot \omega_1^2 + L \cdot k_i \cdot \omega^4 - 7 \cdot L \cdot k_i \cdot \omega^2 \cdot \omega_1^2 + L \cdot k_i \cdot \omega_1^4 - k_p \cdot \omega^4 + k_p^2 \cdot \omega^2 \cdot \omega_1^2 + k_p^2 \cdot \omega_1^4 \\ &\quad - R \cdot k_p \cdot \omega^4 + R \cdot k_p \cdot \omega^2 \cdot \omega_1^2 + R \cdot k_p \cdot \omega_1^4 \\ g_{nd1} &= 2 \cdot k_i \cdot k_p \cdot \omega_1^4 + R \cdot k_i \cdot \omega_1^4 - 3 \cdot L \cdot k_p \cdot \omega^4 \cdot \omega_1^2 - 3 \cdot R \cdot k_i \cdot \omega^2 \cdot \omega_1^2 - 2 \cdot k_i \cdot k_p \cdot \omega^2 \cdot \omega_1^2 \\ g_{nd0} &= -k_i^2 \cdot \omega^2 \cdot \omega_1^2 + k_i^2 \cdot \omega_1^4 + L \cdot k_i \cdot \omega^4 \cdot \omega_1^2 - L \cdot k_i \cdot \omega^2 \cdot \omega_1^4 - k_p^2 \cdot \omega^4 \cdot \omega_1^2 + k_p^2 \cdot \omega^2 \cdot \omega_1^4 - R \cdot k_p \cdot \omega^4 \cdot \omega_1^2 + R \cdot k_p \cdot \omega^2 \cdot \omega_1^4 \end{aligned} \quad (96)$$

And the denominator:

$$\begin{aligned} g_8 &= L^2 \\ g_7 &= 2 \cdot L \cdot k_p + 2 \cdot L \cdot R \\ g_6 &= 4 \cdot L^2 \cdot \omega^2 + 2 \cdot L^2 \cdot \omega_1^2 + 2 \cdot k_i \cdot L + R^2 + 2 \cdot R \cdot k_p + k_p^2 \\ g_5 &= 2 \cdot R \cdot k_i + 2 \cdot k_p \cdot k_i + 6 \cdot L \cdot R \cdot \omega^2 + 4 \cdot L \cdot R \cdot \omega_1^2 + 6 \cdot L \cdot k_p \cdot \omega^2 + 4 \cdot L \cdot k_p \cdot \omega_1^2 \\ g_4 &= 6 \cdot L^2 \cdot \omega^4 + 2 \cdot L^2 \cdot \omega^2 \cdot \omega_1^2 + L^2 \cdot \omega_1^4 + 2 \cdot L \cdot k_i \cdot \omega^2 + 4 \cdot L \cdot k_i \cdot \omega_1^2 + 3 \cdot R \cdot \omega^2 + 2 \cdot R^2 \cdot \omega_1^2 + 6 \cdot R \cdot k_p \cdot \omega^2 \\ &\quad + 4 \cdot R \cdot k_p \cdot \omega_1^2 + k_i^2 + 3 \cdot k_p^2 \cdot \omega^2 + 2 \cdot k_p^2 \cdot \omega_1^2 \\ g_3 &= 4 \cdot k_p \cdot k_i \cdot \omega^2 + 4 \cdot k_p \cdot k_i \cdot \omega_1^2 + 6 \cdot L \cdot R \cdot \omega^4 + 2 \cdot L \cdot R \cdot \omega_1^4 + 6 \cdot L \cdot k_p \cdot \omega^4 + 2 \cdot L \cdot k_p \cdot \omega_1^4 + 4 \cdot R \cdot k_i \cdot \omega^2 + 4 \cdot R \cdot k_i \cdot \omega_1^2 \\ g_2 &= 4 \cdot L^2 \cdot \omega^6 - 2 \cdot L^2 \cdot \omega^4 \cdot \omega_1^2 + 2 \cdot L^2 \cdot \omega^2 \cdot \omega_1^4 - 2 \cdot L \cdot k_i \cdot \omega^4 - 8 \cdot L \cdot k_i \cdot \omega^2 \cdot \omega_1^2 + 2 \cdot L \cdot k_i \cdot \omega_1^4 + 3 \cdot R^2 \cdot \omega^4 \\ &\quad + R^2 \cdot \omega_1^4 + 6 \cdot R \cdot k_p \cdot \omega^4 + 2 \cdot R \cdot k_p \cdot \omega_1^4 + 2 \cdot k_i^2 \cdot \omega^2 + 2 \cdot k_i^2 \cdot \omega_1^2 + 3 \cdot k_p^2 \cdot \omega^4 + k_p^2 \cdot \omega_1^4 \\ g_1 &= 2 \cdot k_p \cdot k_i \cdot \omega^4 + 2 \cdot k_p \cdot k_i \cdot \omega_1^4 + 2 \cdot L \cdot R \cdot \omega^6 + 2 \cdot L \cdot k_p \cdot \omega^6 + 2 \cdot R \cdot k_i \cdot \omega^4 + 2 \cdot R \cdot k_i \cdot \omega_1^4 + 2 \cdot L \cdot R \cdot \omega^2 \cdot \omega_1^4 - 4 \cdot L \cdot R \cdot \omega^4 \cdot \omega_1^2 + 2 \cdot L \cdot k_p \cdot \omega^2 \cdot \omega_1^4 \\ &\quad - 4 \cdot L \cdot k_p \cdot \omega^4 \cdot \omega_1^2 - 4 \cdot R \cdot k_i \cdot \omega^2 \cdot \omega_1^2 - 4 \cdot k_p \cdot k_i \cdot \omega^2 \cdot \omega_1^2 \\ g_0 &= L^2 \cdot \omega^8 - 2 \cdot L^2 \cdot \omega^6 \cdot \omega_1^2 + L^2 \cdot \omega^4 \cdot \omega_1^4 - 2 \cdot L \cdot k_i \cdot \omega^6 + 4 \cdot L \cdot k_i \cdot \omega^4 \cdot \omega_1^2 - 2 \cdot L \cdot k_i \cdot \omega^2 \cdot \omega_1^4 + R^2 \cdot \omega^6 - 2 \cdot R^2 \cdot \omega^4 \cdot \omega_1^2 + R^2 \cdot \omega^2 \cdot \omega_1^4 + 2 \cdot R \cdot k_p \cdot \omega^6 \\ &\quad - 4 \cdot R \cdot k_p \cdot \omega^4 \cdot \omega_1^2 + 2 \cdot R \cdot k_p \cdot \omega^2 \cdot \omega_1^4 + k_i^2 \cdot \omega^4 - 2 \cdot k_i^2 \cdot \omega^2 \cdot \omega_1^2 + k_i^2 \cdot \omega_1^4 + k_p^2 \cdot \omega^6 - 2 \cdot k_p^2 \cdot \omega^4 \cdot \omega_1^2 + k_p^2 \cdot \omega^2 \cdot \omega_1^4 \end{aligned}$$

And for q input current:

$$\frac{G_{\alpha q-s}(s) + G_{\beta q-s}(s)G_{\alpha\beta-s}(s)}{1 - G_{\alpha\beta-s}(s)G_{\beta\alpha-s}(s)} = \frac{g_{nq7} \cdot s^7 + g_{nq6} \cdot s^6 + g_{nq5} \cdot s^5 + g_{nq4} \cdot s^4 + g_{nq3} \cdot s^3 + g_{nq2} \cdot s^2 + g_{nq1} \cdot s + g_{nq0}}{(g_8 \cdot s^8 + g_7 \cdot s^7 + g_6 \cdot s^6 + g_5 \cdot s^5 + g_4 \cdot s^4 + g_3 \cdot s^3 + g_2 \cdot s^2 + g_1 \cdot s + g_0) \cdot s} \quad (97)$$

Being the denominator's coefficients, g_1, g_2, \dots, g_8 equal to the previous expression. While the coefficients of the numerator are:

$$\begin{aligned} g_{nq7} &= -(2 \cdot L \cdot k_p) \cdot \omega \\ g_{nq6} &= -(k_p^2 + R \cdot k_p + 3 \cdot L \cdot k_i) \cdot \omega \\ g_{nq5} &= -(4 \cdot L \cdot k_p \cdot \omega^2 + 2 \cdot R \cdot k_i + 2 \cdot k_i \cdot k_p + 2 \cdot L \cdot k_p \cdot \omega_1^2) \cdot \omega \\ g_{nq4} &= -(k_i^2 + 2 \cdot k_p^2 \cdot \omega^2 + 2 \cdot R \cdot k_p \cdot \omega^2 + 2 \cdot L \cdot k_i \cdot \omega^2 + 4 \cdot L \cdot k_i \cdot \omega_1^2) \cdot \omega \\ g_{nq3} &= -(2 \cdot k_i \cdot k_p \cdot \omega^2 + 2 \cdot L \cdot k_p \cdot \omega^4 + 2 \cdot R \cdot k_i \cdot \omega_1^2 + 4 \cdot L \cdot k_p \cdot \omega^2 \cdot \omega_1^2) \cdot \omega \\ g_{nq2} &= -(k_i \cdot \omega^2 - L \cdot k_i \cdot \omega^4 + 3 \cdot L \cdot k_i \cdot \omega^2 \cdot \omega_1^2 + L \cdot k_i \cdot \omega_1^4 + k_p^2 \cdot \omega^4 + k_p^2 \cdot \omega^2 \cdot \omega_1^2 - k_p^2 \cdot \omega_1^4 + R \cdot k_p \cdot \omega^4 - R \cdot k_p \cdot \omega^2 \cdot \omega_1^2 - R \cdot k_p \cdot \omega_1^4) \cdot \omega \\ g_{nq1} &= -(2 \cdot k_i \cdot k_p \cdot \omega_1^4 + 2 \cdot L \cdot k_p \cdot \omega^4 \cdot \omega_1^2 + 2 \cdot R \cdot k_i \cdot \omega^2 \cdot \omega_1^2 + 2 \cdot k_i \cdot k_p \cdot \omega^2 \cdot \omega_1^2) \cdot \omega \\ g_{nq0} &= -(k_i \cdot k_p \cdot \omega^2 \cdot \omega_1^2 - k_i \cdot \omega_1^4 - L \cdot k_i \cdot \omega^4 \cdot \omega_1^2 + L \cdot k_i \cdot \omega^2 \cdot \omega_1^4 + k_p \cdot \omega^4 \cdot \omega_1^2 + k_p \cdot \omega^2 \cdot \omega_1^4 + R \cdot k_p \cdot \omega^2 \cdot \omega_1^4) \cdot \omega \end{aligned} \quad (98)$$

For current $I_\beta(s)$ the same procedure can be followed and an equivalent expression can be obtained. For simplicity here, it is not shown. Thus, in next Figure 20, the poles and zeros of the system are shown, after numerically substituting the same numerical example used in previous chapter. It is seen again that two complex conjugate pole pairs, with real parts (σ of the exponential terms) of -217 and -288 appear and with imaginary parts $\omega_i=314.159\text{rd/s}$. Then, there are two more pair of conjugate imaginary poles, without real part and with imaginary parts $\omega_i=\omega_l+\omega=1884.9\text{rd/s}$ and $\omega_i=\omega_l-\omega=1256.6\text{rd/s}$, which are the components that create the steady-state current. Note also that there is a conjugate zero pair with imaginary part ω_l in both transfer functions, that is cancelled with the sinus and cosines inputs' poles with imaginary part ω_l .

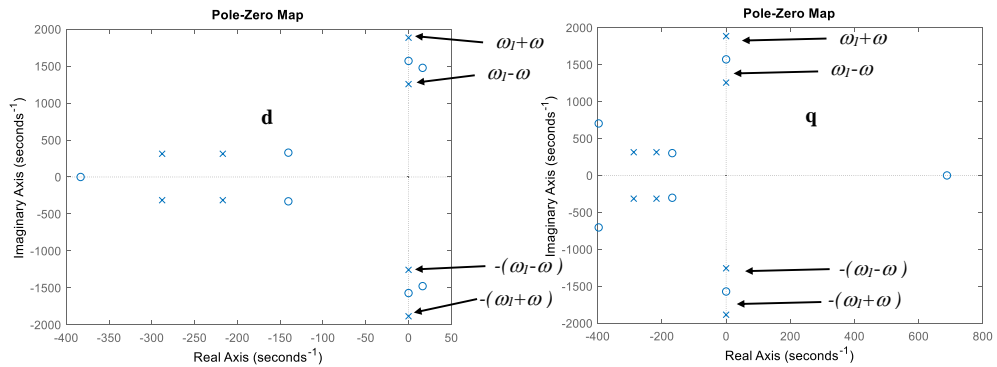


Figure 20. Poles of transfer function of expression (93), for the dq control of currents with sinusoidal current references. Conditions of Appendix E.

Once the transfer functions have been obtained, it is possible to derive the output current expressions. Hence, substituting a sine and cosine inputs at $I_d^*(s)$ and $I_q^*(s)$. The output α current is given by:

$$I_\alpha(s) = \left(\frac{G_{ad-s}(s) + G_{\beta d-s}(s)G_{\alpha\beta-s}(s)}{1 - G_{\alpha\beta-s}(s)G_{\beta\alpha-s}(s)} \right) \left[\frac{\omega_1}{s^2 + \omega_1^2} |I_d^*| \right] + \left(\frac{G_{\alpha q-s}(s) + G_{\beta q-s}(s)G_{\alpha\beta-s}(s)}{1 - G_{\alpha\beta-s}(s)G_{\beta\alpha-s}(s)} \right) \left[\frac{s}{s^2 + \omega_1^2} |I_q^*| \right] \quad (99)$$

What is equal to:

$$I_\alpha(s) = \left(\frac{g_{nd5-} \cdot s^5 + g_{nd4-} \cdot s^4 + g_{nd3-} \cdot s^3 + g_{nd2-} \cdot s^2 + g_{nd1-} \cdot s + g_{nd0-}}{g_8 \cdot s^8 + g_7 \cdot s^7 + g_6 \cdot s^6 + g_5 \cdot s^5 + g_4 \cdot s^4 + g_3 \cdot s^3 + g_2 \cdot s^2 + g_1 \cdot s + g_0} \right) |I_d^*| + \left(\frac{g_{nq5-} \cdot s^5 + g_{nq4-} \cdot s^4 + g_{nq3-} \cdot s^3 + g_{nq2-} \cdot s^2 + g_{nq1-} \cdot s + g_{nq0-}}{g_8 \cdot s^8 + g_7 \cdot s^7 + g_6 \cdot s^6 + g_5 \cdot s^5 + g_4 \cdot s^4 + g_3 \cdot s^3 + g_2 \cdot s^2 + g_1 \cdot s + g_0} \right) |I_q^*| \quad (100)$$

With coefficients of the numerator corresponding to the d input:

$$\begin{aligned} g_{nd5-} &= L \cdot k_p \cdot \omega_1 \\ g_{nd4-} &= \omega_1 \cdot k_p^2 + R \cdot \omega_1 \cdot k_p + L \cdot k_i \cdot \omega_1 \\ g_{nd3-} &= R \cdot k_i \cdot \omega_1 + 2 \cdot k_i \cdot k_p \cdot \omega_1 + L \cdot k_p \cdot \omega_1^3 - 2 \cdot L \cdot k_p \cdot \omega^2 \cdot \omega_1 \\ g_{nd2-} &= k_i^2 \cdot \omega_1 - 6 \cdot L \cdot k_i \cdot \omega^2 \cdot \omega_1 + L \cdot k_i \cdot \omega_1^3 + k_p^2 \cdot \omega_1^3 + R \cdot \omega_1^3 \cdot k_p \\ g_{nd1-} &= 2 \cdot k_i \cdot k_p \cdot \omega_1^3 + R \cdot k_i \cdot \omega_1^3 - 3 \cdot L \cdot k_p \cdot \omega^4 \cdot \omega_1 - 3 \cdot R \cdot k_i \cdot \omega^2 \cdot \omega_1 - 2 \cdot k_i \cdot k_p \cdot \omega^2 \cdot \omega_1 + L \cdot k_p \cdot \omega^2 \cdot \omega_1^3 \\ g_{nd0-} &= -k_i^2 \cdot \omega^2 \cdot \omega_1 + k_i^2 \cdot \omega_1^3 + L \cdot k_i \cdot \omega^4 \cdot \omega_1 - L \cdot k_i \cdot \omega^2 \cdot \omega_1^3 - k_p^2 \cdot \omega^4 \cdot \omega_1 + k_p^2 \cdot \omega^2 \cdot \omega_1^3 - R \cdot k_p \cdot \omega^4 \cdot \omega_1 + R \cdot k_p \cdot \omega^2 \cdot \omega_1^3 \end{aligned} \quad (101)$$

Being obviously the denominator's coefficients, g_1, g_2, \dots, g_8 equal to the previous expressions of transfer functions (93) and (94). While for the q component, the coefficients of the numerator are symbolically represented by:

$$\begin{aligned} g_{nq5-} &= -2 \cdot L \cdot k_p \cdot \omega \\ g_{nq4-} &= -\omega \cdot k_p^2 - R \cdot \omega \cdot k_p - 3 \cdot L \cdot k_i \cdot \omega \\ g_{nq3-} &= -2 \cdot R \cdot k_i \cdot \omega - 2 \cdot k_i \cdot k_p \cdot \omega - 4 \cdot L \cdot k_p \cdot \omega^3 \\ g_{nq2-} &= -k_i^2 \cdot \omega - 2 \cdot L \cdot k_i \cdot \omega^3 \cdot \omega_1 - L \cdot k_i \cdot \omega \cdot \omega_1^2 - 2 \cdot k_p^2 \cdot \omega^3 - 2 \cdot R \cdot \omega^3 \cdot k_p + k_p^2 \cdot \omega \cdot \omega_1^2 + R \cdot k_p \cdot \omega \cdot \omega_1^2 \\ g_{nq1-} &= 2 \cdot k_i \cdot k_p \cdot \omega \cdot \omega_1^2 - 2 \cdot L \cdot k_p \cdot \omega^5 - 2 \cdot R \cdot k_i \cdot \omega^3 - 2 \cdot k_i \cdot k_p \cdot \omega^3 \\ g_{nq0-} &= k_i^2 \cdot \omega \cdot \omega_1^2 - k_i^2 \cdot \omega^3 - L \cdot k_i \cdot \omega^3 \cdot \omega_1^2 + L \cdot k_i \cdot \omega^5 - k_p^2 \cdot \omega^5 + k_p^2 \cdot \omega^3 \cdot \omega_1^2 - R \cdot k_p \cdot \omega^5 + R \cdot k_p \cdot \omega^3 \cdot \omega_1^2 \end{aligned} \quad (102)$$

Finally, by using a partial fraction expansion and applying the inverse Laplace transform, the time domain expression for step inputs of the output current can be obtained from equation (100). Being the time response of the complete final expressions (only $i_\alpha(t)$ current is shown, $i_\beta(t)$ would present an equivalent form):

$$\begin{aligned} i_\alpha(t) &= \left[(2 \cdot B_0) \cdot \cos((\omega_1 + \omega) \cdot t + \arg B_0) + (2 \cdot B_1) \cdot \cos((\omega_1 - \omega) \cdot t + \arg B_1) \right. \\ &\quad \left. + (2 \cdot B_2) \cdot e^{\sigma_2 t} \cdot \cos(\omega_{d2} \cdot t + \arg B_2) + (2 \cdot B_3) \cdot e^{\sigma_3 t} \cdot \cos(\omega_{d3} \cdot t + \arg B_3) \right] |I_d^*| \\ &\quad + \left[(2 \cdot B_4) \cdot \cos((\omega_1 + \omega) \cdot t + \arg B_4) + (2 \cdot B_5) \cdot \cos((\omega_1 - \omega) \cdot t + \arg B_5) \right. \\ &\quad \left. + (2 \cdot B_6) \cdot e^{\sigma_6 t} \cdot \cos(\omega_{d6} \cdot t + \arg B_6) + (2 \cdot B_7) \cdot e^{\sigma_7 t} \cdot \cos(\omega_{d7} \cdot t + \arg B_7) \right] |I_q^*| \end{aligned} \quad (103)$$

To conclude, Table IV shows a numerical example for the previous time domain expression.

Table IV. Numerical solution of expression (103) calculated by using the ‘residue’ function from Matlab Control Toolbox. Conditions of Appendix E.

d	q
$B_0 = 7.70087020305e-02$ $argB_0 = -2.9031908834e+00$ $\omega_1 + \omega = 1.88495559e+03$	$B_4 = 7.700870203052385e-02$ $argB_4 = 2.3840177014250e-01$ $\omega_1 + \omega = 1.8849555921e+03$
$B_1 = 7.700870203052350e-02$ $argB_1 = -2.903190883447285e+00$ $\omega_1 - \omega = 1.25663706143e+03$	$B_5 = 7.700870203052385e-02$ $argB_5 = -2.90319088344e+00$ $\omega_1 - \omega = 1.2566370614e+03$
$B_2 = 3.476903109250930e-01$ $argB_2 = 0$ $\sigma_2 = -2.879436171968e+02$ $\omega_{i2} = 3.141592653589806e+02$	$B_6 = 6.373531952189007e-02$ $argB_6 = -1.570796326794e+00$ $\sigma_6 = -2.87943617196e+02$ $\omega_{i6} = 3.141592653589806e+02$
$B_3 = 1.980290369248264e-01$ $argB_3 = -3.141592653589774e+00$ $\sigma_3 = -2.170563828031060e+02$ $\omega_{i3} = 3.141592653589793e+02$	$B_7 = 2.736412462371267e-02$ $argB_7 = 1.570796326794917e+00$ $\sigma_7 = -2.170563828031e+02$ $\omega_{i7} = 3.141592653589e+02$

Therefore, it is inferred that the transient response or damped terms, oscillate at $\omega_i = 314.159 \text{rd/s}$ (poles with real parts of -217 and -288), while the steady-state (poles without real parts) oscillate at $\omega_1 + \omega = 1884.9 \text{rd/s}$ and $\omega_1 - \omega = 1256.6 \text{rd/s}$.

3.5. Bode Diagram

Once the transfer functions for sine and cosine inputs are obtained, from them it is possible to derive the expressions for the Bode diagram. Hence, from equation (93), for simplicity in the exposition, let us assume that the input $I_q^*(s)$ is zero, what means that we only apply a sinusoidal input at $I_d^*(s)$:

$$I_\alpha(s) = \left(\frac{G_{\alpha d-s}(s) + G_{\beta d-s}(s)G_{\alpha\beta-s}(s)}{1 - G_{\alpha\beta-s}(s)G_{\beta\alpha-s}(s)} \right) I_d^*(s) \quad (104)$$

Therefore, after substituting the sinusoidal input at $I_d^*(s)$ the current yields:

$$\begin{aligned}
 I_{\alpha}(s) = & \left(\frac{\omega_1 + \omega}{s^2 + (\omega_1 + \omega)^2} \right) \left[\left(\frac{k_p}{2} - \frac{k_i \cdot s}{2\omega_1(\omega_1 + \omega)} \right) \left(\frac{(s^2 + \omega^2)A(s)}{A^2(s) + \omega^2(Ls^2 + (\omega^2L - k_i)^2)} \right) - \left(\frac{k_p}{2} \frac{s}{(\omega_1 + \omega)} + \frac{k_i}{2\omega_1} \right) \left(\frac{(s^2 + \omega^2)(\omega(-Ls^2 + (-\omega^2L + k_i)))}{A^2(s) + \omega^2(Ls^2 + (\omega^2L - k_i)^2)} \right) \right] |I_d^*| \\
 & + \left(\frac{\omega_1 - \omega}{s^2 + (\omega_1 - \omega)^2} \right) \left[\left(\frac{k_p}{2} - \frac{k_i \cdot s}{2\omega_1(\omega_1 - \omega)} \right) \left(\frac{(s^2 + \omega^2)A(s)}{A^2(s) + \omega^2(Ls^2 + (\omega^2L - k_i)^2)} \right) + \left(\frac{k_p}{2} \frac{s}{(\omega_1 - \omega)} + \frac{k_i}{2\omega_1} \right) \left(\frac{(s^2 + \omega^2)(\omega(-Ls^2 + (-\omega^2L + k_i)))}{A^2(s) + \omega^2(Ls^2 + (\omega^2L - k_i)^2)} \right) \right] |I_d^*| \quad (105) \\
 & + \left(\frac{(s^2 + \omega^2)A(s)}{A^2(s) + \omega^2(Ls^2 + (\omega^2L - k_i)^2)} \right) \left(\frac{k_i}{\omega_1} \frac{s}{(s^2 + \omega^2)} \right) |I_d^*| + \left(\frac{(s^2 + \omega^2)(\omega(-Ls^2 + (-\omega^2L + k_i)))}{A^2(s) + \omega^2(Ls^2 + (\omega^2L - k_i)^2)} \right) \left(\frac{k_i}{\omega_1} \frac{\omega}{(s^2 + \omega^2)} \right) |I_d^*|
 \end{aligned}$$

Analyzing this last expression, it is possible to see two dominant terms that contribute with two sinusoidal outputs at current $I_{\alpha}(s)$.

One sinusoidal term at $\omega + \omega_1$ frequency:

$$\left(\frac{\omega_1 + \omega}{s^2 + (\omega_1 + \omega)^2} \right) \left[\left(\frac{k_p}{2} - \frac{k_i \cdot s}{2\omega_1(\omega_1 + \omega)} \right) \left(\frac{(s^2 + \omega^2)A(s)}{A^2(s) + \omega^2(Ls^2 + (\omega^2L - k_i)^2)} \right) - \left(\frac{k_p}{2} \frac{s}{(\omega_1 + \omega)} + \frac{k_i}{2\omega_1} \right) \left(\frac{(s^2 + \omega^2)(\omega(-Ls^2 + (-\omega^2L + k_i)))}{A^2(s) + \omega^2(Ls^2 + (\omega^2L - k_i)^2)} \right) \right] |I_d^*| \quad (106)$$

One sinusoidal term at $\omega - \omega_1$ frequency:

$$\left(\frac{\omega_1 - \omega}{s^2 + (\omega_1 - \omega)^2} \right) \left[\left(\frac{k_p}{2} - \frac{k_i \cdot s}{2\omega_1(\omega_1 - \omega)} \right) \left(\frac{(s^2 + \omega^2)A(s)}{A^2(s) + \omega^2(Ls^2 + (\omega^2L - k_i)^2)} \right) + \left(\frac{k_p}{2} \frac{s}{(\omega_1 - \omega)} + \frac{k_i}{2\omega_1} \right) \left(\frac{(s^2 + \omega^2)(\omega(-Ls^2 + (-\omega^2L + k_i)))}{A^2(s) + \omega^2(Ls^2 + (\omega^2L - k_i)^2)} \right) \right] |I_d^*| \quad (107)$$

And two more terms that are a sum of exponential terms in time domain and therefore are made zero at steady-state if the system is stable:

$$\left(\frac{A(s) \left(\frac{sk_i}{\omega_1} \right)}{A^2(s) + \omega^2(Ls^2 + (\omega^2L - k_i)^2)} \right) |I_d^*| + \left(\frac{\omega^2(-Ls^2 + (-\omega^2L + k_i)) \left(\frac{k_i}{\omega_1} \right)}{A^2(s) + \omega^2(Ls^2 + (\omega^2L - k_i)^2)} \right) |I_d^*| \quad (108)$$

Consequently, these last two terms do not contribute to the steady-state, therefore, neither to the Bode diagram. Thus, to calculate the Bode diagram in a classic way [16], it is necessary to substitute the required frequency at which the output is wanted to be considered in the following expressions:

$$\begin{aligned}
 s = j(\omega_1 + \omega) \rightarrow & \left[\left(\frac{k_p}{2} - \frac{k_i \cdot s}{2\omega_1(\omega_1 + \omega)} \right) \left(\frac{(s^2 + \omega^2)A(s)}{A^2(s) + \omega^2(Ls^2 + (\omega^2L - k_i)^2)} \right) - \left(\frac{k_p}{2} \frac{s}{(\omega_1 + \omega)} + \frac{k_i}{2\omega_1} \right) \left(\frac{(s^2 + \omega^2)(\omega(-Ls^2 + (-\omega^2L + k_i)))}{A^2(s) + \omega^2(Ls^2 + (\omega^2L - k_i)^2)} \right) \right] |I_d^*| \\
 s = j(\omega_1 - \omega) \rightarrow & \left[\left(\frac{k_p}{2} - \frac{k_i \cdot s}{2\omega_1(\omega_1 - \omega)} \right) \left(\frac{(s^2 + \omega^2)A(s)}{A^2(s) + \omega^2(Ls^2 + (\omega^2L - k_i)^2)} \right) + \left(\frac{k_p}{2} \frac{s}{(\omega_1 - \omega)} + \frac{k_i}{2\omega_1} \right) \left(\frac{(s^2 + \omega^2)(\omega(-Ls^2 + (-\omega^2L + k_i)))}{A^2(s) + \omega^2(Ls^2 + (\omega^2L - k_i)^2)} \right) \right] |I_d^*| \quad (109)
 \end{aligned}$$

What means that the two sinusoidal output currents at steady-state, can be evaluated in terms of amplitude and phase by applying for instance the Bode function from Matlab of previous expressions. Numerically, this means that for instance by choosing:

$$i_d^*(t) = |I_d^*| \cdot \sin(\omega_l t) \quad \rightarrow \quad i_d^*(t) = 1 \cdot \sin(250 \cdot 2 \cdot \pi \cdot t) \quad (110)$$

$$i_q^*(t) = 0 \quad (111)$$

At the output current $i_d(t)$, we obtain 0.154A at 200Hz and 0.154A at 300Hz, which corresponds with -16.2dB at both frequencies as noticed in next Figure 21. Note that at both output frequencies $\omega + \omega_l$ and $\omega - \omega_l$, this control in dq reference frame with cancellation of coupling terms, curiously obtains the same amplitudes at the output current. It is important to notice the fact that at the Bode itself, the ω_l frequency also appears.

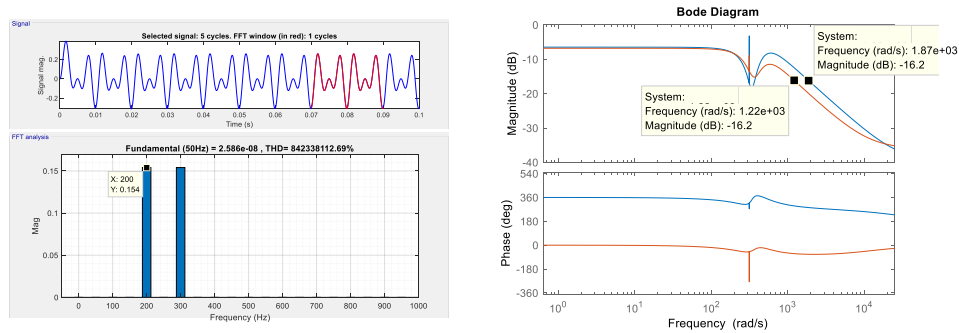


Figure 21. Time domain and Bode correspondence of currents expressed in $\alpha\beta$ reference frame, of dq control of currents with cancellation of coupling terms. Conditions of Appendix E and:

$$i_d^*(t) = 1 \cdot \sin(250 \cdot 2 \cdot \pi \cdot t), \quad i_q^*(t) = 0.$$

On the other hand, if we now evaluate the time domain response and Bode diagram in synchronous rotating dq reference frame, as can be seen in Figure 22, $i_d(t)$ oscillates at ω_l frequency, with an amplitude of 0.308A. This value corresponds with -10.22dB, which is exactly the gain given by the Bode diagram at ω_l frequency.

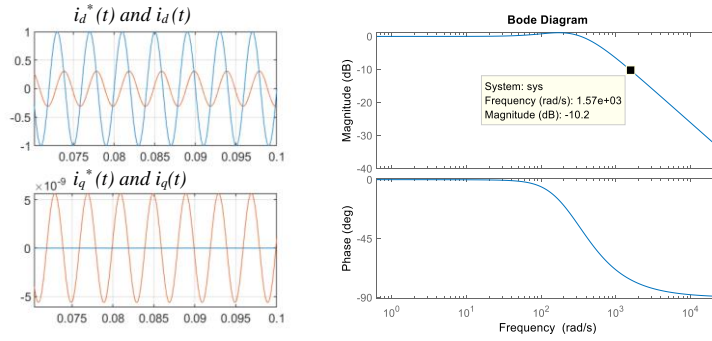


Figure 22. Time domain responses of $i_d(t)$ and $i_q(t)$ and Bode correspondence in currents expressed in a synchronous rotating dq reference frame. Conditions of Appendix E and:

$$i_d^*(t) = 1 \cdot \sin(250 \cdot 2 \cdot \pi \cdot t), \quad i_q^*(t) = 0$$

If we compare both time domain responses in synchronous rotating dq reference frame and stationary $\alpha\beta$ reference frame, we see that the amplitude of the obtained two outputs at $\omega_r + \omega$ and $\omega_r - \omega$, is 0.154A in $\alpha\beta$, while the output obtained at ω_r is 0.308A in dq , is just the double. What means that the amplitude of the oscillating current in dq , is divided equally into two oscillating currents in $\alpha\beta$. This fact is schematically represented in Table V.

Table V. Comparison of output currents in synchronous rotating dq reference frame and stationary $\alpha\beta$ reference frame

input	Output in dq reference frame	Output in $\alpha\beta$ reference frame
$i_d^*(t) = 1 \cdot \sin(250 \cdot 2 \cdot \pi \cdot t)$	$i_d(t)$:	$i_\alpha(t)$:
$i_q^*(t) = 0$	ω_r and 0.308 A amplitude	$\omega_r + \omega$ and 0.308/2 A amplitude + $\omega_r - \omega$ and 0.308/2 A amplitude

Chapter 4.

Control of currents in rotating reference frame (dq control) without cancellation of coupling terms

The control block diagram studied in this chapter is depicted in Figure 23, [6]-[7]. It is exactly the same control strategy as presented in previous chapter, but in this case, the unique difference is that the cancellation of the current coupling terms is not carried out.

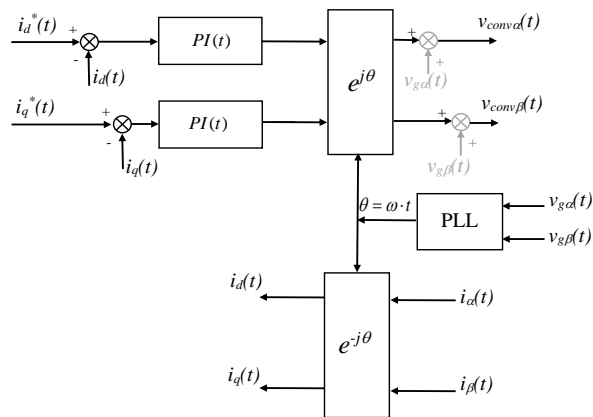


Figure 23. Current control block diagram in rotating reference frame (dq) with two PI controllers and no cancellation of current coupling terms.

This control block diagram, can be represented as an equivalent 'black box' either in time domain and also in 's' domain, as shown in Figure 24.

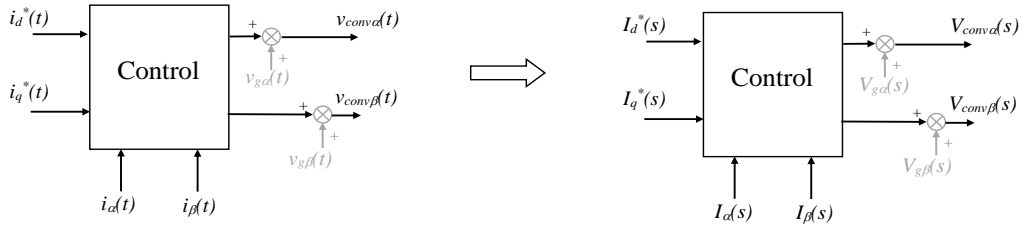


Figure 24. Current control blocks in time and 's' domains.

The α and β components of the converter voltages, considering the grid voltage feedforward terms, are mathematically represented in time domain as follows (Note that the harmonics created by the converter are neglected):

$$v_{conv\alpha}(t) = \left(\left[i_d^*(t) - i_d(t) \right] \otimes PI(t) \right) \cdot \cos(\omega t) - \left(\left[i_q^*(t) - i_q(t) \right] \otimes PI(t) \right) \cdot \sin(\omega t) + v_{g\alpha}(t) \quad (112)$$

$$v_{conv\beta}(t) = \left(\left[i_d^*(t) - i_d(t) \right] \otimes PI(t) \right) \cdot \sin(\omega t) - \left(\left[i_q^*(t) - i_q(t) \right] \otimes PI(t) \right) \cdot \cos(\omega t) + v_{g\beta}(t) \quad (113)$$

Which is equal to:

$$\begin{aligned} v_{conv\alpha}(t) = & \left(\left[i_d^*(t) - (i_\alpha(t) \cdot \cos(\omega t) + i_\beta(t) \cdot \sin(\omega t)) \right] \otimes PI(t) \right) \cdot \cos(\omega t) \\ & - \left(\left[i_q^*(t) - (-i_\alpha(t) \cdot \sin(\omega t) + i_\beta(t) \cdot \cos(\omega t)) \right] \otimes PI(t) \right) \cdot \sin(\omega t) \\ & + v_{g\alpha}(t) \end{aligned} \quad (114)$$

$$\begin{aligned} v_{conv\beta}(t) = & \left(\left[i_d^*(t) - (i_\alpha(t) \cdot \cos(\omega t) + i_\beta(t) \cdot \sin(\omega t)) \right] \otimes PI(t) \right) \cdot \sin(\omega t) \\ & - \left(\left[i_q^*(t) - (-i_\alpha(t) \cdot \sin(\omega t) + i_\beta(t) \cdot \cos(\omega t)) \right] \otimes PI(t) \right) \cdot \cos(\omega t) \\ & + v_{g\beta}(t) \end{aligned} \quad (115)$$

4.1. Mathematical model in $\alpha\beta$ with a step input

Considering **step** inputs at at both $I_d^*(s)$ and $I_q^*(s)$ and assuming that the grid voltage is ideal and not perturbed, i.e., assuming no angle jumps and ω constant, the previous time domain expressions can be transformed into the 's' domain as follows (see appendix C omitting the coupling terms cancellation):

$$\begin{aligned}
 V_{conv\alpha}(s) = & -\left(k_p + \frac{k_i s}{s^2 + \omega^2}\right) I_\alpha(s) + \left(\frac{\omega k_i}{s^2 + \omega^2}\right) I_\beta(s) \\
 & + \left(\frac{k_p s^2}{s^2 + \omega^2} + \frac{k_i s(s^2 - \omega^2)}{(s^2 + \omega^2)^2}\right) I_d^*(s) - \left(\frac{k_p \omega s}{s^2 + \omega^2} - \frac{2\omega k_i s^2}{(s^2 + \omega^2)^2}\right) I_q^*(s) + V_{g\alpha}(s)
 \end{aligned} \tag{116}$$

$$\begin{aligned}
 V_{conv\beta}(s) = & -\left(\frac{\omega k_i}{s^2 + \omega^2}\right) I_\alpha(s) - \left(k_p + \frac{k_i s}{s^2 + \omega^2}\right) I_\beta(s) \\
 & + \left(\frac{k_p \omega s}{s^2 + \omega^2} - \frac{2\omega k_i s^2}{(s^2 + \omega^2)^2}\right) I_d^*(s) + \left(\frac{k_p s^2}{s^2 + \omega^2} + \frac{k_i s(s^2 - \omega^2)}{(s^2 + \omega^2)^2}\right) I_q^*(s) + V_{g\beta}(s)
 \end{aligned} \tag{117}$$

Being these expressions only valid for a step input at both $I_d^*(s)$ and $I_q^*(s)$:

$$I_d^*(s) = \frac{|I_d^*|}{s} \qquad I_q^*(s) = \frac{|I_q^*|}{s} \tag{118}$$

As done in previous chapter, combining the last two control law expressions with the power circuit electric expressions, it is possible to derive the closed loop equation for both α and β currents:

$$I_\alpha(s) = \left(k_p s + \frac{k_i(s^2 - \omega^2)}{s^2 + \omega^2}\right) \left(\frac{s}{A(s)}\right) I_d^*(s) - \left(k_p + \frac{2k_i s}{s^2 + \omega^2}\right) \left(\frac{\omega s}{A(s)}\right) I_q^*(s) + \left(\frac{k_i \omega}{A(s)}\right) I_\beta(s) \tag{119}$$

$$I_\beta(s) = \left(k_p + \frac{2k_i s}{s^2 + \omega^2}\right) \left(\frac{\omega s}{A(s)}\right) I_d^*(s) + \left(k_p s + \frac{k_i(s^2 - \omega^2)}{s^2 + \omega^2}\right) \left(\frac{s}{A(s)}\right) I_q^*(s) - \left(\frac{k_i \omega}{A(s)}\right) I_\alpha(s) \tag{120}$$

Being again:

$$A(s) = Ls^3 + (k_p + R)s^2 + (L\omega^2 + k_i)s + (k_p + R)\omega^2 \tag{121}$$

Thus now substituting in both inputs a step, the output currents yields:

$$I_\alpha(s) = \left(\frac{k_p s^3 + k_i s^2 + k_p \omega^2 s - k_i \omega^2}{(s^2 + \omega^2)A(s)}\right) |I_d^*| - \left(\frac{k_p \omega s^2 + 2k_i \omega s + k_p \omega^3}{(s^2 + \omega^2)A(s)}\right) |I_q^*| + \left(\frac{k_i \omega}{A(s)}\right) I_\beta(s) \tag{122}$$

$$I_\beta(s) = \left(\frac{k_p \omega s^2 + 2k_i \omega s + k_p \omega^3}{(s^2 + \omega^2)A(s)}\right) |I_d^*| + \left(\frac{k_p s^3 + k_i s^2 + k_p \omega^2 s - k_i \omega^2}{(s^2 + \omega^2)A(s)}\right) |I_q^*| - \left(\frac{k_i \omega}{A(s)}\right) I_\alpha(s) \tag{123}$$

Which is equal to:

$$\begin{aligned}
 I_\alpha(s) = & \left(\frac{k_p s^3 + k_i s^2 + k_p \omega^2 s - k_i \omega^2}{Ls^5 + (k_p + R)s^4 + (2L\omega^2 + k_i)s^3 + 2\omega^2(k_p + R)s^2 + (L\omega^2 + k_i)\omega^2 s + \omega^4(k_p + R)} \right) |I_d^*| \\
 & - \left(\frac{k_p \omega s^2 + 2k_i \omega s + k_p \omega^3}{Ls^5 + (k_p + R)s^4 + (2L\omega^2 + k_i)s^3 + 2\omega^2(k_p + R)s^2 + (L\omega^2 + k_i)\omega^2 s + \omega^4(k_p + R)} \right) |I_q^*| \\
 & + \left(\frac{k_i \omega}{Ls^3 + (k_p + R)s^2 + (L\omega^2 + k_i)s + (k_p + R)\omega^2} \right) I_\beta(s)
 \end{aligned} \tag{124}$$

$$\begin{aligned}
 I_\beta(s) = & \left(\frac{k_p \omega s^2 + 2k_i \omega s + k_p \omega^3}{Ls^5 + (k_p + R)s^4 + (2L\omega^2 + k_i)s^3 + 2\omega^2(k_p + R)s^2 + (L\omega^2 + k_i)\omega^2 s + \omega^4(k_p + R)} \right) |I_d^*| \\
 & + \left(\frac{k_p s^3 + k_i s^2 + k_p \omega^2 s - k_i \omega^2}{Ls^5 + (k_p + R)s^4 + (2L\omega^2 + k_i)s^3 + 2\omega^2(k_p + R)s^2 + (L\omega^2 + k_i)\omega^2 s + \omega^4(k_p + R)} \right) |I_q^*| \\
 & - \left(\frac{k_i \omega}{Ls^3 + (k_p + R)s^2 + (L\omega^2 + k_i)s + (k_p + R)\omega^2} \right) I_\alpha(s)
 \end{aligned} \tag{125}$$

As can be noticed from the previous expressions and as occurred in previous chapter when the current coupling terms were cancelled, there is a coupling between α and β . What means that $I_\alpha(s)$ depends on $I_\beta(s)$ and vice versa. This coupling, can be represented graphically as in Figure 25.

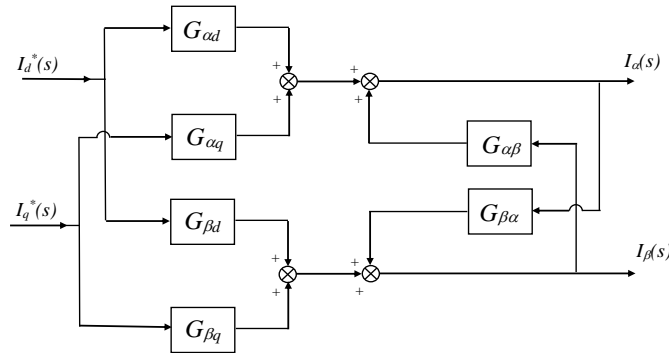


Figure 25. Block diagram of the control of currents in *dq* with cancellation of coupling terms.

Seeking to eliminate this coupling, we rename the expressions (122) and (123) as follows:

$$I_\alpha(s) = G_{ad}I_d^*(s) + G_{\alpha q}I_q^*(s) + G_{\alpha\beta}I_\beta(s) \tag{126}$$

$$I_\beta(s) = G_{\beta d}I_d^*(s) + G_{\beta q}I_q^*(s) + G_{\beta\alpha}I_\alpha(s) \tag{127}$$

Combining these two expressions, the decoupled input-output transfer functions are obtained:

$$I_{\alpha}(s) = \left(\frac{G_{\alpha d}(s) + G_{\beta d}(s)G_{\alpha\beta}(s)}{1 - G_{\alpha\beta}(s)G_{\beta\alpha}(s)} \right) I_d^*(s) + \left(\frac{G_{\alpha q}(s) + G_{\beta q}(s)G_{\alpha\beta}(s)}{1 - G_{\alpha\beta}(s)G_{\beta\alpha}(s)} \right) I_q^*(s) \quad (128)$$

$$I_{\beta}(s) = \left(\frac{G_{\beta d}(s) + G_{\alpha d}(s)G_{\beta\alpha}(s)}{1 - G_{\alpha\beta}(s)G_{\beta\alpha}(s)} \right) I_d^*(s) + \left(\frac{G_{\beta q}(s) + G_{\alpha q}(s)G_{\beta\alpha}(s)}{1 - G_{\alpha\beta}(s)G_{\beta\alpha}(s)} \right) I_q^*(s) \quad (129)$$

The decoupled transfer functions are graphically represented in block diagrams in next Figure 26:

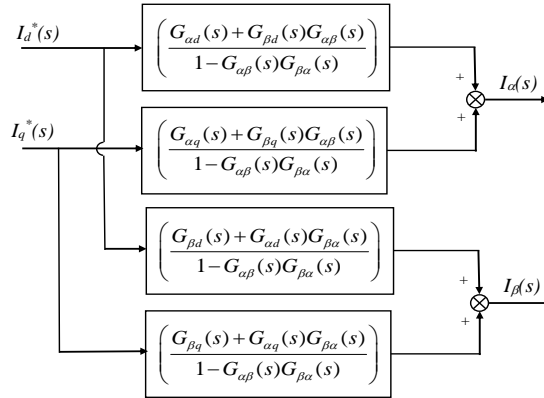


Figure 26. Equivalent block diagram of the control of currents in *dq* without cancellation of coupling terms. Note that its structure is equal to one shown in Figure 16, but the poles and zeros are different.

By solving $I_{\alpha}(s)$ expressions using a symbolic Toolbox from Matlab for instance, it is possible to obtain for *d* input current:

$$\frac{G_{\alpha d}(s) + G_{\beta d}(s)G_{\alpha\beta}(s)}{1 - G_{\alpha\beta}(s)G_{\beta\alpha}(s)} = \frac{g_{nd5} \cdot s^5 + g_{nd4} \cdot s^4 + g_{nd3} \cdot s^3 + g_{nd2} \cdot s^2 + g_{nd1} \cdot s}{g_6 \cdot s^6 + g_5 \cdot s^5 + g_4 \cdot s^4 + g_3 \cdot s^3 + g_2 \cdot s^2 + g_1 \cdot s + g_0} \quad (130)$$

Being each coefficient of the resulting transfer function:

$$\begin{aligned}
 g_{nd5} &= L \cdot k_p \\
 g_{nd4} &= k_p^2 + R \cdot k_p + L \cdot k_i \\
 g_{nd3} &= L \cdot k_p \cdot \omega^2 + R \cdot k_i + 2 \cdot k_i \cdot k_p \\
 g_{nd2} &= k_i^2 - L \cdot k_i \cdot \omega^2 + k_p^2 \cdot \omega^2 + R \cdot k_p \cdot \omega^2 \\
 g_{nd1} &= -R \cdot k_i \cdot \omega^2
 \end{aligned}$$

$$\begin{aligned}
 g_6 &= L^2 \\
 g_5 &= 2 \cdot L \cdot k_p + 2 \cdot L \cdot R \\
 g_4 &= 2 \cdot L^2 \cdot \omega^2 + 2 \cdot k_i \cdot L + R^2 + 2 \cdot R \cdot k_p + k_p^2 \\
 g_3 &= 2 \cdot R \cdot k_i + 2 \cdot k_i \cdot k_p + 4 \cdot L \cdot R \cdot \omega^2 + 4 \cdot L \cdot k_p \cdot \omega^2 \\
 g_2 &= L^2 \cdot \omega^4 + 2 \cdot L \cdot k_i \cdot \omega^2 + 2 \cdot R^2 \cdot \omega^2 + 4 \cdot R \cdot k_p \cdot \omega^2 + k_i^2 + 2 \cdot k_p^2 \cdot \omega^2 \\
 g_1 &= 2 \cdot k_i \cdot k_p \cdot \omega^2 + 2 \cdot L \cdot R \cdot \omega^4 + 2 \cdot L \cdot k_p \cdot \omega^4 + 2 \cdot R \cdot k_i \cdot \omega^2 \\
 g_0 &= R^2 \cdot \omega^4 + 2 \cdot R \cdot k_p \cdot \omega^4 + k_i^2 \cdot \omega^2 + k_p^2 \cdot \omega^4
 \end{aligned} \tag{131}$$

And for q input current:

$$\frac{G_{\alpha q}(s) + G_{\beta q}(s)G_{\alpha\beta}(s)}{1 - G_{\alpha\beta}(s)G_{\beta\alpha}(s)} = \frac{g_{nq4} \cdot s^4 + g_{nq3} \cdot s^3 + g_{nq2} \cdot s^2 + g_{nq1} \cdot s}{g_6 \cdot s^6 + g_5 \cdot s^5 + g_4 \cdot s^4 + g_3 \cdot s^3 + g_2 \cdot s^2 + g_1 \cdot s + g_0} \tag{132}$$

Being the denominator' coefficients, g_1, g_2, \dots equal to the previous expression. While the coefficients of the numerator are:

$$\begin{aligned}
 g_{nq4} &= -(L \cdot k_p) \cdot \omega \\
 g_{nq3} &= -(k_p^2 + R \cdot k_p + 2 \cdot L \cdot k_i) \cdot \omega \\
 g_{nq2} &= -(L \cdot k_p \cdot \omega^2 + 2 \cdot R \cdot k_i + 2 \cdot k_i \cdot k_p) \cdot \omega \\
 g_{nq1} &= -(k_i^2 + k_p^2 \cdot \omega^2 + R \cdot k_p \cdot \omega^2) \cdot \omega
 \end{aligned} \tag{133}$$

Thus, in next Figure 27, the poles and zeros of the system are shown, after substituting the same numerical example used in previous chapters. Comparing the poles with the control that cancels the coupling terms, it is seen that the real and imaginary parts of the poles that conform the natural or transient response, have been moved considerably. Now it is seen that there is a pole that has increased considerably its imaginary part (bigger oscillating frequency) and it has reduced considerably its real part (it is damped slower). On the other hand, the other pole has decreased considerably its imaginary part (smaller oscillating frequency) and it has increased considerably its real part (it is damped faster). This fact occurs due to the presence of the current coupling terms that are not cancelled by this control. In this way, the coupling terms operate analogously to a perturbation action that affects to the behavior of the entire closed loops system.

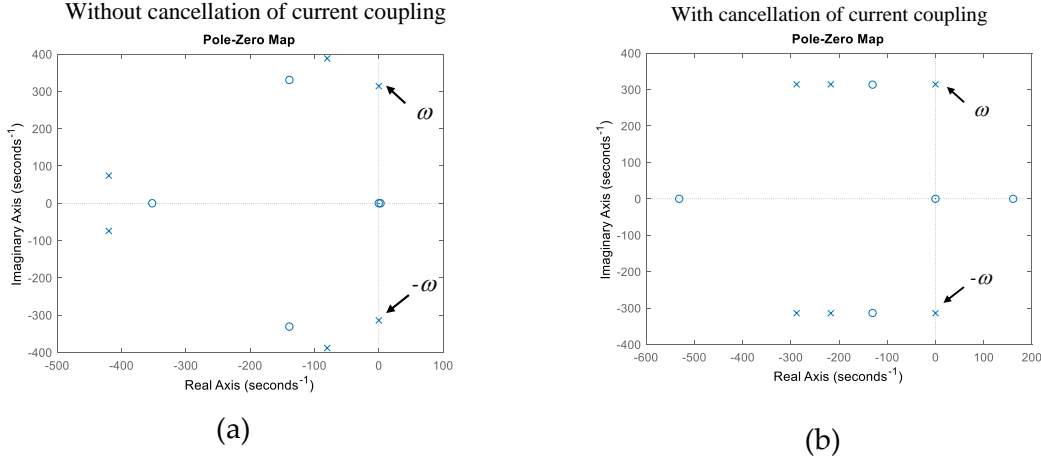


Figure 27. Poles in stationary reference frame ($\alpha\beta$) for $I_\alpha(s)$ of expression (128) (a) without cancellation of current coupling terms, (b) with cancellation of current coupling terms. Conditions of Appendix E.

After this, by substituting step inputs at at both $I_d^*(s)$ and $I_q^*(s)$, the output alfa current results:

$$I_\alpha(s) = \left(\frac{G_{\alpha d}(s) + G_{\beta d}(s)G_{\alpha\beta}(s)}{1 - G_{\alpha\beta}(s)G_{\beta\alpha}(s)} \right) \frac{|I_d^*|}{s} + \left(\frac{G_{\alpha q}(s) + G_{\beta q}(s)G_{\alpha\beta}(s)}{1 - G_{\alpha\beta}(s)G_{\beta\alpha}(s)} \right) \frac{|I_q^*|}{s} \quad (134)$$

What is equal to:

$$I_\alpha(s) = \left(\frac{g_{nd5} \cdot s^4 + g_{nd4} \cdot s^3 + g_{nd3} \cdot s^2 + g_{nd2} \cdot s + g_{nd1}}{g_6 \cdot s^6 + g_5 \cdot s^5 + g_4 \cdot s^4 + g_3 \cdot s^3 + g_2 \cdot s^2 + g_1 \cdot s + g_0} \right) |I_d^*| + \left(\frac{g_{nq4} \cdot s^3 + g_{nq3} \cdot s^2 + g_{nq2} \cdot s^1 + g_{nq1}}{g_6 \cdot s^6 + g_5 \cdot s^5 + g_4 \cdot s^4 + g_3 \cdot s^3 + g_2 \cdot s^2 + g_1 \cdot s + g_0} \right) |I_q^*| \quad (135)$$

By using a partial fraction expansion and applying the inverse Laplace transform, the time domain expression for step inputs of the output current can be obtained from previous equation. Being the time response of the complete final expressions (only $i_\alpha(t)$ current is shown, $i_\beta(t)$ would present an equivalent form):

$$i_\alpha(t) = \left((2 \cdot B_0) \cdot e^{\sigma_0 t} \cdot \cos(\omega_{d0} \cdot t + \arg B_0) + (2 \cdot B_1) \cdot e^{\sigma_1 t} \cdot \cos(\omega_{d1} \cdot t + \arg B_1) + (2 \cdot B_2) \cdot \cos(\omega \cdot t) \right) |I_d^*| + \left((2 \cdot B_3) \cdot e^{\sigma_3 t} \cdot \cos(\omega_{d3} \cdot t + \arg B_3) + (2 \cdot B_4) \cdot e^{\sigma_4 t} \cdot \cos(\omega_{d4} \cdot t + \arg B_4) + (2 \cdot B_5) \cdot \cos(\omega \cdot t + \pi/2) \right) |I_q^*| \quad (136)$$

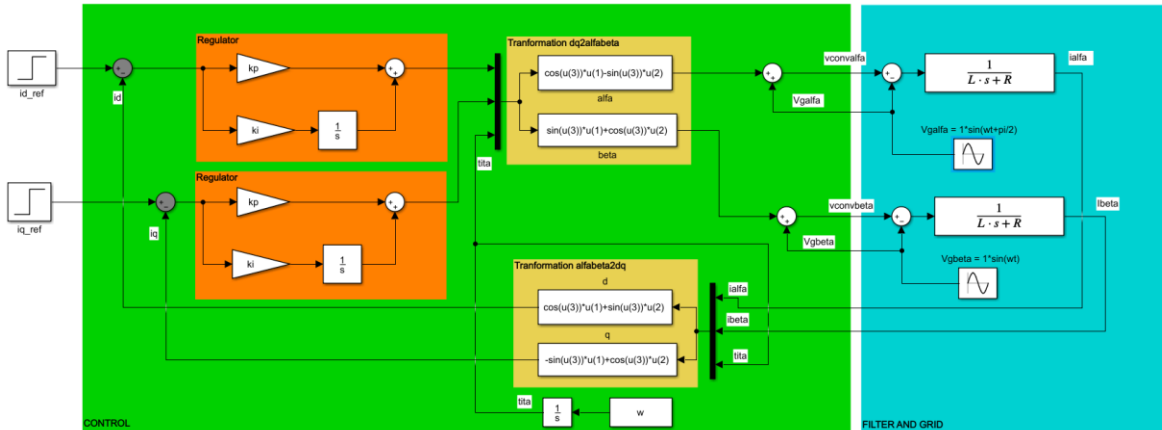
In the following Table VI, the numerical parameters and constants of the previous expressions are provided. In accordance with the poles depicted in Figure 27, it is seen that the two conjugate pole pairs that conform the transient response (natural response) present now very distant real and imaginary parts. There is now a much slower pole, with a damping constant (real part) of $\sigma_1 = -8.032e+01$ and oscillates at $\omega_{d1} = 3.8743e+02$ rd/s (imaginary part). This pole becomes dominant in the transient response, because it present much longer time constant than the other pole denoted by B_0 , $\arg B_0$, σ_0 and ω_{d0} . Then,

regarding the steady-state conforming pole pair, nothing special or new can be said, in comparison with what occurred with the control that cancels the current coupling terms. Finally, note that the poles and/or parameters corresponding to the $I_d(s)$ input are almost the same that the ones corresponding to the $I_q(s)$ input, the only difference can be found on the arguments of the cosine terms that come from a slight difference on the zeros.

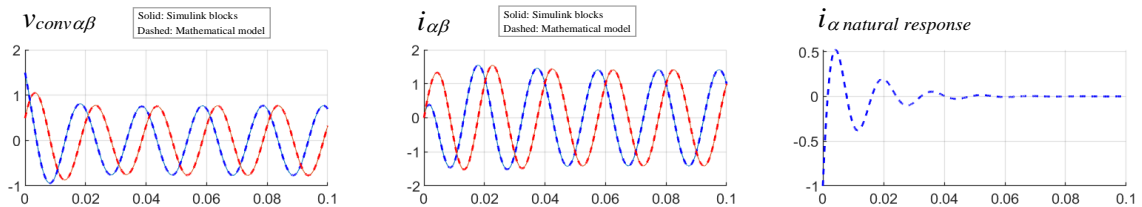
Table VI. Numerical solution of expression (136) by using the 'residue' function from Matlab Control Toolbox. Conditions of Appendix E.

d	q
$B_0 = 3.66059470414e-01$ $argB_0 = -2.38756461679e+00$ $\sigma_0 = -4.24679933020e+02$ $\omega_{d0} = 7.32759410267e+01$	$B_3 = 3.66059470414e-01$ $argB_3 = 2.32482436358e+00$ $\sigma_3 = -4.24679933020e+02$ $\omega_{d3} = 7.32759410267e+01$
$B_1 = 3.422939427312006e-01$ $argB_1 = -2.320176782313537e+00$ $\sigma_1 = -8.032006697983152e+01$ $\omega_{d1} = 3.874352063857773e+02$	$B_4 = 3.42293942731e-01$ $argB_4 = -7.49380455518e-01$ $\sigma_4 = -8.03200669798e+01$ $\omega_{d4} = 3.87435206385e+02$
$B_2 = 5.00000e-01$ $\omega = 3.141592653589798e+02$	$B_5 = 5.00000e-01$ $\omega = 3.14159265358e+02$

Finally, the time domain step response is shown in the next Figure 28. It is seen a good agreement between the derived mathematical expressions and the Simulink based model.



(a)



(b)

Figure 28. (a) Block diagram of control in synchronous reference frame (dq) without current coupling cancellation, (b) time domain responses in $\alpha\beta$ reference frame of control in dq frame without current coupling cancellation, to a unit step input in $i_d^*(t)$ and $i_q^*(t)$. Conditions of Appendix E.

4.2. Mathematical model in $\alpha\beta$ with sinusoidal and cosenoidal input

Now considering **sine** and **cosine** inputs at $I_d^*(s)$ and $I_q^*(s)$ respectively and again assuming that the grid voltage is ideal, i.e., assuming no angle phase shift and ω constant, the time domain expressions (112) and (113) can be transformed into the 's' domain as follows (see appendix D omitting cancellation of coupling terms):

$$\begin{aligned}
 V_{conv\alpha}(s) = & -\left(k_p + \frac{k_i s}{s^2 + \omega^2}\right) I_\alpha(s) + \left(\frac{k_i \omega}{s^2 + \omega^2}\right) I_\beta(s) \\
 & + \left(\frac{k_p}{2}\right) \left(\frac{s^2 + \omega_1^2}{\omega_1}\right) \left(\frac{\omega_1 + \omega}{s^2 + (\omega_1 + \omega)^2} + \frac{\omega_1 - \omega}{s^2 + (\omega_1 - \omega)^2}\right) I_d^*(s) \\
 & - \left(\frac{k_i}{2}\right) \left(\frac{s^2 + \omega_1^2}{\omega_1^2}\right) \left(\frac{s}{s^2 + (\omega_1 + \omega)^2} + \frac{s}{s^2 + (\omega_1 - \omega)^2} + \frac{2s}{s^2 + \omega^2}\right) I_d^*(s) \\
 & - \left(\frac{k_p}{2}\right) \left(\frac{s^2 + \omega_1^2}{s}\right) \left(\frac{\omega_1 + \omega}{s^2 + (\omega_1 + \omega)^2} - \frac{\omega_1 - \omega}{s^2 + (\omega_1 - \omega)^2}\right) I_q^*(s) \\
 & - \left(\frac{k_i}{2\omega_1}\right) \left(\frac{s^2 + \omega_1^2}{s}\right) \left(\frac{s}{s^2 + (\omega_1 + \omega)^2} - \frac{s}{s^2 + (\omega_1 - \omega)^2}\right) I_q^*(s) + V_{g\alpha}(s)
 \end{aligned} \tag{137}$$

$$\begin{aligned}
 V_{conv\beta}(s) = & -\left(k_p + \frac{k_i s}{s^2 + \omega^2}\right) I_\beta(s) - \left(\frac{k_i \omega}{s^2 + \omega^2}\right) I_\alpha(s) \\
 & - \left(\frac{k_i}{2}\right) \left(\frac{s^2 + \omega_1^2}{\omega_1^2}\right) \left(\frac{\omega_1 + \omega}{s^2 + (\omega_1 + \omega)^2} - \frac{\omega_1 - \omega}{s^2 + (\omega_1 - \omega)^2} - \frac{2\omega}{s^2 + \omega^2}\right) I_d^*(s) \\
 & + \left(\frac{k_p}{2}\right) \left(\frac{s^2 + \omega_1^2}{\omega_1}\right) \left(\frac{s}{s^2 + (\omega_1 - \omega)^2} - \frac{s}{s^2 + (\omega_1 + \omega)^2}\right) I_d^*(s) \\
 & + \left(\frac{k_i}{2\omega_1}\right) \left(\frac{s^2 + \omega_1^2}{s}\right) \left(\frac{\omega_1 + \omega}{s^2 + (\omega_1 + \omega)^2} + \frac{\omega_1 - \omega}{s^2 + (\omega_1 - \omega)^2}\right) I_q^*(s) \\
 & + \left(\frac{k_p}{2}\right) \left(\frac{s^2 + \omega_1^2}{s}\right) \left(\frac{s}{s^2 + (\omega_1 + \omega)^2} + \frac{s}{s^2 + (\omega_1 - \omega)^2}\right) I_q^*(s) + V_{g\beta}(s)
 \end{aligned} \tag{138}$$

Being these expressions only valid for a **sine** and **cosine** inputs at $I_d^*(s)$ and $I_q^*(s)$:

$$i_d^*(t) = |I_d^*| \cdot \sin(\omega_1 t) \quad \rightarrow \quad I_d^*(s) = \frac{\omega_1}{s^2 + \omega_1^2} |I_d^*| \tag{139}$$

$$i_q^*(t) = |I_q^*| \cdot \cos(\omega_1 t) \quad \rightarrow \quad I_q^*(s) = \frac{s}{s^2 + \omega_1^2} |I_q^*| \tag{140}$$

Then, combining these last two expressions in 's' domain, with the power circuit model equations, the closed loop expressions of the currents can be obtained:

$$I_\alpha(s) = \left(\frac{(s^2 + \omega^2) \cdot D_\alpha(s)}{A(s)}\right) I_d^*(s) - \left(\frac{(s^2 + \omega^2) \cdot Q_\alpha(s)}{A(s)}\right) I_q^*(s) + \left(\frac{k_i \omega}{A(s)}\right) I_\beta(s) \tag{141}$$

$$I_\beta(s) = \left(\frac{(s^2 + \omega^2) \cdot D_\beta(s)}{A(s)}\right) I_d^*(s) + \left(\frac{(s^2 + \omega^2) \cdot Q_\beta(s)}{A(s)}\right) I_q^*(s) - \left(\frac{k_i \omega}{A(s)}\right) I_\alpha(s) \tag{142}$$

With:

$$D_\alpha(s) = \left(\frac{s^2 + \omega_1^2}{\omega_1}\right) \left[\left(\frac{k_p}{2}\right) \left(\frac{\omega_1 + \omega}{s^2 + (\omega_1 + \omega)^2} + \frac{\omega_1 - \omega}{s^2 + (\omega_1 - \omega)^2}\right) - \left(\frac{k_i}{2\omega_1}\right) \left(\frac{s}{s^2 + (\omega_1 + \omega)^2} + \frac{s}{s^2 + (\omega_1 - \omega)^2}\right) + \left(\frac{k_i}{\omega_1}\right) \left(\frac{s}{s^2 + \omega^2}\right)\right] \tag{143}$$

$$Q_\alpha(s) = \left(\frac{k_p}{2}\right) \left(\frac{s^2 + \omega_1^2}{s}\right) \left(\frac{\omega_1 + \omega}{s^2 + (\omega_1 + \omega)^2} - \frac{\omega_1 - \omega}{s^2 + (\omega_1 - \omega)^2}\right) + \left(\frac{k_i}{2\omega_1}\right) \left(\frac{s^2 + \omega_1^2}{s}\right) \left(\frac{s}{s^2 + (\omega_1 - \omega)^2} - \frac{s}{s^2 + (\omega_1 + \omega)^2}\right) \quad (144)$$

And

$$D_\beta(s) = \left(\frac{s^2 + \omega_1^2}{\omega_1}\right) \left[\left(\frac{k_i}{\omega_1}\right) \left(\frac{\omega}{s^2 + \omega^2}\right) + \left(\frac{k_p}{2}\right) \left(-\frac{s}{s^2 + (\omega_1 + \omega)^2} + \frac{s}{s^2 + (\omega_1 - \omega)^2}\right) - \left(\frac{k_i}{2\omega_1}\right) \left(\frac{\omega_1 + \omega}{s^2 + (\omega_1 + \omega)^2} - \frac{\omega_1 - \omega}{s^2 + (\omega_1 - \omega)^2}\right)\right] \quad (145)$$

$$Q_\beta(s) = \left(\frac{s^2 + \omega_1^2}{s}\right) \left[\left(\frac{k_p}{2}\right) \left(\frac{s}{s^2 + (\omega_1 + \omega)^2} + \frac{s}{s^2 + (\omega_1 - \omega)^2}\right) + \left(\frac{k_i}{2\omega_1}\right) \left(\frac{\omega_1 + \omega}{s^2 + (\omega_1 + \omega)^2} + \frac{\omega_1 - \omega}{s^2 + (\omega_1 - \omega)^2}\right)\right] \quad (146)$$

Being again, these expressions only valid for a **sine** and **cosine** inputs at $I_d^*(s)$ and $I_q^*(s)$. (147)-(148). By representing the previous expressions in a more compact form:

$$I_\alpha(s) = G_{\alpha d-s} I_d^*(s) + G_{\alpha q-s} I_q^*(s) + G_{\alpha\beta-s} I_\beta(s) \quad (149)$$

$$I_\beta(s) = G_{\beta d-s} I_d^*(s) + G_{\beta q-s} I_q^*(s) + G_{\beta\alpha-s} I_\alpha(s) \quad (150)$$

It is seen that there is again a coupling between two output currents that influence one in the other. Repeating again the same procedure developed in the previous chapter, the decoupled input-output transfer functions are obtained:

$$I_\alpha(s) = \left(\frac{G_{\alpha d-s}(s) + G_{\beta d-s}(s)G_{\alpha\beta-s}(s)}{1 - G_{\alpha\beta-s}(s)G_{\beta\alpha-s}(s)}\right) I_d^*(s) + \left(\frac{G_{\alpha q-s}(s) + G_{\beta q-s}(s)G_{\alpha\beta-s}(s)}{1 - G_{\alpha\beta-s}(s)G_{\beta\alpha-s}(s)}\right) I_q^*(s) \quad (151)$$

$$I_\beta(s) = \left(\frac{G_{\beta d-s}(s) + G_{\alpha d-s}(s)G_{\beta\alpha-s}(s)}{1 - G_{\alpha\beta-s}(s)G_{\beta\alpha-s}(s)}\right) I_d^*(s) + \left(\frac{G_{\beta q-s}(s) + G_{\alpha q-s}(s)G_{\beta\alpha-s}(s)}{1 - G_{\alpha\beta-s}(s)G_{\beta\alpha-s}(s)}\right) I_q^*(s) \quad (152)$$

The decoupled transfer functions are graphically represented in block diagrams in next figure:

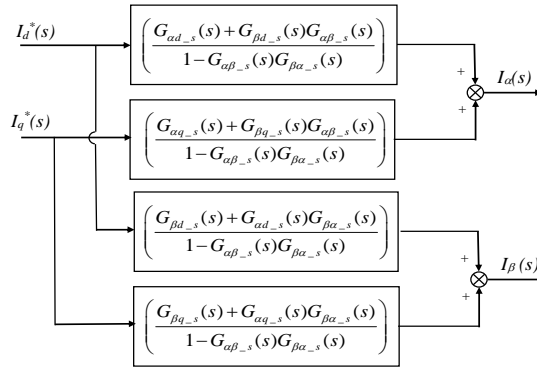


Figure 29. Equivalent block diagram of the currents control in *dq* frame without cancellation of coupling terms. Note that its structure is equal to one shown in Figure 19, but the poles and zeros are different.

By solving $I_\alpha(s)$ expressions using a symbolic Toolbox from Matlab for instance, it is possible to obtain for *d* and *q* inputs current:

$$\frac{G_{ad-s} + G_{\beta d-s} G_{\alpha\beta-s}}{1 - G_{\alpha\beta-s} G_{\beta\alpha-s}} = \frac{g_{nd7} \cdot s^7 + g_{nd6} \cdot s^6 + g_{nd5} \cdot s^5 + g_{nd4} \cdot s^4 + g_{nd3} \cdot s^3 + g_{nd2} \cdot s^2 + g_{nd1} \cdot s + g_{nd0}}{g_8 \cdot s^8 + g_7 \cdot s^7 + g_6 \cdot s^6 + g_5 \cdot s^5 + g_4 \cdot s^4 + g_3 \cdot s^3 + g_2 \cdot s^2 + g_1 \cdot s + g_0} \quad (153)$$

$$\frac{G_{\alpha q-s} + G_{\beta q-s} G_{\alpha\beta-s}}{1 - G_{\alpha\beta-s} G_{\beta\alpha-s}} = \frac{g_{nq7} \cdot s^7 + g_{nq6} \cdot s^6 + g_{nq5} \cdot s^5 + g_{nq4} \cdot s^4 + g_{nq3} \cdot s^3 + g_{nq2} \cdot s^2 + g_{nq1} \cdot s + g_{nq0}}{(g_8 \cdot s^8 + g_7 \cdot s^7 + g_6 \cdot s^6 + g_5 \cdot s^5 + g_4 \cdot s^4 + g_3 \cdot s^3 + g_2 \cdot s^2 + g_1 \cdot s + g_0) \cdot s}$$

Thus, in next Figure 30, the poles and zeros of the system are shown, after numerically substituting the same numerical example used in previous chapter. It is seen again that two complex conjugate pole pairs conforming the transient response or natural response, have been moved in comparison with the poles of a control with cancellation of current coupling terms. Both the real and the imaginary part of these poles now are different one from each other.

Then, the other two pair of conjugate imaginary poles, without real part and with imaginary parts $\omega_l = \omega_l + \omega = 1884.9 \text{rd/s}$ and $\omega_l = \omega_l - \omega = 1256.6 \text{rd/s}$, which are the components that create the steady-state current are still there. Note also that there is a conjugate zero pair with imaginary part ω_l in both transfer functions, that is cancelled with the sinus and cosines inputs' poles with imaginary part ω_l .

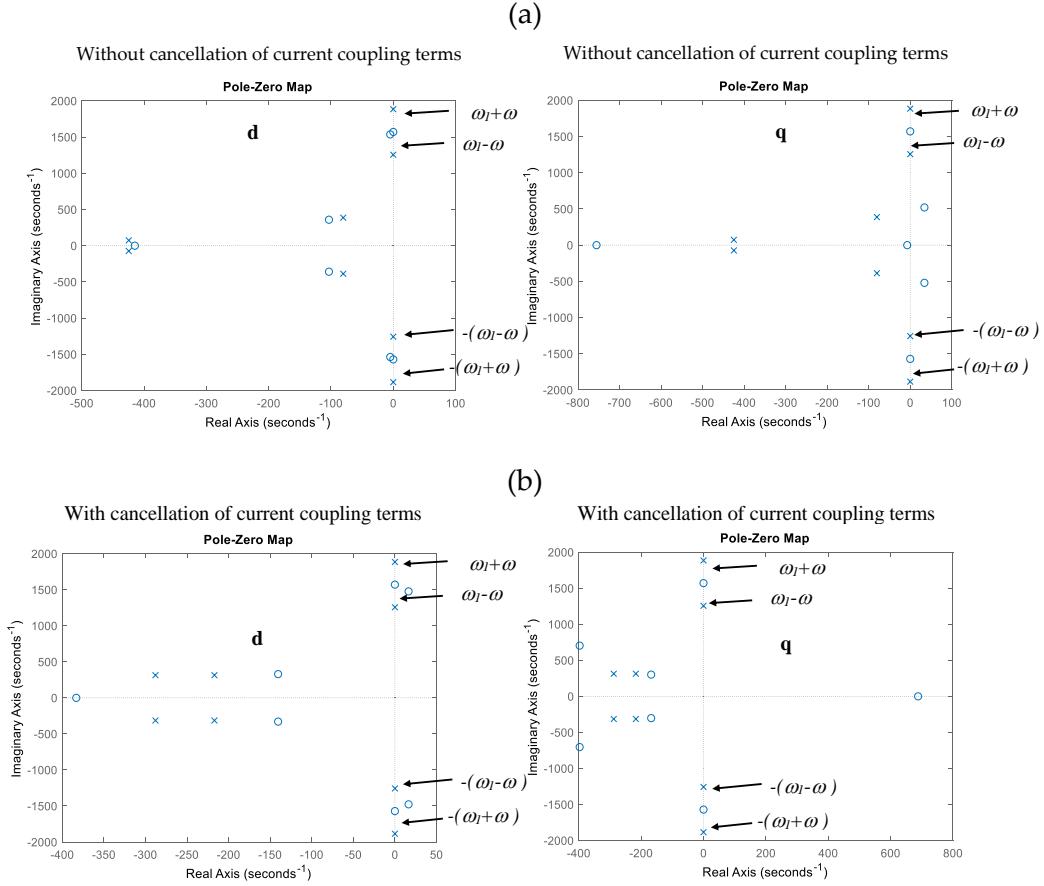


Figure 30. *dq* control of currents. (a) Poles in stationary reference frame ($\alpha\beta$) for $I_\alpha(s)/I_d^*(s)$ and $I_\alpha(s)/I_q^*(s)$ **without** the current coupling terms cancellation, (b) Poles in stationary reference frame ($\alpha\beta$) for $I_\alpha(s)/I_d^*(s)$ and $I_\alpha(s)/I_q^*(s)$ **with** the current coupling terms cancellation. Conditions of Appendix E.

Once the transfer functions have been obtained, it is possible to derive the output current expressions. Hence, substituting a sine and cosine inputs at $I_d^*(s)$ and $I_q^*(s)$. The output alfa current is given by:

$$I_\alpha(s) = \left(\frac{G_{\alpha d_s}(s) + G_{\beta d_s}(s)G_{\alpha\beta_s}(s)}{1 - G_{\alpha\beta_s}(s)G_{\beta\alpha_s}(s)} \right) \left[\frac{\omega_1}{s^2 + \omega_1^2} |I_d^*| \right] + \left(\frac{G_{\alpha q_s}(s) + G_{\beta q_s}(s)G_{\alpha\beta_s}(s)}{1 - G_{\alpha\beta_s}(s)G_{\beta\alpha_s}(s)} \right) \left[\frac{s}{s^2 + \omega_1^2} |I_q^*| \right] \quad (154)$$

What is equal to:

$$I_\alpha(s) = \left(\frac{g_{nd5_-} \cdot s^5 + g_{nd4_-} \cdot s^4 + g_{nd3_-} \cdot s^3 + g_{nd2_-} \cdot s^2 + g_{nd1_-} \cdot s + g_{nd0_-}}{g_8 \cdot s^8 + g_7 \cdot s^7 + g_6 \cdot s^6 + g_5 \cdot s^5 + g_4 \cdot s^4 + g_3 \cdot s^3 + g_2 \cdot s^2 + g_1 \cdot s + g_0} \right) |I_d^*| + \left(\frac{g_{nq5_-} \cdot s^5 + g_{nq4_-} \cdot s^4 + g_{nq3_-} \cdot s^3 + g_{nq2_-} \cdot s^2 + g_{nq1_-} \cdot s^1 + g_{nq0_-}}{g_8 \cdot s^8 + g_7 \cdot s^7 + g_6 \cdot s^6 + g_5 \cdot s^5 + g_4 \cdot s^4 + g_3 \cdot s^3 + g_2 \cdot s^2 + g_1 \cdot s + g_0} \right) |I_q^*| \quad (155)$$

With coefficients of the numerator and denominator corresponding to the *d* input:

$$\begin{aligned}
g_{nd5_} &= L \cdot k_p \cdot \omega_1 \\
g_{nd4_} &= \omega_1 \cdot k_p^2 + R \cdot \omega_1 \cdot k_p + L \cdot k_i \cdot \omega_1 \\
g_{nd3_} &= R \cdot k_i \cdot \omega_1 + 2 \cdot k_i \cdot k_p \cdot \omega_1 + L \cdot k_p \cdot \omega_1^3 \\
g_{nd2_} &= k_i^2 \cdot \omega_1 - 3 \cdot L \cdot k_i \cdot \omega^2 \cdot \omega_1 + L \cdot k_i \cdot \omega_1^3 + k_p^2 \cdot \omega_1^3 + R \cdot \omega_1^3 \cdot k_p \\
g_{nd1_} &= 2 \cdot k_i \cdot k_p \cdot \omega_1^3 + R \cdot k_i \cdot \omega_1^3 - L \cdot k_p \cdot \omega^4 \cdot \omega_1 - 3 \cdot R \cdot k_i \cdot \omega^2 \cdot \omega_1 - 2 \cdot k_i \cdot k_p \cdot \omega^2 \cdot \omega_1 + L \cdot k_p \cdot \omega^2 \cdot \omega_1^3 \\
g_{nd0_} &= -k_i^2 \cdot \omega^2 \cdot \omega_1 + k_i^2 \cdot \omega_1^3 - k_p^2 \cdot \omega^4 \cdot \omega_1 + k_p^2 \cdot \omega^2 \cdot \omega_1^3 - R \cdot k_p \cdot \omega^4 \cdot \omega_1 + R \cdot k_p \cdot \omega^2 \cdot \omega_1^3 \\
\\
g_8 &= L^2 \\
g_7 &= 2 \cdot L \cdot k_p + 2 \cdot L \cdot R \\
g_6 &= 3 \cdot L^2 \cdot \omega^2 + 2 \cdot L^2 \cdot \omega_1^2 + 2 \cdot k_i \cdot L + R^2 + 2 \cdot R \cdot k_p + k_p^2 \\
g_5 &= 2 \cdot R \cdot k_i + 2 \cdot k_p \cdot k_i + 6 \cdot L \cdot R \cdot \omega^2 + 4 \cdot L \cdot R \cdot \omega_1^2 + 6 \cdot L \cdot k_p \cdot \omega^2 + 4 \cdot L \cdot k_p \cdot \omega_1^2 \\
g_4 &= 3 \cdot L^2 \cdot \omega^4 + L^2 \cdot \omega_1^4 + 4 \cdot L \cdot k_i \cdot \omega^2 + 4 \cdot L \cdot k_i \cdot \omega_1^2 + 3 \cdot R^2 \cdot \omega^2 + 2 \cdot R^2 \cdot \omega_1^2 \\
&+ 6 \cdot R \cdot k_p \cdot \omega^2 + 4 \cdot R \cdot k_p \cdot \omega_1^2 + k_i^2 + 3 \cdot k_p^2 \cdot \omega^2 + 2 \cdot k_p^2 \cdot \omega_1^2 \\
g_3 &= 4 \cdot k_p \cdot k_i \cdot \omega^2 + 4 \cdot k_p \cdot k_i \cdot \omega_1^2 + 6 \cdot L \cdot R \cdot \omega^4 + 2 \cdot L \cdot R \cdot \omega_1^4 + 6 \cdot L \cdot k_p \cdot \omega^4 + 2 \cdot L \cdot k_p \cdot \omega_1^4 + 4 \cdot R \cdot k_i \cdot \omega^2 + 4 \cdot R \cdot k_i \cdot \omega_1^2 \\
g_2 &= L^2 \cdot \omega^6 - 2 \cdot L^2 \cdot \omega^4 \cdot \omega_1^2 + L^2 \cdot \omega^2 \cdot \omega_1^4 + 2 \cdot L \cdot k_i \cdot \omega^4 - 4 \cdot L \cdot k_i \cdot \omega^2 \cdot \omega_1^2 + 2 \cdot L \cdot k_i \cdot \omega_1^4 + 3 \cdot R^2 \cdot \omega^4 + R^2 \cdot \omega_1^4 \\
&+ 6 \cdot R \cdot k_p \cdot \omega^4 + 2 \cdot R \cdot k_p \cdot \omega_1^4 + 2 \cdot k_i^2 \cdot \omega^2 + 2 \cdot k_i^2 \cdot \omega_1^2 + 3 \cdot k_p^2 \cdot \omega^4 + k_p^2 \cdot \omega_1^4 \\
g_1 &= 2 \cdot k_p \cdot k_i \cdot \omega^4 + 2 \cdot k_p \cdot k_i \cdot \omega_1^4 + 2 \cdot L \cdot R \cdot \omega^6 + 2 \cdot L \cdot k_p \cdot \omega^6 + 2 \cdot R \cdot k_i \cdot \omega^4 + 2 \cdot R \cdot k_i \cdot \omega_1^4 + 2 \cdot L \cdot R \cdot \omega^2 \cdot \omega_1^4 - 4 \cdot L \cdot R \cdot \omega^4 \cdot \omega_1^2 \\
&+ 2 \cdot L \cdot k_p \cdot \omega^2 \cdot \omega_1^4 - 4 \cdot L \cdot k_p \cdot \omega^4 \cdot \omega_1^2 - 4 \cdot R \cdot k_i \cdot \omega^2 \cdot \omega_1^2 - 4 \cdot R \cdot k_i \cdot \omega^2 \cdot \omega_1^2 \\
g_0 &= R^2 \cdot \omega^6 - 2 \cdot R^2 \cdot \omega^4 \cdot \omega_1^2 + R^2 \cdot \omega^2 \cdot \omega_1^4 + 2 \cdot R \cdot k_p \cdot \omega^6 - 4 \cdot R \cdot k_p \cdot \omega^4 \cdot \omega_1^2 + 2 \cdot R \cdot k_p \cdot \omega^2 \cdot \omega_1^4 + k_i^2 \cdot \omega^4 - 2 \cdot k_i^2 \cdot \omega^2 \cdot \omega_1^2 + k_i^2 \cdot \omega_1^4 \\
&+ k_p^2 \cdot \omega^6 - 2 \cdot k_p^2 \cdot \omega^4 \cdot \omega_1^2 + k_p^2 \cdot \omega^2 \cdot \omega_1^4
\end{aligned} \tag{156}$$

While for the q component, the coefficients of the numerator are symbolically represented by:

$$\begin{aligned}
g_{nq5_} &= -L \cdot k_p \cdot \omega \\
g_{nq4_} &= -\omega \cdot k_p^2 - R \cdot \omega \cdot k_p - 2 \cdot L \cdot k_i \cdot \omega \\
g_{nq3_} &= L \cdot k_p \cdot \omega \cdot \omega_1^2 - 2 \cdot R \cdot k_i \cdot \omega - 2 \cdot k_i \cdot k_p \cdot \omega - 2 \cdot L \cdot k_p \cdot \omega^3 \\
g_{nq2_} &= -k_i^2 \cdot \omega - 2 \cdot L \cdot k_i \cdot \omega^3 - 2 \cdot k_p^2 \cdot \omega^3 + k_p^2 \cdot \omega \cdot \omega_1^2 - 2 \cdot R \cdot \omega^3 \cdot k_p + R \cdot k_p \cdot \omega \cdot \omega_1^2 \\
g_{nq1_} &= 2 \cdot k_i \cdot k_p \cdot \omega \cdot \omega_1^2 - L \cdot k_p \cdot \omega^5 - 2 \cdot R \cdot k_i \cdot \omega^3 - 2 \cdot k_i \cdot k_p \cdot \omega^3 + L \cdot k_p \cdot \omega^3 \omega_1^2 \\
g_{nq0_} &= k_i^2 \cdot \omega \cdot \omega_1^2 - k_i^2 \cdot \omega^3 - k_p^2 \cdot \omega^5 + k_p^2 \cdot \omega^3 \cdot \omega_1^2 - R \cdot k_p \cdot \omega^5 + R \cdot k_p \cdot \omega^3 \cdot \omega_1^2
\end{aligned} \tag{157}$$

By using a partial fraction expansion and applying the inverse Laplace transform, the time domain expression for sinus and cosines inputs of the output current can be obtained from equation (155). Being the time response of the complete final expressions (only $i_\alpha(t)$ current is shown, $i_\beta(t)$ would present an equivalent form):

$$\begin{aligned}
i_\alpha(t) &= \left[(2 \cdot B_0) \cdot \cos((\omega_1 + \omega) \cdot t + \arg B_0) + (2 \cdot B_1) \cdot \cos((\omega_1 - \omega) \cdot t + \arg B_1) \right. \\
&\quad \left. + (2 \cdot B_2) \cdot e^{\sigma_2 t} \cdot \cos(\omega_{d2} \cdot t + \arg B_2) + (2 \cdot B_3) \cdot e^{\sigma_3 t} \cdot \cos(\omega_{d3} \cdot t + \arg B_3) \right] | I_d^* | \\
&+ \left[(2 \cdot B_4) \cdot \cos((\omega_1 + \omega) \cdot t + \arg B_4) + (2 \cdot B_5) \cdot \cos((\omega_1 - \omega) \cdot t + \arg B_5) \right. \\
&\quad \left. + (2 \cdot B_6) \cdot e^{\sigma_6 t} \cdot \cos(\omega_{d6} \cdot t + \arg B_6) + (2 \cdot B_7) \cdot e^{\sigma_7 t} \cdot \cos(\omega_{d7} \cdot t + \arg B_7) \right] | I_q^* |
\end{aligned} \tag{158}$$

Finally, Table VII shows a numerical solution of expression (158) by using the the ‘residue’ function from Matlab Control Toolbox. Therefore, it is inferred that in contrast to the control with cancellation of coupling terms, the transient response or damped terms (natural response), oscillate at different $\omega=314.159$ rd/s (different imaginary parts) and are damped with different time constants (real parts), while the steady-state terms (poles without real parts) oscillate at $\omega_1+\omega=1884.9$ rd/s and $\omega_1-\omega=1256.6$ rd/s.

Table VII. Numerical solution of expression (158) by using the the ‘residue’ function from Matlab Control Toolbox. Conditions of Appendix E.

d	q
$B_0 = 6.48967586678e-02$	$B_4 = 6.489675866781006e-02$
$argB_0 = -2.9031908834e+00$	$argB_4 = 1.869371989665175e-01$
$\omega_1 + \omega = 1.88495559e+03$	$\omega_1 + \omega = 1.8849555921e+03$
$B_1 = 9.42325130201e-02$	$B_5 = 9.423251302016845e-02$
$argB_1 = -2.82842575621e+00$	$argB_5 = -2.828425756210602e+00$
$\omega_1 - \omega = 1.25663706143e+03$	$\omega_1 - \omega = 1.2566370614e+03$
$B_2 = 1.312085249117193e-01$	$B_6 = 4.801766349698532e-02$
$argB_2 = 1.454573489016104e-01$	$argB_6 = 9.766847868259755e-01$
$\sigma_2 = -4.246799330201682e+02$	$\sigma_6 = -4.246799330201682e+02$
$\omega_{d2} = 7.327594102679845e+01$	$\omega_{d6} = 7.327594102679845e+01$
$B_3 = 2.368128003266055e-02$	$B_7 = 1.639103833170650e-03$
$argB_3 = 8.661548497401336e-02$	$argB_7 = -2.223749730691358e+00$
$\sigma_3 = -8.032006697983110e+01$	$\sigma_7 = -8.032006697983110e+01$
$\omega_{d3} = 3.874352063857774e+02$	$\omega_{d7} = 3.874352063857774e+02$

4.3. Bode Diagram

Once the transfer functions for sine and cosine inputs are obtained, from them it is possible to derive the expressions for computation of the Bode diagram. Hence, from equation (151), as we did in previous chapter, for simplicity in the exposition, let us assume that the input $I_q^*(s)$ is zero, what means that we only apply a sinusoidal input at $I_d^*(s)$:

$$I_\alpha(s) = \left(\frac{G_{\alpha d-s}(s) + G_{\beta d-s}(s)G_{\alpha\beta-s}(s)}{1 - G_{\alpha\beta-s}(s)G_{\beta\alpha-s}(s)} \right) I_d^*(s) \quad (159)$$

Therefore, after substituting the sinusoidal input at $I_d^*(s)$ the current yields:

$$\begin{aligned}
 I_\alpha(s) = & \left(\frac{\omega_1 + \omega}{s^2 + (\omega_1 + \omega)^2} \right) \left[\left(\frac{k_p}{2} - \frac{k_i \cdot s}{2\omega_1(\omega_1 + \omega)} \right) \left(\frac{(s^2 + \omega^2)A(s)}{A^2(s) + (k_i\omega)^2} \right) - \left(\frac{k_p}{2} \frac{s}{(\omega_1 + \omega)} + \frac{k_i}{2\omega_1} \right) \left(\frac{(s^2 + \omega^2)(k_i\omega)}{A^2(s) + (k_i\omega)^2} \right) \right] | I_d^* | \\
 & + \left(\frac{\omega_1 - \omega}{s^2 + (\omega_1 - \omega)^2} \right) \left[\left(\frac{k_p}{2} - \frac{k_i \cdot s}{2\omega_1(\omega_1 - \omega)} \right) \left(\frac{(s^2 + \omega^2)A(s)}{A^2(s) + (k_i\omega)^2} \right) + \left(\frac{k_p}{2} \frac{s}{(\omega_1 - \omega)} + \frac{k_i}{2\omega_1} \right) \left(\frac{(s^2 + \omega^2)(k_i\omega)}{A^2(s) + (k_i\omega)^2} \right) \right] | I_d^* | \\
 & + \left(\frac{(s^2 + \omega^2)A(s)}{A^2(s) + (k_i\omega)^2} \right) \left(\frac{k_i}{\omega_1} \frac{s}{(s^2 + \omega^2)} \right) | I_d^* | + \left(\frac{(s^2 + \omega^2)(k_i \cdot \omega)}{A^2(s) + (k_i\omega)^2} \right) \left(\frac{k_i}{\omega_1} \frac{\omega}{(s^2 + \omega^2)} \right) | I_d^* |
 \end{aligned} \quad (160)$$

As occurred in the control with cancellation of the current coupling terms, analyzing this last expression, it is possible to see two dominant terms that contribute with two sinusoidal outputs at current $I_d(s)$.

One sinusoidal term at $\omega + \omega_l$ frequency:

$$\left(\frac{\omega_1 + \omega}{s^2 + (\omega_1 + \omega)^2} \right) \left[\left(\frac{k_p}{2} - \frac{k_i \cdot s}{2\omega_1(\omega_1 + \omega)} \right) \left(\frac{(s^2 + \omega^2)A(s)}{A^2(s) + (k_i\omega)^2} \right) - \left(\frac{k_p}{2} \frac{s}{(\omega_1 + \omega)} + \frac{k_i}{2\omega_1} \right) \left(\frac{(s^2 + \omega^2)(k_i\omega)}{A^2(s) + (k_i\omega)^2} \right) \right] |I_d^*| \quad (161)$$

One sinusoidal term at $\omega - \omega_l$ frequency:

$$\left(\frac{\omega_1 - \omega}{s^2 + (\omega_1 - \omega)^2} \right) \left[\left(\frac{k_p}{2} - \frac{k_i \cdot s}{2\omega_1(\omega_1 - \omega)} \right) \left(\frac{(s^2 + \omega^2)A(s)}{A^2(s) + (k_i\omega)^2} \right) + \left(\frac{k_p}{2} \frac{s}{(\omega_1 - \omega)} + \frac{k_i}{2\omega_1} \right) \left(\frac{(s^2 + \omega^2)(k_i\omega)}{A^2(s) + (k_i\omega)^2} \right) \right] |I_d^*| \quad (162)$$

And two more terms that are a sum of exponential terms and therefore are made zero at steady-state if the system is stable:

$$\frac{A(s) \left(\frac{sk_i}{\omega_1} \right)}{A^2(s) + (k_i\omega)^2} |I_d^*| + \frac{(k_i\omega) \left(\frac{k_i}{\omega_1} \right)}{A^2(s) + (k_i\omega)^2} |I_d^*| \quad (163)$$

Consequently, these last two terms do not contribute to the steady-state, therefore, neither to the Bode diagram. Thus, to calculate the Bode diagram in a classic way, it is necessary to substitute the required frequency at which the output is wanted to be considered in the following expressions:

$$s = j(\omega_1 + \omega) \rightarrow \left[\left(\frac{k_p}{2} - \frac{k_i \cdot s}{2\omega_1(\omega_1 + \omega)} \right) \left(\frac{(s^2 + \omega^2)A(s)}{A^2(s) + (k_i\omega)^2} \right) - \left(\frac{k_p}{2} \frac{s}{(\omega_1 + \omega)} + \frac{k_i}{2\omega_1} \right) \left(\frac{(s^2 + \omega^2)(k_i\omega)}{A^2(s) + (k_i\omega)^2} \right) \right] |I_d^*| \quad (164)$$

$$s = j(\omega_1 - \omega) \rightarrow \left[\left(\frac{k_p}{2} - \frac{k_i \cdot s}{2\omega_1(\omega_1 - \omega)} \right) \left(\frac{(s^2 + \omega^2)A(s)}{A^2(s) + (k_i\omega)^2} \right) + \left(\frac{k_p}{2} \frac{s}{(\omega_1 - \omega)} + \frac{k_i}{2\omega_1} \right) \left(\frac{(s^2 + \omega^2)(k_i\omega)}{A^2(s) + (k_i\omega)^2} \right) \right] |I_d^*|$$

What means that the two sinusoidal output currents at steady-state, can be evaluated in terms of amplitude and phase by applying for instance 'Bode function' in Matlab of previous expressions (164). Numerically, this means that for instance by choosing:

$$i_d^*(t) = |I_d^*| \cdot \sin(\omega_1 t) \quad \rightarrow \quad i_d^*(t) = 1 \cdot \sin(250 \cdot 2 \cdot \pi \cdot t) \quad (165)$$

$$i_q^*(t) = 0 \quad (166)$$

At the output current $i_d(t)$, we obtain 0.1885A at 200Hz and 0.1298A at 300Hz, which corresponds with -14.5dB and -17.7dB respectively, as noticed in next Figure 31. It can be inferred that there is not correspondence between this Bode diagram and the one with the

control that cancels the current coupling terms (Figure 21). However, this Bode diagram matches with the bode Diagram of the control with resonant controller of Figure 7. Note also that in this case, it is problematic to compare the resulted Bode diagram with its corresponding in dq reference frame, since there is not cancellation of coupling terms and they affect to the steady-state.

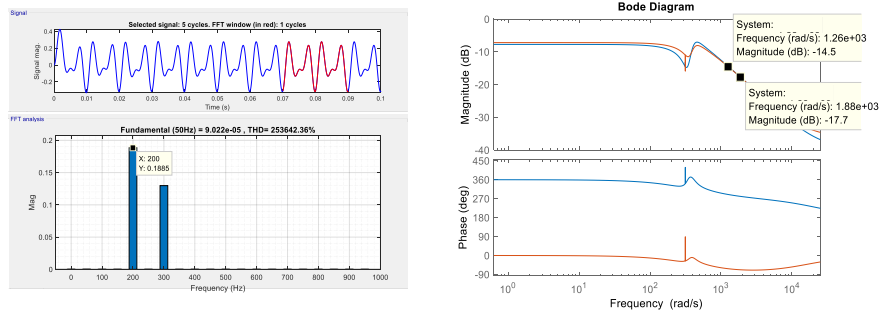


Figure 31. Time domain and Bode correspondence of currents expressed in $\alpha\beta$ frame, for control in dq without cancellation of coupling terms. Conditions of Appendix E. $i_d^*(t) = 1 \cdot \sin(250 \cdot 2 \cdot \pi \cdot t)$, $i_q^*(t) = 0$

Chapter 5.

Comparison and analysis

In this chapter, a summary of the time domain responses, pole-zero map and Bode is presented for the three studied controls. The three controls are excited by the same inputs and the three controls also use the same filter and k_p - k_i gains for their regulators. For an easier comparison, the results of the simulations are grouped into three columns, each one of them dedicated for a control.

Hence, first of all in Figure 32 the time domain responses to a unit step input in $i_d^*(t)$ and $i_q^*(t)$, are presented. Above, the voltages created by the control are shown. Then below, the current $i_\alpha(t)$ and $i_\beta(t)$, while finally, at the bottom, the natural response (only exponential terms of the time domain response) of $i_\alpha(t)$ is shown.

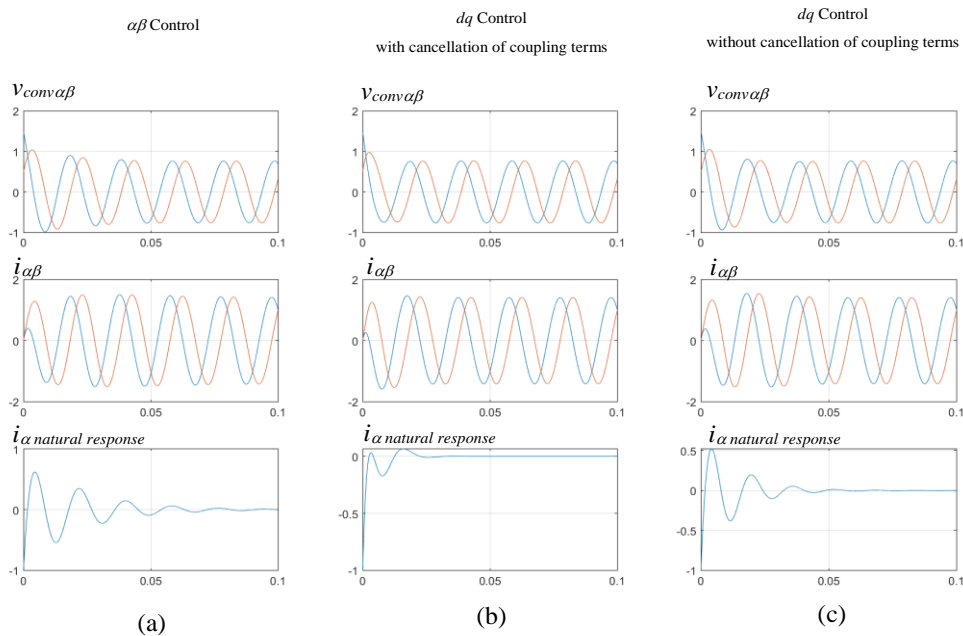


Figure 32. Time domain responses to an unit step input in $i_d^*(t)$ and $i_q^*(t)$, for the three types of controls studied, (a) Control in stationary reference frame ($\alpha\beta$), (b) Control in synchronous reference frame (dq) with current coupling cancellation, (c) Control in synchronous reference frame (dq) without current coupling cancellation. Conditions of Appendix E.

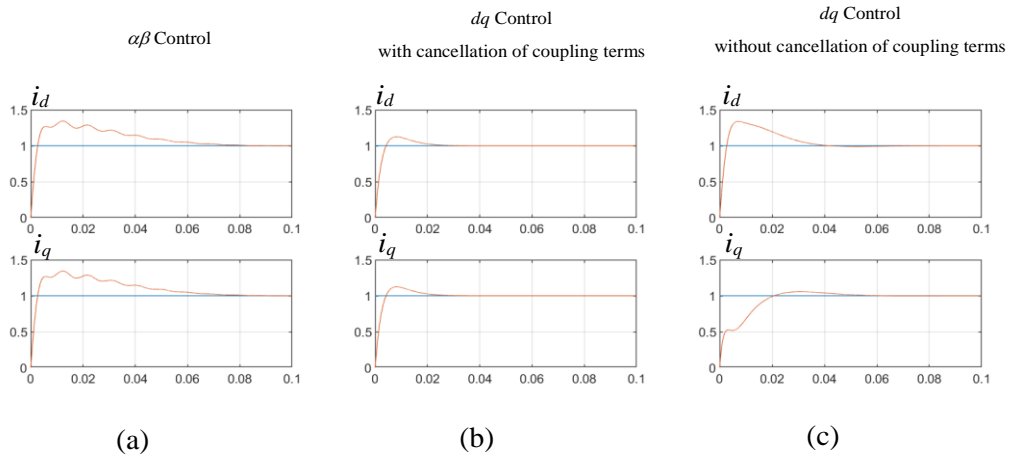


Figure 33. Time domain responses to an unit step input in $i_d^*(t)$ and $i_q^*(t)$, for the three types of controls studied and only current in dq reference frame are shown. (a) Control in stationary reference frame ($\alpha\beta$), (b) Control in synchronous reference frame (dq) with current coupling cancellation, (c) Control in synchronous reference frame (dq) without current coupling cancellation. Conditions of Appendix E.

It is seen that for the same values of k_p-k_i , the control in dq with cancellation of current coupling terms achieves the steady-state faster than the other two controls. Nevertheless, the differences are not very significant. However, it must be remarked that by changing the gain values of k_p-k_i , the dq control without cancellation of coupling terms and the $\alpha\beta$ control, probably could achieve faster dynamic response.

Then, in Figure 33 it is also seen the behavior of the same currents under the same experiment but after being transformed into dq reference frame. In this case also occurs that the fastest dynamic is achieved, by the control in dq with cancellation of current coupling terms. It is remarkable also that in $\alpha\beta$ control, it appears an small oscillatory current when transformed the $\alpha\beta$ currents to dq reference frame.

The dynamic response behavior of these controls, is in good agreement with the pole-zero maps shown in Figure 34. It is possible to see how the $\alpha\beta$ control and the dq control without cancellation of coupling terms, present a pair of conjugate pole pair with smallest real part around -50 and -80 respectively, while the control in dq with cancellation of coupling terms presents a lowest real part of conjugate pole around -210. Thus, by checking the smallest real part of the poles, it is deduced that the control in dq with cancellation of coupling terms presents a natural response that is damped between 3 or 4 times faster than the other two controls.

Figure 34 also shows the Bodes of the three studied controls. The biggest remarkable difference is that only in dq control with cancellation of coupling terms, achieves the same gain at both frequencies $\omega_l + \omega$ and $\omega_l - \omega$.

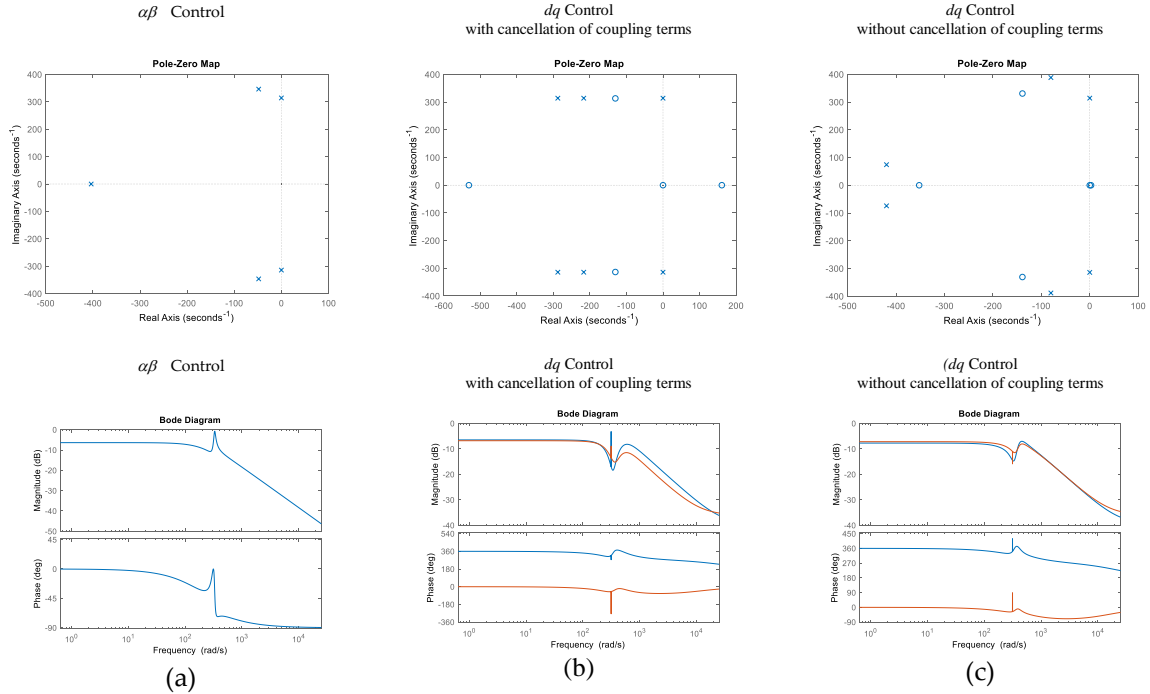


Figure 34. Poles to a step input and Bode diagrams of transfer function $I_\alpha(s)/I_d^*(s)$, for the three types of controls studied (rest of transfer functions present very similar behavior: $I_\alpha(s)/I_q^*(s)$, $I_\beta(s)/I_d^*(s)$, $I_\beta(s)/I_q^*(s)$). (a) Control in stationary reference frame ($\alpha\beta$), (b) Control in synchronous reference frame (dq) with current coupling cancellation, (c) Control in synchronous reference frame (dq) without current coupling cancellation. Conditions of Appendix E.

Coming back again to the poles, Figure 35 shows the poles to a step input of control in synchronous reference frame (dq) with current coupling cancellation. It is seen that this control achieves to maintain the real part of the poles responsible of the dynamic response to a step input, in both dq and $\alpha\beta$ representation. This means that damping factors, σ , of the current dynamic is equal in both dq and $\alpha\beta$ representation of the currents. Note that in reality, a perfect cancellation of current coupling terms is very difficult due to the effect of delays of filters and computation delays mainly, as later will be shown more under detail.

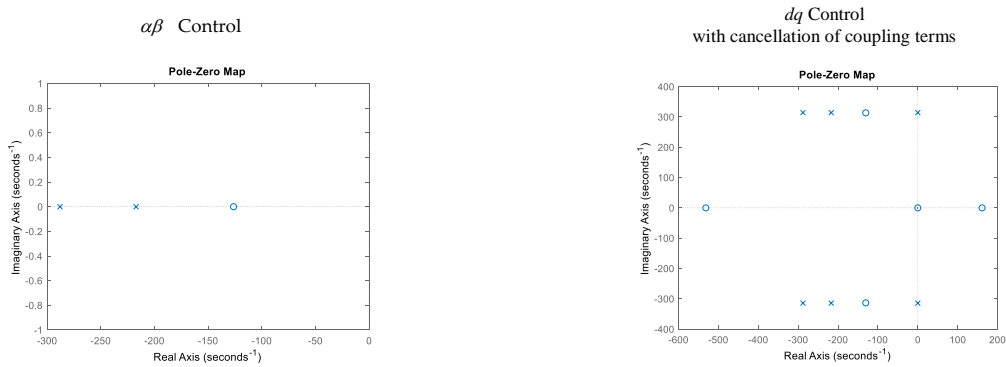


Figure 35. Poles to a step input of control in synchronous reference frame (dq) with current coupling cancellation. (a) Current in dq reference frame, i.e.: Transfer function: $I_d(s)/I_d^*(s)$ (b) Current in $\alpha\beta$ reference frame, i.e.: Transfer function: $I_\alpha(s)/I_\alpha^*(s)$. Conditions of Appendix E.

Finally, in Figure 36, poles, time domain responses and Bode diagrams of the three studied controls ($I_\alpha(s)/I_\alpha^*(s)$ and $i_\alpha(t)$ time domain responses) at different conditions of the regulators are shown. It is seen how the poles and zeros are affected by a different tuning of the regulator, how the time domain responses are affected and finally, how the Bode diagrams are also modified. A remarkable difference is that for the gains k_p and k_i evaluated at least, there is a clear tendency of control in dq with cancellation of the coupling terms, to be more stable. Being more specific, for the evaluated gains, the dq control with cancellation maintains the real part of the poles further away from the imaginary axis, producing also less oscillatory step responses.

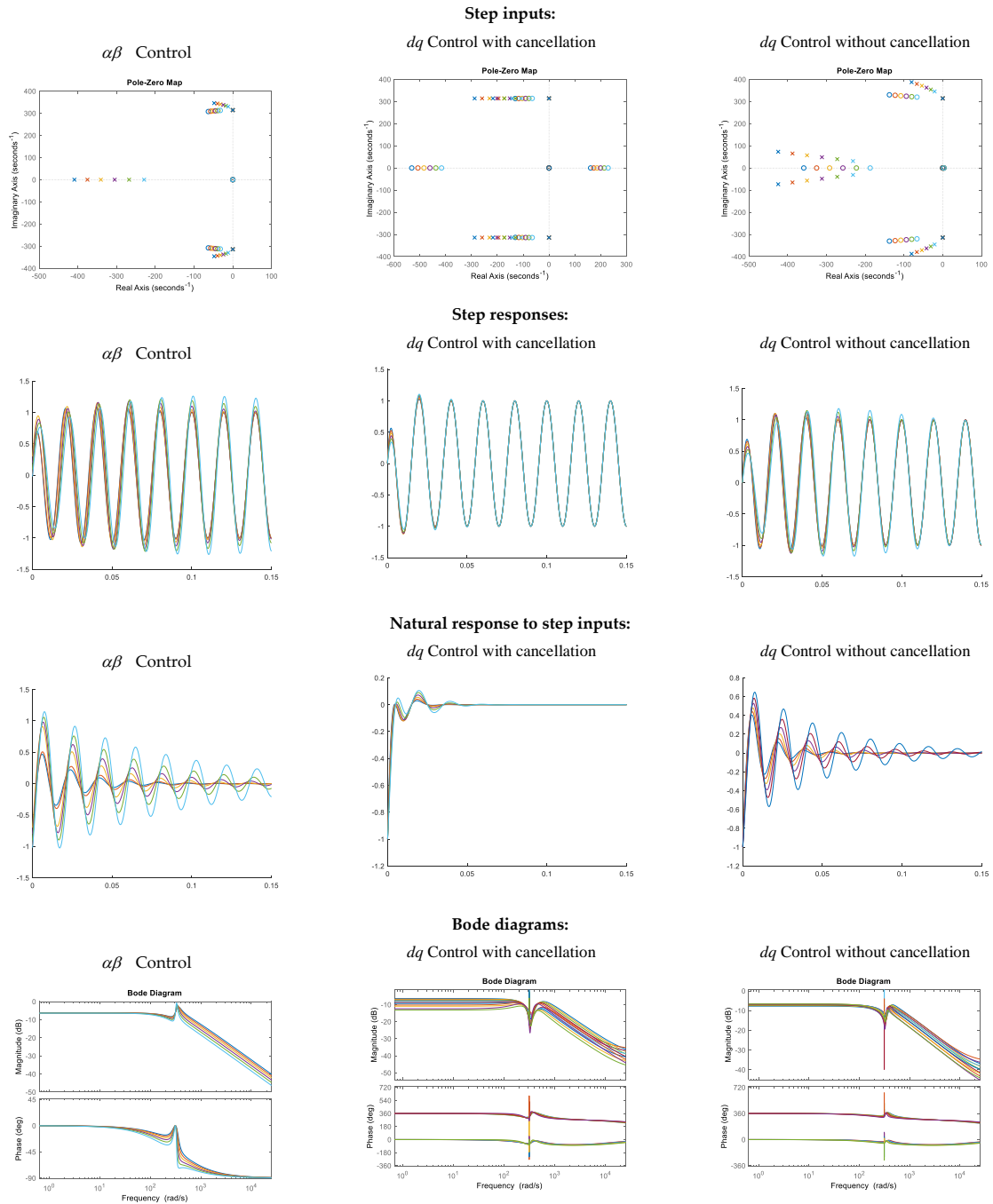


Figure 36. Poles, time domain responses and Bode diagrams of the three studied controls of $I_d(s)/I_d^*(s)$ at different conditions of the regulator. Conditions: $R = 1\Omega$, $L = 1\text{mH}$, $\xi = 1.01$ and $\omega_n = (R/L) \cdot 25 \cdot [1, 0.9, 0.8, 0.7, 0.6, 0.5]$.

Finally, the following tables show a summary of the most relevant equations for the studied controls.

Table VIII. Most relevant expressions of the three control studied for step inputs (β magnitudes are not shown for simplicity).

$\alpha\beta$ control	dq control with cancellation of coupling terms	dq control without cancellation of coupling terms
Step inputs		
$V_{convz}(s) =$ $-\left(k_p + \frac{k_i s}{s^2 + \omega^2}\right) I_\alpha(s)$ $+ \left(\frac{k_p s^2}{s^2 + \omega^2} + \frac{k_i s^3}{(s^2 + \omega^2)^2}\right) I_d^*(s)$ $- \left(\frac{k_p \omega s}{s^2 + \omega^2} + \frac{\omega k_i s^2}{(s^2 + \omega^2)^2}\right) I_q^*(s)$ $+ V_{ga}(s)$	$V_{convz}(s) =$ $-\left(k_p + \frac{k_i s}{s^2 + \omega^2}\right) I_\alpha(s)$ $+ \left(\frac{-\omega L s^2 + (k_i \omega - \omega^3 L)}{s^2 + \omega^2}\right) I_\beta(s)$ $+ \left(\frac{k_p s^2}{s^2 + \omega^2} + \frac{k_i s(s^2 - \omega^2)}{(s^2 + \omega^2)^2}\right) I_d^*(s)$ $- \left(\frac{k_p \omega s}{s^2 + \omega^2} - \frac{2\omega k_i s^2}{(s^2 + \omega^2)^2}\right) I_q^*(s)$ $+ V_{ga}(s)$	$V_{convz}(s) =$ $-\left(k_p + \frac{k_i s}{s^2 + \omega^2}\right) I_\alpha(s)$ $+ \left(\frac{\omega k_i}{s^2 + \omega^2}\right) I_\beta(s)$ $+ \left(\frac{k_p s^2}{s^2 + \omega^2} + \frac{k_i s(s^2 - \omega^2)}{(s^2 + \omega^2)^2}\right) I_d^*(s)$ $- \left(\frac{k_p \omega s}{s^2 + \omega^2} - \frac{2\omega k_i s^2}{(s^2 + \omega^2)^2}\right) I_q^*(s)$ $+ V_{ga}(s)$
$I_\alpha(s) =$ $\left(k_p + \frac{k_i s}{s^2 + \omega^2}\right) \left(\frac{s^2}{A(s)}\right) I_d^*(s)$ $- \left(k_p + \frac{k_i s}{s^2 + \omega^2}\right) \left(\frac{\omega s}{A(s)}\right) I_q^*(s)$	$I_\alpha(s) =$ $\left(k_p s + \frac{k_i(s^2 - \omega^2)}{s^2 + \omega^2}\right) \left(\frac{s}{A(s)}\right) I_d^*(s)$ $- \left(k_p + \frac{2k_i s}{s^2 + \omega^2}\right) \left(\frac{\omega s}{A(s)}\right) I_q^*(s)$ $+ \left(\frac{-\omega L s^2 + (k_i \omega - \omega^3 L)}{A(s)}\right) I_\beta(s)$ <p style="text-align: center;">↓</p> $I_\alpha(s) =$ $\left(\frac{G_{\alpha d}(s) + G_{\beta d}(s)G_{\alpha\beta}(s)}{1 - G_{\alpha\beta}(s)G_{\beta\alpha}(s)}\right) I_d^*(s)$ $+ \left(\frac{G_{\alpha q}(s) + G_{\beta q}(s)G_{\alpha\beta}(s)}{1 - G_{\alpha\beta}(s)G_{\beta\alpha}(s)}\right) I_q^*(s)$ <p style="text-align: center;">(See chapter 3 for solutions)</p>	$I_\alpha(s) =$ $\left(k_p s + \frac{k_i(s^2 - \omega^2)}{s^2 + \omega^2}\right) \left(\frac{s}{A(s)}\right) I_d^*(s)$ $- \left(k_p + \frac{2k_i s}{s^2 + \omega^2}\right) \left(\frac{\omega s}{A(s)}\right) I_q^*(s)$ $+ \left(\frac{k_i \omega}{A(s)}\right) I_\beta(s)$ <p style="text-align: center;">↓</p> $I_\alpha(s) =$ $\left(\frac{G_{\alpha d}(s) + G_{\beta d}(s)G_{\alpha\beta}(s)}{1 - G_{\alpha\beta}(s)G_{\beta\alpha}(s)}\right) I_d^*(s)$ $+ \left(\frac{G_{\alpha q}(s) + G_{\beta q}(s)G_{\alpha\beta}(s)}{1 - G_{\alpha\beta}(s)G_{\beta\alpha}(s)}\right) I_q^*(s)$ <p style="text-align: center;">(See chapter 4 for solutions)</p>
$i_\alpha(t) =$ $\left((B_0) \cdot e^{\sigma t} + (2 \cdot B_1) \cdot e^{\sigma t} \cdot \cos(\omega_{d1} \cdot t + \arg B_1)\right)$ $+ (2 \cdot B_2) \cdot \cos(\omega \cdot t) I_d^* $ $+ \left((B_3) \cdot e^{\sigma t} + (2 \cdot B_4) \cdot e^{\sigma t} \cdot \cos(\omega_{d3} \cdot t + \arg B_4)\right)$ $+ (2 \cdot B_5) \cdot \cos(\omega \cdot t + \pi/2) I_q^* $	$i_\alpha(t) =$ $\left((2 \cdot B_0) \cdot e^{\sigma t} \cdot \cos(\omega_{d0} \cdot t + \arg B_0)\right)$ $+ (2 \cdot B_1) \cdot e^{\sigma t} \cdot \cos(\omega_{d1} \cdot t + \arg B_1) + (2 \cdot B_2) \cdot \cos(\omega \cdot t) I_d^* $ $+ \left((2 \cdot B_3) \cdot e^{\sigma t} \cdot \cos(\omega_{d3} \cdot t + \arg B_3)\right)$ $+ (2 \cdot B_4) \cdot e^{\sigma t} \cdot \cos(\omega_{d4} \cdot t + \arg B_4) + (2 \cdot B_5) \cdot \cos(\omega \cdot t + \pi/2) I_q^* $	$i_\alpha(t) =$ $\left((2 \cdot B_0) \cdot e^{\sigma t} \cdot \cos(\omega_{d0} \cdot t + \arg B_0)\right)$ $+ (2 \cdot B_1) \cdot e^{\sigma t} \cdot \cos(\omega_{d1} \cdot t + \arg B_1) + (2 \cdot B_2) \cdot \cos(\omega \cdot t) I_d^* $ $+ \left((2 \cdot B_3) \cdot e^{\sigma t} \cdot \cos(\omega_{d3} \cdot t + \arg B_3)\right)$ $+ (2 \cdot B_4) \cdot e^{\sigma t} \cdot \cos(\omega_{d4} \cdot t + \arg B_4) + (2 \cdot B_5) \cdot \cos(\omega \cdot t + \pi/2) I_q^* $
$A(s) = Ls^3 + (k_p + R)s^2 + (L\omega^2 + k_i)s + (k_p + R)\omega^2$		

Table IX. Most relevant expressions of the three control studied for sinusoidal and cosenoidal inputs (β magnitudes are not shown for simplicity).

$\alpha\beta$ control	dq control with cancellation of coupling terms	dq control without cancellation of coupling terms
Sinusoidal inputs		
$V_{\text{comm}}(s) = \left(k_p + \frac{k_i s}{s^2 + \omega^2}\right) [-I_\alpha(s) + \left(\frac{1}{2}\right) \left(\frac{s^2 + \omega_1^2}{\omega_1}\right) \left(\frac{\omega_1 + \omega}{s^2 + (\omega_1 + \omega)^2} + \frac{\omega_1 - \omega}{s^2 + (\omega_1 - \omega)^2}\right) I_d^*(s) - \left(\frac{1}{2}\right) \left(\frac{s^2 + \omega_1^2}{s}\right) \left(\frac{\omega_1 + \omega}{s^2 + (\omega_1 + \omega)^2} - \frac{\omega_1 - \omega}{s^2 + (\omega_1 - \omega)^2}\right) I_q^*(s)] + V_{\text{ref}}(s)$	$V_{\text{comm}}(s) = -\left(k_p + \frac{k_i s}{s^2 + \omega^2}\right) I_\alpha(s) + \left(\frac{-\omega L s^2 + (k_i \omega - \omega^2 L)}{s^2 + \omega^2}\right) I_\beta(s) + \left(\frac{k_p}{2}\right) \left(\frac{s^2 + \omega_1^2}{\omega_1}\right) \left(\frac{\omega_1 + \omega}{s^2 + (\omega_1 + \omega)^2} + \frac{\omega_1 - \omega}{s^2 + (\omega_1 - \omega)^2}\right) I_d^*(s) - \left(\frac{k_i}{2}\right) \left(\frac{s^2 + \omega_1^2}{\omega_1^2}\right) \left(\frac{s}{s^2 + (\omega_1 + \omega)^2} + \frac{s}{s^2 + (\omega_1 - \omega)^2} + \frac{2s}{s^2 + \omega^2}\right) I_d^*(s) - \left(\frac{k_p}{2}\right) \left(\frac{s^2 + \omega_1^2}{s}\right) \left(\frac{\omega_1 + \omega}{s^2 + (\omega_1 + \omega)^2} - \frac{\omega_1 - \omega}{s^2 + (\omega_1 - \omega)^2}\right) I_q^*(s) - \left(\frac{k_i}{2\omega_1}\right) \left(\frac{s^2 + \omega_1^2}{s}\right) \left(\frac{s}{s^2 + (\omega_1 + \omega)^2} - \frac{s}{s^2 + (\omega_1 - \omega)^2}\right) I_q^*(s) + V_{\text{ref}}(s)$	$V_{\text{comm}}(s) = -\left(k_p + \frac{k_i s}{s^2 + \omega^2}\right) I_\alpha(s) + \left(\frac{k_i \omega}{s^2 + \omega^2}\right) I_\beta(s) + \left(\frac{k_p}{2}\right) \left(\frac{s^2 + \omega_1^2}{\omega_1}\right) \left(\frac{\omega_1 + \omega}{s^2 + (\omega_1 + \omega)^2} + \frac{\omega_1 - \omega}{s^2 + (\omega_1 - \omega)^2}\right) I_d^*(s) - \left(\frac{k_i}{2}\right) \left(\frac{s^2 + \omega_1^2}{\omega_1^2}\right) \left(\frac{s}{s^2 + (\omega_1 + \omega)^2} + \frac{s}{s^2 + (\omega_1 - \omega)^2} + \frac{2s}{s^2 + \omega^2}\right) I_d^*(s) - \left(\frac{k_p}{2}\right) \left(\frac{s^2 + \omega_1^2}{s}\right) \left(\frac{\omega_1 + \omega}{s^2 + (\omega_1 + \omega)^2} - \frac{\omega_1 - \omega}{s^2 + (\omega_1 - \omega)^2}\right) I_q^*(s) - \left(\frac{k_i}{2\omega_1}\right) \left(\frac{s^2 + \omega_1^2}{s}\right) \left(\frac{s}{s^2 + (\omega_1 + \omega)^2} - \frac{s}{s^2 + (\omega_1 - \omega)^2}\right) I_q^*(s) + V_{\text{ref}}(s)$
$I_\alpha(s) = \left(\frac{k_p s^2 + k_i s + k_p \omega^2}{A(s)}\right) \left(\frac{1}{2}\right) \left[\left(\frac{s^2 + \omega_1^2}{\omega_1}\right) \left(\frac{\omega_1 + \omega}{s^2 + (\omega_1 + \omega)^2} + \frac{\omega_1 - \omega}{s^2 + (\omega_1 - \omega)^2}\right) I_d^*(s) - \left(\frac{s^2 + \omega_1^2}{s}\right) \left(\frac{\omega_1 + \omega}{s^2 + (\omega_1 + \omega)^2} - \frac{\omega_1 - \omega}{s^2 + (\omega_1 - \omega)^2}\right) I_q^*(s)\right]$	$I_\alpha(s) = \left(\frac{(s^2 + \omega^2) \cdot D_\alpha(s)}{A(s)}\right) I_d^*(s) - \left(\frac{(s^2 + \omega^2) \cdot Q_\alpha(s)}{A(s)}\right) I_q^*(s) + \left(\frac{-\omega L s^2 + (k_i \omega - \omega^2 L)}{A(s)}\right) I_\beta(s)$ <p style="text-align: center;">↓</p> $I_\alpha(s) = \left(\frac{G_{\alpha d \rightarrow s}(s) + G_{\beta d \rightarrow s}(s) G_{\alpha \beta \rightarrow s}(s)}{1 - G_{\alpha \beta \rightarrow s}(s) G_{\beta \alpha \rightarrow s}(s)}\right) I_d^*(s) + \left(\frac{G_{\alpha q \rightarrow s}(s) + G_{\beta q \rightarrow s}(s) G_{\alpha \beta \rightarrow s}(s)}{1 - G_{\alpha \beta \rightarrow s}(s) G_{\beta \alpha \rightarrow s}(s)}\right) I_q^*(s)$ <p style="text-align: center;">(See chapter 3 for solutions)</p>	$I_\alpha(s) = \left(\frac{(s^2 + \omega^2) \cdot D_\alpha(s)}{A(s)}\right) I_d^*(s) - \left(\frac{(s^2 + \omega^2) \cdot Q_\alpha(s)}{A(s)}\right) I_q^*(s) + \left(\frac{k_i \omega}{A(s)}\right) I_\beta(s)$ <p style="text-align: center;">↓</p> $I_\alpha(s) = \left(\frac{G_{\alpha d \rightarrow s}(s) + G_{\beta d \rightarrow s}(s) G_{\alpha \beta \rightarrow s}(s)}{1 - G_{\alpha \beta \rightarrow s}(s) G_{\beta \alpha \rightarrow s}(s)}\right) I_d^*(s) + \left(\frac{G_{\alpha q \rightarrow s}(s) + G_{\beta q \rightarrow s}(s) G_{\alpha \beta \rightarrow s}(s)}{1 - G_{\alpha \beta \rightarrow s}(s) G_{\beta \alpha \rightarrow s}(s)}\right) I_q^*(s)$ <p style="text-align: center;">(See chapter 4 for solutions)</p>
$i_\alpha(t) = \left((B_0) \cdot e^{\sigma t} + (2 \cdot B_1) \cdot e^{\sigma t} \cdot \cos(\omega_{a1} \cdot t + \arg B_1) + (2 \cdot B_2) \cdot \cos((\omega_1 + \omega) \cdot t + \arg B_2) + (2 \cdot B_3) \cdot \cos((\omega_1 - \omega) \cdot t + \arg B_3)\right) I_d^* + \left((B_4) \cdot e^{\sigma t} + (2 \cdot B_5) \cdot e^{\sigma t} \cdot \cos(\omega_{a5} \cdot t + \arg B_5) + (2 \cdot B_6) \cdot \cos((\omega_1 + \omega) \cdot t + \arg B_6) + (2 \cdot B_7) \cdot \cos((\omega_1 - \omega) \cdot t + \arg B_7)\right) I_q^* $	$i_\alpha(t) = [(2 \cdot B_0) \cdot \cos((\omega_1 + \omega) \cdot t + \arg B_0) + (2 \cdot B_1) \cdot \cos((\omega_1 - \omega) \cdot t + \arg B_1) + (2 \cdot B_2) \cdot e^{\sigma t} \cdot \cos(\omega_{a2} \cdot t + \arg B_2) + (2 \cdot B_3) \cdot e^{\sigma t} \cdot \cos(\omega_{a3} \cdot t + \arg B_3)] I_d^* + [(2 \cdot B_4) \cdot \cos((\omega_1 + \omega) \cdot t + \arg B_4) + (2 \cdot B_5) \cdot \cos((\omega_1 - \omega) \cdot t + \arg B_5) + (2 \cdot B_6) \cdot e^{\sigma t} \cdot \cos(\omega_{a6} \cdot t + \arg B_6) + (2 \cdot B_7) \cdot e^{\sigma t} \cdot \cos(\omega_{a7} \cdot t + \arg B_7)] I_q^* $	$i_\alpha(t) = [(2 \cdot B_0) \cdot \cos((\omega_1 + \omega) \cdot t + \arg B_0) + (2 \cdot B_1) \cdot \cos((\omega_1 - \omega) \cdot t + \arg B_1) + (2 \cdot B_2) \cdot e^{\sigma t} \cdot \cos(\omega_{a2} \cdot t + \arg B_2) + (2 \cdot B_3) \cdot e^{\sigma t} \cdot \cos(\omega_{a3} \cdot t + \arg B_3)] I_d^* + [(2 \cdot B_4) \cdot \cos((\omega_1 + \omega) \cdot t + \arg B_4) + (2 \cdot B_5) \cdot \cos((\omega_1 - \omega) \cdot t + \arg B_5) + (2 \cdot B_6) \cdot e^{\sigma t} \cdot \cos(\omega_{a6} \cdot t + \arg B_6) + (2 \cdot B_7) \cdot e^{\sigma t} \cdot \cos(\omega_{a7} \cdot t + \arg B_7)] I_q^* $
$A(s) = Ls^3 + (k_p + R)s^2 + (L\omega^2 + k_i)s + (k_p + R)\omega^2$		
$D_\alpha(s) = \left(\frac{s^2 + \omega_1^2}{\omega_1}\right) \left[\left(\frac{k_p}{2}\right) \left(\frac{\omega_1 + \omega}{s^2 + (\omega_1 + \omega)^2} + \frac{\omega_1 - \omega}{s^2 + (\omega_1 - \omega)^2}\right) - \left(\frac{k_i}{2\omega_1}\right) \left(\frac{s}{s^2 + (\omega_1 + \omega)^2} + \frac{s}{s^2 + (\omega_1 - \omega)^2}\right) + \left(\frac{k_i}{\omega_1}\right) \left(\frac{s}{s^2 + \omega^2}\right)\right]$ $Q_\alpha(s) = \left(\frac{k_p}{2}\right) \left(\frac{s^2 + \omega_1^2}{s}\right) \left(\frac{\omega_1 + \omega}{s^2 + (\omega_1 + \omega)^2} - \frac{\omega_1 - \omega}{s^2 + (\omega_1 - \omega)^2}\right) + \left(\frac{k_i}{2\omega_1}\right) \left(\frac{s^2 + \omega_1^2}{s}\right) \left(\frac{s}{s^2 + (\omega_1 - \omega)^2} - \frac{s}{s^2 + (\omega_1 + \omega)^2}\right)$		

Chapter 6.

Experimental validation of the analytical models

In this chapter, the experimental validation of the mathematical model equations derived in previous chapters is carried out. The experimental platform employed is presented in Figure 37. Its main parameters and characteristics are specified in appendix F. The control block diagrams implemented are depicted in Figure 38. Note that the power system does not present a DC voltage source, what means that the active power exchange with grid cannot be controlled freely. Consequently, it is necessary to incorporate a DC bus voltage control loop as depicted in Figure 38.

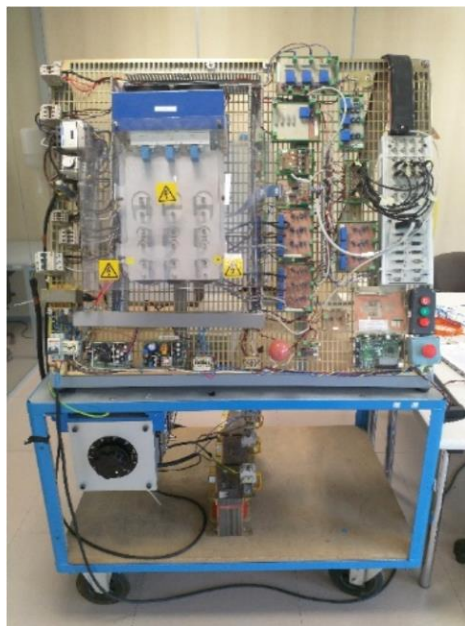


Figure 37. Experimental platform of the grid connected converter. Main characteristics: Appendix F.

Trying to simplify the set of results presented in this validation, only one input response is evaluated for all the controls. More specifically, a q axis current step change is applied to the controls studied in this book, and the experimental response obtained is compared with the mathematical model equations derived. Thus, the obtained results are depicted in Figures 39 and fig 40.

In Figure 39, the three studied control of this book are evaluated in a step response of 4 Amps at i_q . In this set of results the employed gains for the PIR and PI regulators are: $k_p = 10$ and $k_i = 3500$. In all the controls and variables shown, the experimental and analytical models show a reasonably good agreement both at steady-state and transient response.

Then, in Figure 39, the same experiment is carried out but in this case, with a smaller gains at the PIR and PI regulators: $k_p = 4.4$ and $k_i = 395$. This choice, produces a slower dynamic response of the currents. Under these regulators gains, it has been observed that the PIR regulators did present difficulties for stabilization (mainly due to the high frequency current ripple present and the discretization method employed for the regulators), so only controls in dq (with and without cancellation of the current coupling terms) are evaluated. The agreement under these conditions between the experimental behavior and the mathematical models is reasonably good as well.

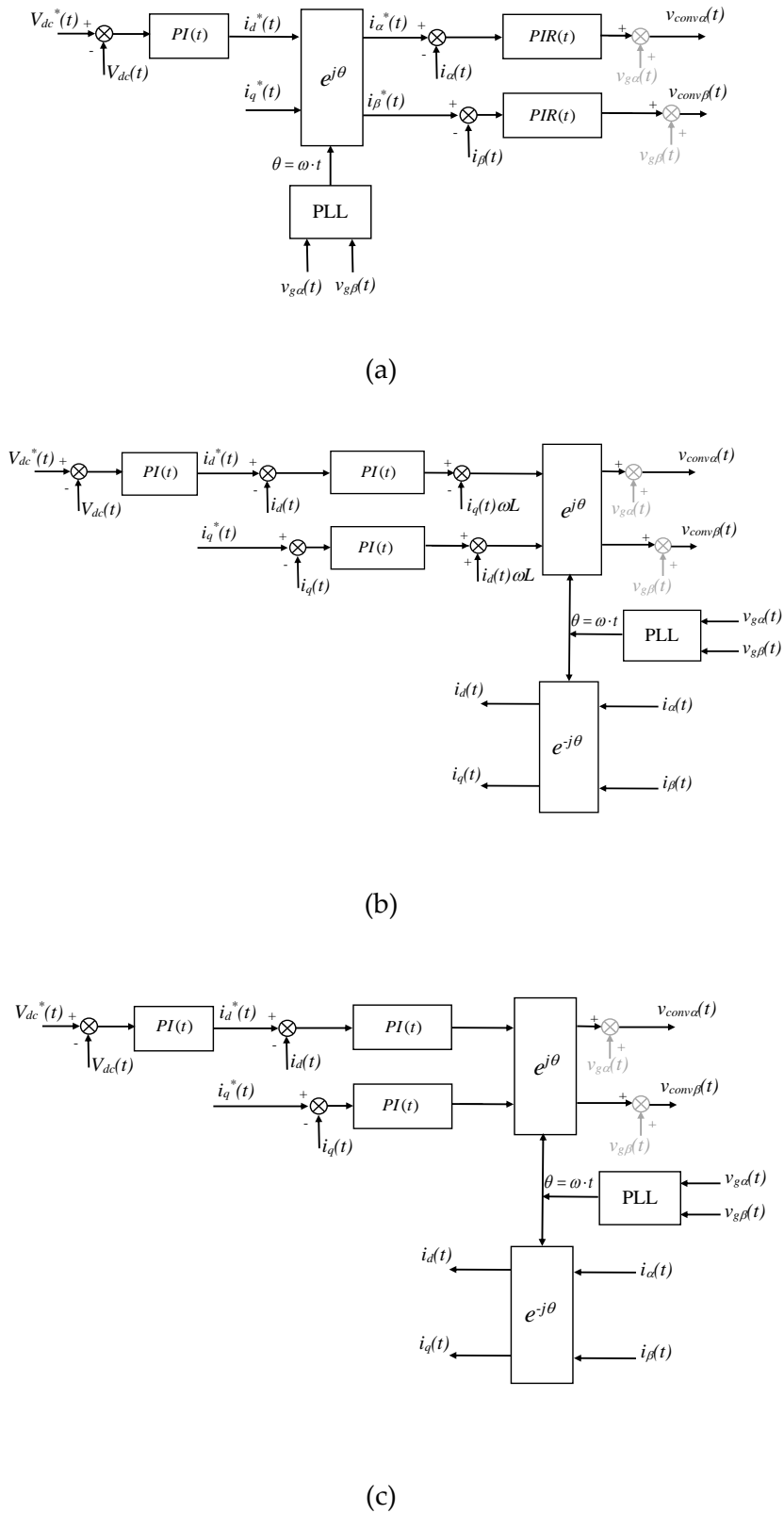


Figure 38. Control block diagram of the three studied controls, with inclusion of the DC bus voltage control loop.

These tests have been repeated under many other operating conditions, but due to lack of space are not shown in this book. In all the cases, the agreement between both experimental and analytical results have been observed to be reasonably good, very similar to what it has been shown in Figure 39 and Figure 40.

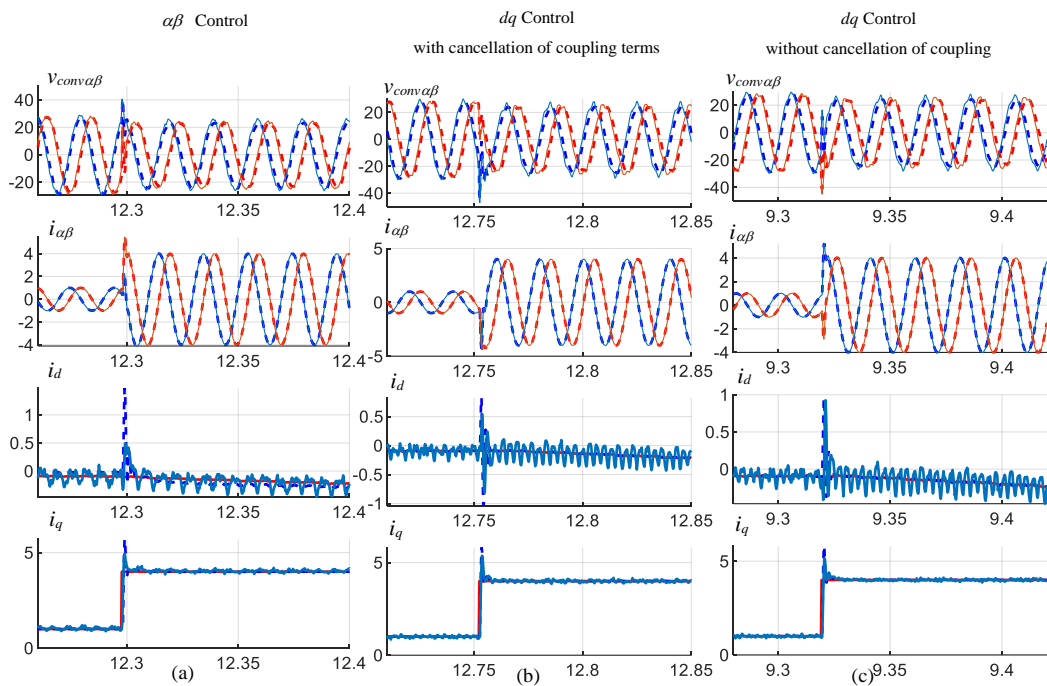


Figure 39. Time domain responses to a 4 Amps step input in $i_q^*(t)$, for the three types of controls studied: Experimental -> continuous lines, Mathematical models -> dashed lines, (a) Control in stationary reference frame ($\alpha\beta$), (b) Control in synchronous reference frame (dq) with current coupling cancellation, (c) Control in synchronous reference frame (dq) without current coupling cancellation. Conditions of Appendix F. Gains for the PIR and PI regulators: $k_p = 10$ and $k_i = 3500$.

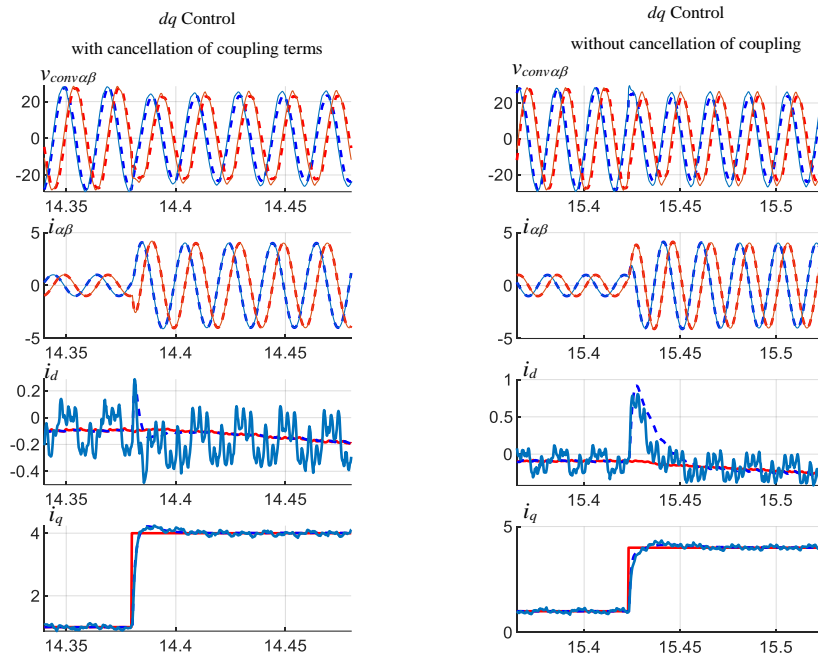


Figure 40. Time domain responses to a 4 Amps step input in $i_q^*(t)$, for two of the controls studied: Experimental \rightarrow continuous lines, Mathematical models \rightarrow dashed lines, (a) Control in synchronous reference frame (dq) with current coupling cancellation, (b) Control in synchronous reference frame (dq) without current coupling cancellation. Conditions of Appendix F. Gains for the PIR and PI regulators: $k_p = 4.4$ and $k_i = 395$.

Chapter 7.

Inclusion of delay and filter at current measurement

7.1. Control of currents in stationary reference frame ($\alpha\beta$) for step inputs

Approaching to a more realistic modelling of the control under some specific contexts, let us now consider the inevitable delay between the voltage reference generation and the actual synthetization, $Del(t)$, and the low pass filter that is normally employed at the current measurements $F_i(t)$, to reduce the current ripple seen by the control. This is represented in block diagram of Figure 41. Note that at the grid voltages no filter has been considered, because at strong grids, this voltage is not severely corrupted by ripple or other perturbations.

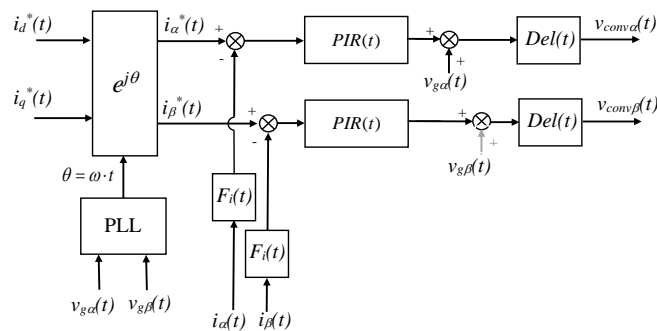


Figure 41. Current control block diagram in stationary reference frame ($\alpha\beta$) with two resonant controllers and inclusion of converter's delay and filter for current measurement.

Thus, the α and β components of the converter voltages, considering the grid voltage feedforward terms, are mathematically represented in time domain as follows (Note that the harmonics created by the converter are neglected):

$$v_{conv\alpha}(t) = \left[\left(i_d^*(t) \cdot \cos(\omega t) - i_q^*(t) \cdot \sin(\omega t) \right) \otimes PIR(t) - \left(i_\alpha(t) \otimes F_i(t) \right) \otimes PIR(t) + v_{g\alpha}(t) \right] \otimes Del(t) \quad (167)$$

$$v_{conv\beta}(t) = \left[\left(i_d^*(t) \cdot \sin(\omega t) + i_q^*(t) \cdot \cos(\omega t) \right) \otimes PIR(t) - \left(i_\beta(t) \otimes F_i(t) \right) \otimes PIR(t) + v_{g\beta}(t) \right] \otimes Del(t) \quad (168)$$

Considering **step** inputs at both $I_d^*(s)$ and $I_q^*(s)$ and assuming that the grid voltage is ideal or not perturbed, i.e., assuming no angle phase shift and ω constant, the previous time domain expressions can be transformed into the 's' domain as follows:

$$V_{conv\alpha}(s) = \left[- \left(k_p + \frac{k_i s}{s^2 + \omega^2} \right) \cdot F_i(s) \cdot I_\alpha(s) + \left(\frac{k_p s^2}{s^2 + \omega^2} + \frac{k_i s^3}{(s^2 + \omega^2)^2} \right) I_d^*(s) - \left(\frac{k_p \omega s}{s^2 + \omega^2} + \frac{\omega k_i s^2}{(s^2 + \omega^2)^2} \right) I_q^*(s) + V_{g\alpha}(s) \right] \cdot Del(s) \quad (169)$$

$$V_{conv\beta}(s) = \left[- \left(k_p + \frac{k_i s}{s^2 + \omega^2} \right) \cdot F_i(s) \cdot I_\beta(s) + \left(\frac{k_p \omega s}{s^2 + \omega^2} + \frac{\omega k_i s^2}{(s^2 + \omega^2)^2} \right) I_d^*(s) + \left(\frac{k_p s^2}{s^2 + \omega^2} + \frac{k_i s^3}{(s^2 + \omega^2)^2} \right) I_q^*(s) + V_{g\beta}(s) \right] \cdot Del(s) \quad (170)$$

Knowing also that the 's' domain equations of the power circuit are:

$$V_{conv\alpha}(s) - V_{g\alpha}(s) = I_\alpha(s) \cdot (R + Ls) \quad (171)$$

$$V_{conv\beta}(s) - V_{g\beta}(s) = I_\beta(s) \cdot (R + Ls) \quad (172)$$

Combining these expressions with the voltage applied by the control in equations (169) and (170), the closed loop current expression yield:

$$I_\alpha(s) = \left(k_p + \frac{k_i s}{s^2 + \omega^2} \right) \left(\frac{s^2}{s^2 + \omega^2} \right) \left(\frac{Del(s)}{B(s)} \right) I_d^*(s) - \left(k_p + \frac{k_i s}{s^2 + \omega^2} \right) \left(\frac{\omega s}{s^2 + \omega^2} \right) \left(\frac{Del(s)}{B(s)} \right) I_q^*(s) - \left(\frac{1 - Del(s)}{B(s)} \right) \cdot V_{g\alpha}(s) \quad (173)$$

$$\begin{aligned}
 I_{\beta}(s) &= \left(k_p + \frac{k_i s}{s^2 + \omega^2} \right) \left(\frac{\omega s}{s^2 + \omega^2} \right) \left(\frac{Del(s)}{B(s)} \right) I_d^*(s) \\
 &+ \left(k_p + \frac{k_i s}{s^2 + \omega^2} \right) \left(\frac{s^2}{s^2 + \omega^2} \right) \left(\frac{Del(s)}{B(s)} \right) I_q^*(s) - \left(\frac{1 - Del(s)}{B(s)} \right) \cdot V_{g\beta}(s)
 \end{aligned} \tag{174}$$

Being:

$$B(s) = \left(k_p + \frac{k_i s}{s^2 + \omega^2} \right) \cdot F_i(s) \cdot Del(s) + R + Ls \tag{175}$$

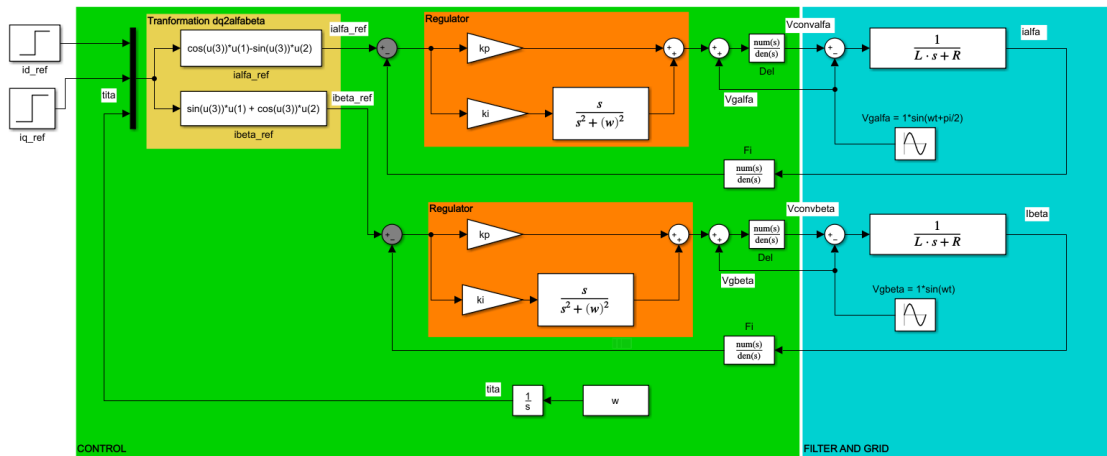
Then, the current filter and the delay can be modelled in a simple manner, for instance as follows:

$$F_i(s) = \frac{1}{T_i s + 1} \quad Del(s) = \frac{1}{T_d s + 1} \tag{176}$$

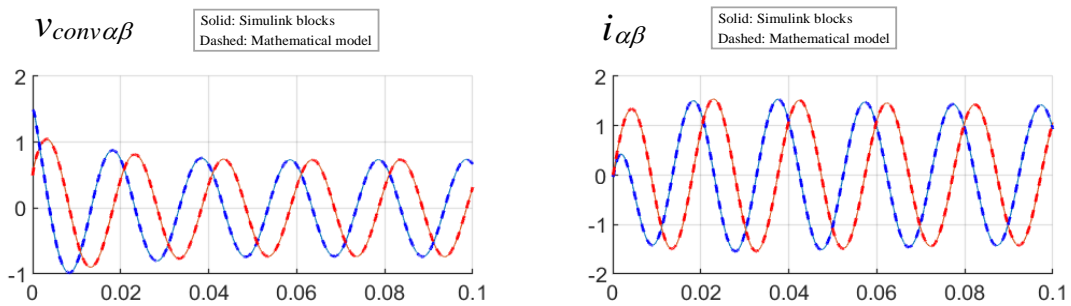
Note that is believed is more accurate any other filter and delay models could be substituted at previous expressions. Thus for instance, for modelling the delay a Pade approximation is also quite common. Next, equation shows as an example, a fourth order Pade approximation for a delay of 200µseg:

$$Del(s) = \frac{s^4 + a_3 s^3 + a_2 s^2 + a_1 s + a_0}{s^4 + b_3 s^3 + b_2 s^2 + b_1 s + b_0} \tag{177}$$

With; $a_3 = -9.9999e+04$, $a_2 = 4.4999e+09$, $a_1 = -1.05e+14$, $a_0 = 1.05e+18$, $b_3 = 9.9999e+04$, $b_2 = 4.4999e+09$, $b_1 = 1.05e+14$, $b_0 = 1.05e+18$. Nevertheless, in forthcoming analysis and for simplicity, both delay and filter are modelled as a first order system as described in equation (176). Hence, the following figure' results show that the time domain responses to step inputs, are perfectly described with the derived mathematical equations in correspondence with the Simulink blocks.



(a)



(b)

Figure 42. (a) Simulink model for evaluating the Step response, (b) Unit step (at both inputs) response of control of currents in stationary reference frame $\alpha\beta$. Conditions of Appendix E. With delay ($Del(s)=1/(Tas+1)$) and $Ta=1/5000/3sec$ and low pass filter at current measurements ($Fi(s)=1/(Tis+1)$) with time constant $T=1/5000sec$.

7.2. Control of currents in rotating reference frame (dq) with cancellation of coupling current terms for step inputs

This section includes also the inevitable delay between the voltage reference generation and the actual synthetization $Del(t)$ and the low pass filter at the current measurements $Fi(t)$. This is represented in block diagram of Figure 43. Note that at the grid voltages no filter has been considered, because at strong grids, this voltage is not corrupted by ripple or other perturbations.

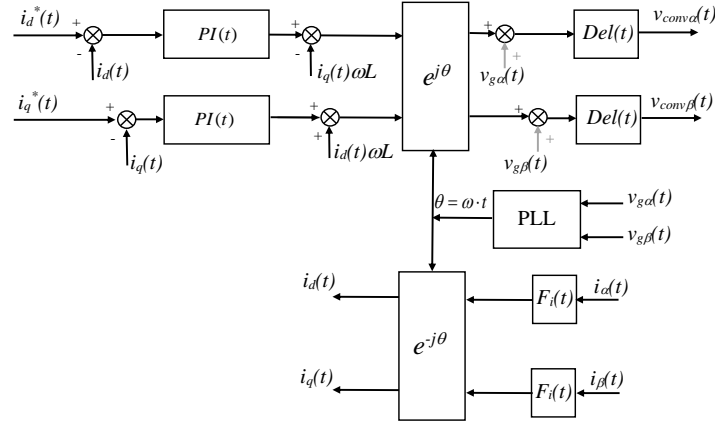


Figure 43. Current control block diagram in rotating reference frame (dq) with two PI controllers and cancellation of current coupling terms and inclusion of converter's delay and filter for current measurement.

The α and β components of the converter voltages, are mathematically represented in time domain as follows:

$$v_{conv\alpha}(t) = \left\{ \left(\left[i_d^*(t) - i_d(t) \right] \otimes PI(t) \right) \cdot \cos(\omega t) - \left(\left[i_q^*(t) - i_q(t) \right] \otimes PI(t) \right) \cdot \sin(\omega t) - \omega \cdot L \cdot i_q(t) \cdot \cos(\omega t) - \omega \cdot L \cdot i_d(t) \cdot \sin(\omega t) + v_{g\alpha}(t) \right\} \otimes Del(t) \quad (178)$$

$$v_{conv\beta}(t) = \left\{ \left(\left[i_d^*(t) - i_d(t) \right] \otimes PI(t) \right) \cdot \sin(\omega t) - \left(\left[i_q^*(t) - i_q(t) \right] \otimes PI(t) \right) \cdot \cos(\omega t) - \omega \cdot L \cdot i_q(t) \cdot \sin(\omega t) + \omega \cdot L \cdot i_d(t) \cdot \cos(\omega t) + v_{g\beta}(t) \right\} \otimes Del(t) \quad (179)$$

Which is equal to:

$$v_{conv\alpha}(t) = \left\{ \left(\left[i_d^*(t) - \left((i_\alpha(t) \otimes F_i(t)) \cdot \cos(\omega t) + (i_\beta(t) \otimes F_i(t)) \cdot \sin(\omega t) \right) \right] \otimes PI(t) \right) \cdot \cos(\omega t) - \left(\left[i_q^*(t) - \left(-(i_\alpha(t) \otimes F_i(t)) \cdot \sin(\omega t) + (i_\beta(t) \otimes F_i(t)) \cdot \cos(\omega t) \right) \right] \otimes PI(t) \right) \cdot \sin(\omega t) - \omega \cdot L \cdot \left(-(i_\alpha(t) \otimes F_i(t)) \cdot \sin(\omega t) + (i_\beta(t) \otimes F_i(t)) \cdot \cos(\omega t) \right) \cdot \cos(\omega t) - \omega \cdot L \cdot \left((i_\alpha(t) \otimes F_i(t)) \cdot \cos(\omega t) + (i_\beta(t) \otimes F_i(t)) \cdot \sin(\omega t) \right) \cdot \sin(\omega t) + v_{g\alpha}(t) \right\} \otimes Del(t) \quad (180)$$

$$v_{conv\beta}(t) = \left\{ \left(\left[i_d^*(t) - \left((i_\alpha(t) \otimes F_i(t)) \cdot \cos(\omega t) + (i_\beta(t) \otimes F_i(t)) \cdot \sin(\omega t) \right) \right] \otimes PI(t) \right) \cdot \sin(\omega t) - \left(\left[i_q^*(t) - \left(-(i_\alpha(t) \otimes F_i(t)) \cdot \sin(\omega t) + (i_\beta(t) \otimes F_i(t)) \cdot \cos(\omega t) \right) \right] \otimes PI(t) \right) \cdot \cos(\omega t) - \omega \cdot L \cdot \left(-(i_\alpha(t) \otimes F_i(t)) \cdot \sin(\omega t) + (i_\beta(t) \otimes F_i(t)) \cdot \cos(\omega t) \right) \cdot \sin(\omega t) + \omega \cdot L \cdot \left((i_\alpha(t) \otimes F_i(t)) \cdot \cos(\omega t) + (i_\beta(t) \otimes F_i(t)) \cdot \sin(\omega t) \right) \cdot \cos(\omega t) + v_{g\beta}(t) \right\} \otimes Del(t) \quad (181)$$

Considering **step** inputs at both $I_d^*(s)$ and $I_q^*(s)$ and assuming that the grid voltage is not perturbed so it is purely sinusoidal, i.e., assuming no angle jumps and ω constant, the previous time domain expressions can be transformed into the 's' domain as follows:

$$V_{conv\alpha}(s) = \left[-\left(k_p + \frac{k_i s}{s^2 + \omega^2} \right) \cdot F_i(s) \cdot I_\alpha(s) + \left(\frac{-\omega L s^2 + (k_i \omega - \omega^3 L)}{s^2 + \omega^2} \right) \cdot F_i(s) \cdot I_\beta(s) \right. \\ \left. + \left(\frac{k_p s^2}{s^2 + \omega^2} + \frac{k_i s(s^2 - \omega^2)}{(s^2 + \omega^2)^2} \right) I_d^*(s) - \left(\frac{k_p \omega s}{s^2 + \omega^2} - \frac{2\omega k_i s^2}{(s^2 + \omega^2)^2} \right) I_q^*(s) + V_{g\alpha}(s) \right] \cdot Del(s) \quad (182)$$

$$V_{conv\beta}(s) = \left[-\left(\frac{-\omega L s^2 + (k_i \omega - \omega^3 L)}{s^2 + \omega^2} \right) \cdot F_i(s) \cdot I_\alpha(s) - \left(k_p + \frac{k_i s}{s^2 + \omega^2} \right) \cdot F_i(s) \cdot I_\beta(s) \right. \\ \left. + \left(\frac{k_p \omega s}{s^2 + \omega^2} - \frac{2\omega k_i s^2}{(s^2 + \omega^2)^2} \right) I_d^*(s) + \left(\frac{k_p s^2}{s^2 + \omega^2} + \frac{k_i s(s^2 - \omega^2)}{(s^2 + \omega^2)^2} \right) I_q^*(s) + V_{g\beta}(s) \right] \cdot Del(s) \quad (183)$$

Being these expressions only valid for a step input at both $I_d^*(s)$ and $I_q^*(s)$:

$$I_d^*(s) = \frac{|I_d^*|}{s} \quad I_q^*(s) = \frac{|I_q^*|}{s} \quad (184)$$

As done in previous chapters, combining the last two control law expressions with the power circuit electric expressions, it is possible to derive the closed loop equation for both α and β currents:

$$I_\alpha(s) = \left(k_p s + \frac{k_i(s^2 - \omega^2)}{s^2 + \omega^2} \right) \left(\frac{s}{s^2 + \omega^2} \right) \left(\frac{Del(s)}{B(s)} \right) I_d^*(s) - \left(k_p + \frac{2k_i s}{s^2 + \omega^2} \right) \left(\frac{\omega s}{s^2 + \omega^2} \right) \left(\frac{Del(s)}{B(s)} \right) I_q^*(s) \\ + \left(\frac{-\omega L s^2 + (k_i \omega - \omega^3 L)}{s^2 + \omega^2} \right) \left(\frac{F_i(s) \cdot Del(s)}{B(s)} \right) I_\beta(s) - \left(\frac{1 - Del(s)}{B(s)} \right) \cdot V_{g\alpha}(s) \quad (185)$$

$$I_\beta(s) = \left(k_p + \frac{2k_i s}{s^2 + \omega^2} \right) \left(\frac{\omega s}{s^2 + \omega^2} \right) \left(\frac{Del(s)}{B(s)} \right) I_d^*(s) + \left(k_p s + \frac{k_i(s^2 - \omega^2)}{s^2 + \omega^2} \right) \left(\frac{s}{s^2 + \omega^2} \right) \left(\frac{Del(s)}{B(s)} \right) I_q^*(s) \\ - \left(\frac{-\omega L s^2 + (k_i \omega - \omega^3 L)}{A(s)} \right) \left(\frac{F_i(s) \cdot Del(s)}{B(s)} \right) I_\alpha(s) - \left(\frac{1 - Del(s)}{B(s)} \right) \cdot V_{g\beta}(s) \quad (186)$$

Being again:

$$B(s) = \left(k_p + \frac{k_i s}{s^2 + \omega^2} \right) \cdot F_i(s) \cdot Del(s) + R + Ls \quad (187)$$

In order to derive decoupled expressions that connect the outputs ($I_\alpha(s)$ and $I_\beta(s)$) directly to the inputs ($I_d^*(s)$ and $I_q^*(s)$), a further mathematical development must be carried out. Hence, by renaming the expressions (185) and (186) as follows:

$$I_\alpha(s) = G_{\alpha d}(s)I_d^*(s) + G_{\alpha q}(s)I_q^*(s) + G_{\alpha\beta}(s)I_\beta(s) + G_v(s)V_{g\alpha}(s) \quad (188)$$

$$I_\beta(s) = G_{\beta d}(s)I_d^*(s) + G_{\beta q}(s)I_q^*(s) + G_{\beta\alpha}(s)I_\alpha(s) + G_v(s)V_{g\beta}(s) \quad (189)$$

If we combine both equations seeking to eliminate $I_\alpha(s)$ from the second equation and $I_\beta(s)$ from the first equation, the decoupled input-output transfer functions can be obtained as:

$$\begin{aligned} I_\alpha(s) = & \left(\frac{G_{\alpha d}(s) + G_{\beta d}(s)G_{\alpha\beta}(s)}{1 - G_{\alpha\beta}(s)G_{\beta\alpha}(s)} \right) I_d^*(s) + \left(\frac{G_{\alpha q}(s) + G_{\beta q}(s)G_{\alpha\beta}(s)}{1 - G_{\alpha\beta}(s)G_{\beta\alpha}(s)} \right) I_q^*(s) \\ & + \left(\frac{G_v(s)}{1 - G_{\alpha\beta}(s)G_{\beta\alpha}(s)} \right) V_{g\alpha}(s) + \left(\frac{G_v(s)G_{\alpha\beta}(s)}{1 - G_{\alpha\beta}(s)G_{\beta\alpha}(s)} \right) V_{g\beta}(s) \end{aligned} \quad (190)$$

$$\begin{aligned} I_\beta(s) = & \left(\frac{G_{\beta d}(s) + G_{\alpha d}(s)G_{\beta\alpha}(s)}{1 - G_{\alpha\beta}(s)G_{\beta\alpha}(s)} \right) I_d^*(s) + \left(\frac{G_{\beta q}(s) + G_{\alpha q}(s)G_{\beta\alpha}(s)}{1 - G_{\alpha\beta}(s)G_{\beta\alpha}(s)} \right) I_q^*(s) \\ & + \left(\frac{G_v(s)G_{\beta\alpha}(s)}{1 - G_{\alpha\beta}(s)G_{\beta\alpha}(s)} \right) V_{g\alpha}(s) + \left(\frac{G_v(s)}{1 - G_{\alpha\beta}(s)G_{\beta\alpha}(s)} \right) V_{g\beta}(s) \end{aligned} \quad (191)$$

The decoupled transfer functions are graphically represented in block diagrams of next figure:

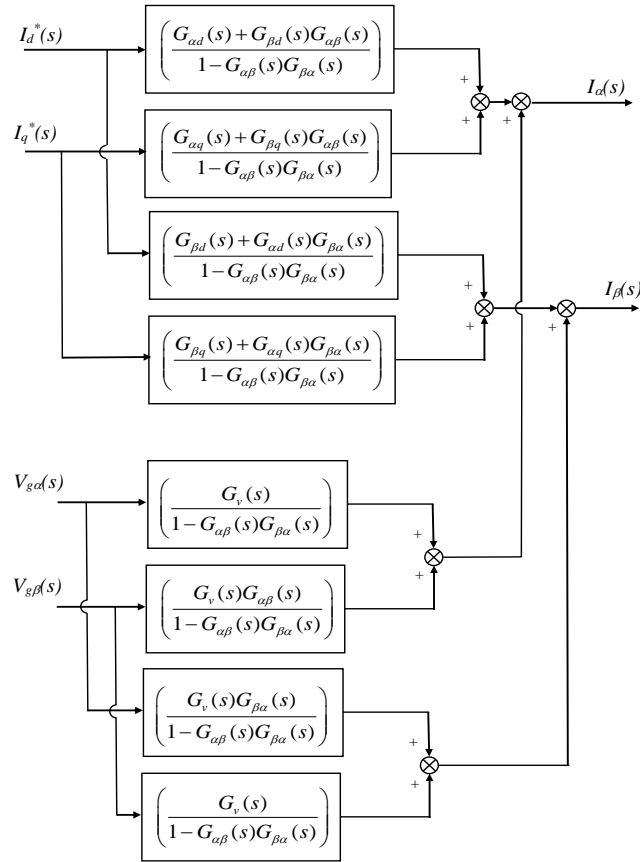
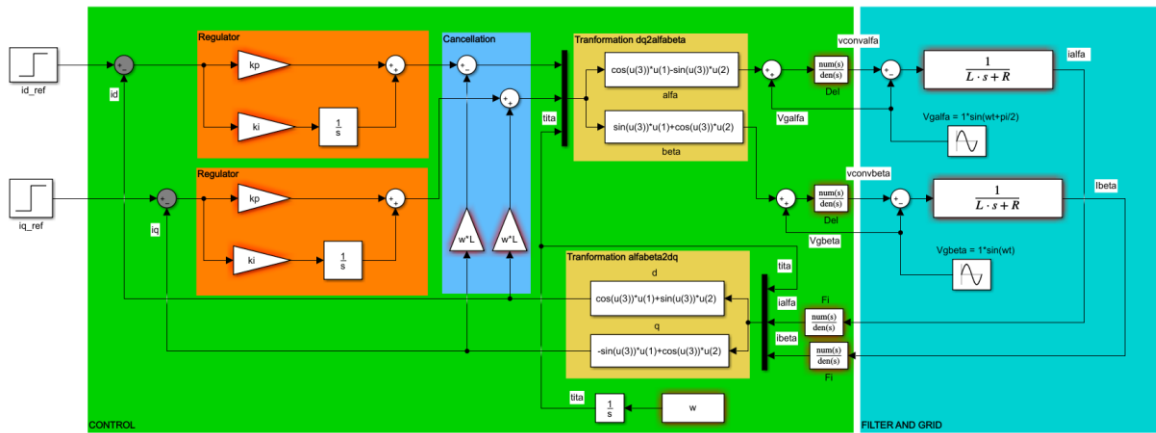
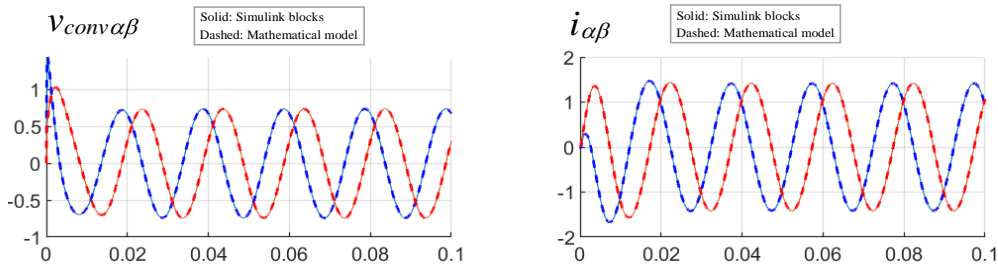


Figure 44. Equivalent block diagram of the currents control in dq with cancellation of coupling terms and inclusion of delay and filter at measurements.

In this case, the resulting symbolic expressions maybe are too long to be represented here. It is perhaps simpler to solve them numerically if further analysis is wanted to carry out. Note that the terms multiplying the stator voltages, $G_v(s)$ are made zero very quickly so their effect is only appreciated at the beginning when connecting the converter to the grid. Afterwards, if the grid voltage does not change, the effect of the grid voltage in equations (190) and (191) will be zero as well. Note that many other analysis could be carried out at this point, as for instance, transient behavior analysis under different delays or filter conditions. However, this is left as a future study in a different book to this.



(a)



(b)

Figure 45. (a) Simulink model for evaluating the step response, (b) Unit step (at both inputs) response of control of currents in rotating reference frame (dq) with cancellation of coupling current terms. Conditions of Appendix E. With delay ($Del(s)=1/(T_d s+1)$) and $T_d=1/5000/3\text{sec}$ and low pass filter at current measurements ($F_i(s)=1/(T_i s+1)$) with time constant $T_i=1/5000\text{sec}$.

7.3. Stability analysis of both controls: pole location for step inputs

This chapter evaluates how the filter at current measurement and the delay affects to the stability of the closed loop current control, in both studied control techniques: Control in stationary reference frame ($\alpha\beta$) and control in rotating reference frame (dq) with cancellation of current coupling terms. This affection, for simplicity will be only studied for a step input.

First, in Figure 46, the poles to a step input of different controls (Transfer function $I_\alpha(s)/I_\alpha^*(s)$) are evaluated, with a low pass filter at current measurements ($F_i(s)=1/(T_i s+1)$) with different time constants. It is clearly seen that the control in dq is affected much more severely by this filter, altering the real part of the dominant poles significantly (poles affecting to the natural response).

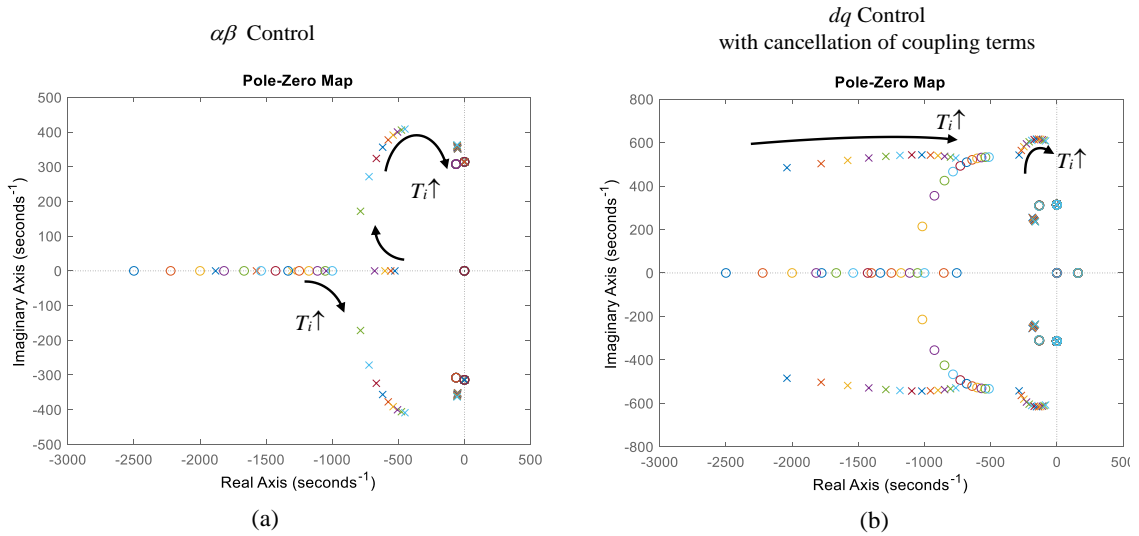


Figure 46. Poles to a step input of different controls of Transfer function $I_\alpha(s)/I_d^*(s)$, with low pass filter at current measurements ($F_i(s)=1/(T_i s+1)$) with different time constants: ($T_i=2/5000 \div 4.4/5000$, increments: $0.2/5000$). (a) Current control in $\alpha\beta$ reference frame, (b) Current control in dq reference frame with cancellation of coupling terms. Conditions of Appendix E.

Second, in Figure 47, the poles to a step input of different controls (Transfer function $I_\alpha(s)/I_d^*(s)$) are evaluated, with different delays. Again, it is seen that the control in dq is affected more severely by this delay, altering the real and imaginary parts of more dominant poles (poles affecting to the natural response).

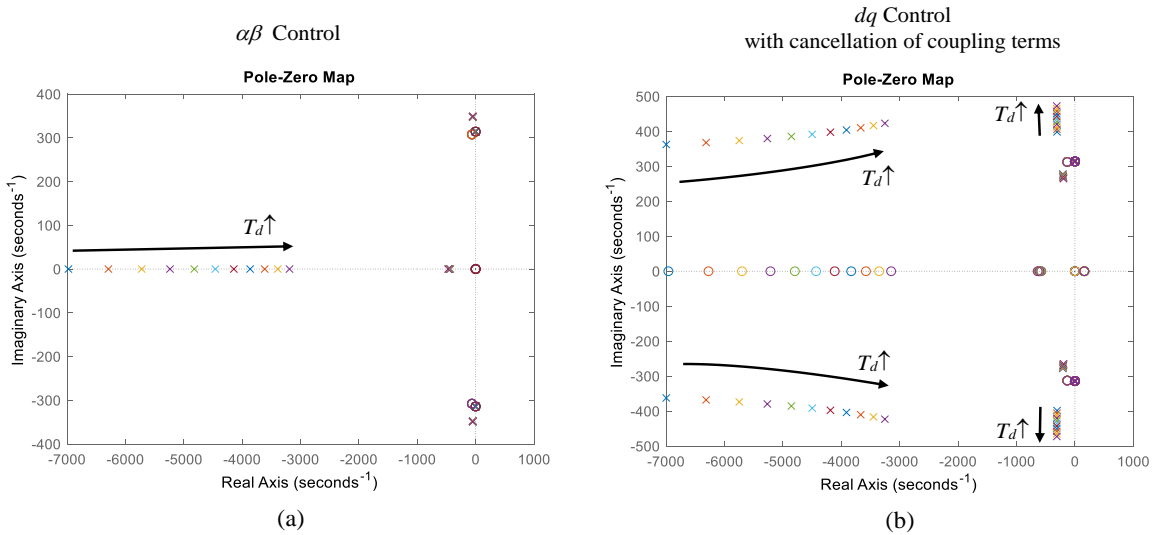


Figure 47. Poles to a step input of different controls of Transfer function $I_\alpha(s)/I_d^*(s)$, with different delays ($Del(s)=1/(T_d s+1)$): ($T_d=2/5000 \div 4/5000$, increments: $0.2/5000$). (a) Current control in $\alpha\beta$ reference frame, (b) Current control in dq reference frame with cancellation of coupling terms. Conditions of Appendix E.

Finally, in Figure 48, both effects of filter and delay are evaluated in the poles and zeros of the closed loop systems. It is seen that combination of both phenomena move the poles more significantly than in previous two analyzed cases, being again the control in dq the most sensitive one. It is also seen that if the filter time constant T_i is made very big (severe filter with big delay in current measurement) the system can become unstable.

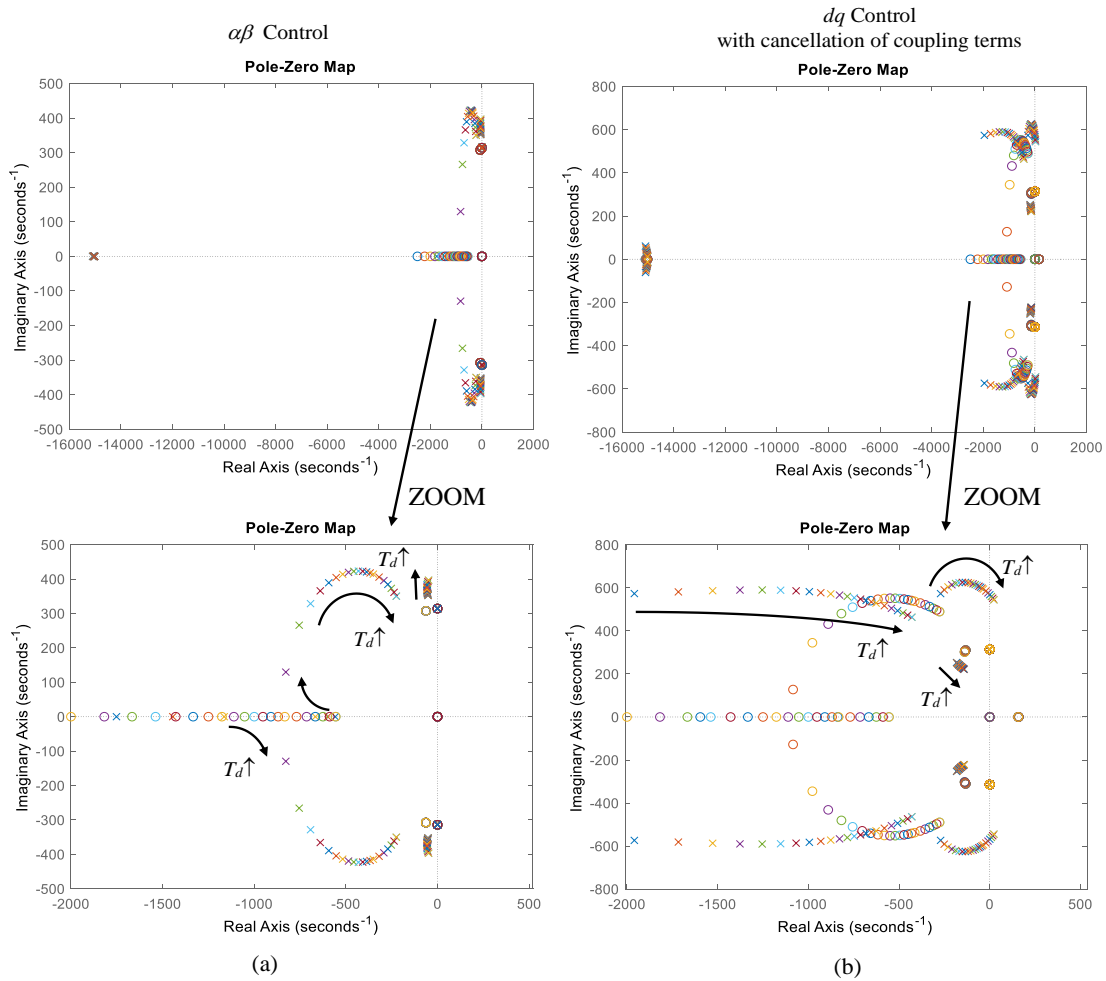


Figure 48. Poles to a step input of different controls of Transfer function $I_\alpha(s)/I_\alpha^*(s)$, with constant delay ($Del(s)=1/(T_d s+1)$) of $T_d = 1/5000/3\text{sec}$ and with low pass filter at current measurements ($F_i(s)=1/(T_i s+1)$) with different time constants: ($T_i=2/5000 \div 9/5000$, increments: $0.25/5000$). (a) Current control in $\alpha\beta$ reference frame, (b) Current control in dq reference frame with cancellation, Conditions of Appendix E.

Chapter 8.

Step response analysis in a weak grid

This chapter provides an introductory or simplified analysis of what occurs in grid-connected converters, when the grid to what is connected is weak. As shown in Figure 49, it is supposed now that the series impedance of the grid L_g is considerable big in comparison with the filter inductance L , so it cannot be assumed to be neglectable. This scenario is quite common in some grids and commonly this grid's impedance is quantified as the Short Circuit Ratio (SCR). Hence, the following chapter shortly analyzes how the mathematical expressions derived in previous chapters for both controls in $\alpha\beta$ and dq are affected under these conditions.

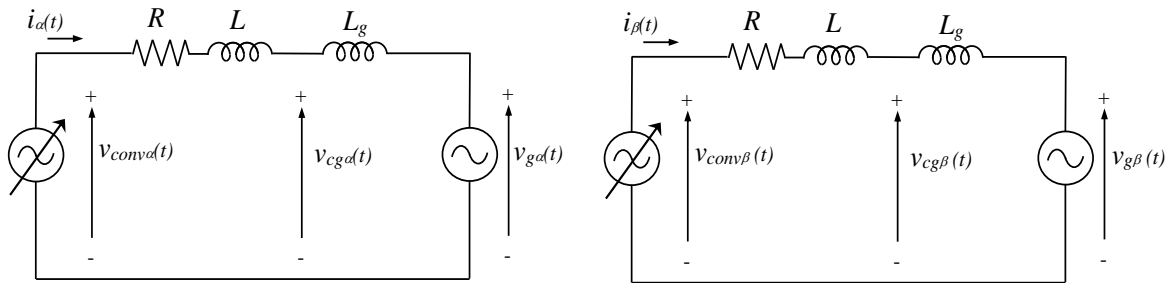


Figure. 49. $\alpha\beta$ equivalent electric circuit connected to a weak grid with impedance L_g .

In the following figure, it is graphically shown how the steady-state vector diagram is modified after a variation of the operating point. More specifically, after an increase of active power.

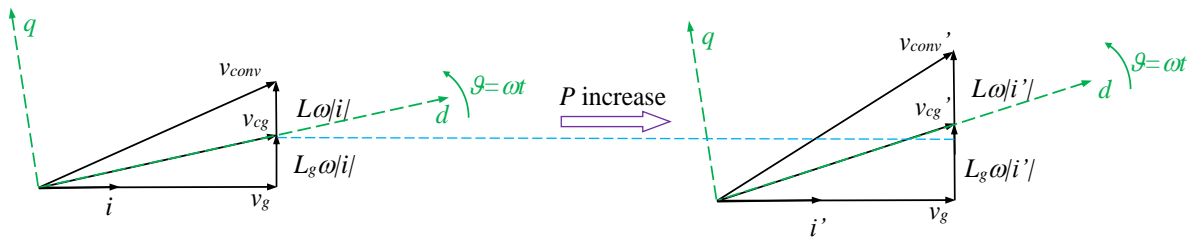


Figure. 50. Steady-state phasor diagrams under a change of active current operating point in a weak grid (effect of resistance R neglected).

8.1. Control of currents in stationary reference frame ($\alpha\beta$ control) with a PLL tuned dynamically slow

First of all, the performance of the current control in stationary reference frame is studied. For simplicity in the analysis, it is assumed the ideal control block diagram utilized in chapter 2 as shown in Figure 51, not considering filter at current measurement and delay between control and converter synthesis of the output voltage. This choice helps a decoupled analysis, understanding the effect of different phenomena separately.

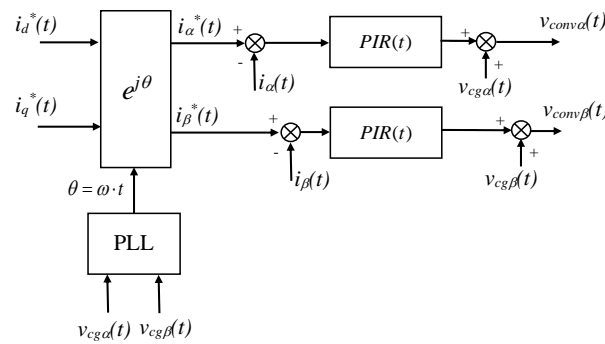


Figure 51. Current control block diagram in stationary reference frame ($\alpha\beta$) with two resonant controllers and converter connected to a weak grid.

It is important to highlight the fact that the converter's control now sees voltages $v_{cg\alpha}(t)$ and $v_{cg\beta}(t)$, which are affected by the current exchange due to the presence of the grid's impedance L_g . Therefore, the input voltage that goes to the PLL and the voltage feed forward terms are $v_{cg\alpha}(t)$ and $v_{cg\beta}(t)$. Then, regarding to the behavior of the PLL, for this analysis, it is supposed that it has been tuned with a slow dynamic response. This means that when for instance, a step is performed at the input current references, although the currents during the transient response make $v_{cg\alpha}(t)$ and $v_{cg\beta}(t)$ voltages change, we will consider that the PLL will synchronize with the new phase angle a time later. In other words, we will consider that the PLL has been tuned, so that detects the phase changes due to the current changes, a time later than they occur. This behavior is typical in some power electronic applications such as for instance some type of battery chargers.

Therefore, considering this, when the step is performed at the reference currents, since θ angle is assumed that does not change, the voltage reference generated by the control is equivalent to expressions (4) and (5), but only changes the voltage feedforward terms (expressions only valid for step inputs):

$$V_{conv\alpha}(s) = -\left(k_p + \frac{k_i s}{s^2 + \omega^2}\right) I_\alpha(s) + \left(\frac{k_p s^2}{s^2 + \omega^2} + \frac{k_i s^3}{(s^2 + \omega^2)^2}\right) I_d^*(s) - \left(\frac{k_p \omega s}{s^2 + \omega^2} + \frac{\omega k_i s^2}{(s^2 + \omega^2)^2}\right) I_q^*(s) + V_{cg\alpha}(s) \quad (192)$$

$$V_{conv\beta}(s) = -\left(k_p + \frac{k_i s}{s^2 + \omega^2}\right) I_\beta(s) + \left(\frac{k_p \omega s}{s^2 + \omega^2} + \frac{\omega k_i s^2}{(s^2 + \omega^2)^2}\right) I_d^*(s) + \left(\frac{k_p s^2}{s^2 + \omega^2} + \frac{k_i s^3}{(s^2 + \omega^2)^2}\right) I_q^*(s) + V_{cg\beta}(s) \quad (193)$$

On the other hand, the electric power circuit equations in Laplace domain are:

$$V_{conv\alpha}(s) = I_\alpha(s) \cdot (R + Ls) + V_{cg\alpha}(s) = I_\alpha(s) \cdot (R + Ls) + I_\alpha(s) \cdot (L_g s) + V_{g\alpha}(s) \quad (194)$$

$$V_{conv\beta}(s) = I_\beta(s) \cdot (R + Ls) + V_{cg\beta}(s) = I_\beta(s) \cdot (R + Ls) + I_\beta(s) \cdot (L_g s) + V_{g\beta}(s) \quad (195)$$

By combining these last four equations and as commented before, if the voltage feed-forward term is used and no delay is assumed in this measurement at the voltage synthesis, the $V_{cg\alpha}(s)$ and $V_{cg\beta}(s)$ are effectively cancelled and we obtain the closed loop current expressions, which are equal to ones obtained in chapter 2, in a strong grid:

$$I_\alpha(s) = \left(k_p + \frac{k_i s}{s^2 + \omega^2}\right) \left(\frac{s^2}{A(s)}\right) I_d^*(s) - \left(k_p + \frac{k_i s}{s^2 + \omega^2}\right) \left(\frac{\omega s}{A(s)}\right) I_q^*(s) \quad (196)$$

$$I_\beta(s) = \left(k_p + \frac{k_i s}{s^2 + \omega^2}\right) \left(\frac{\omega s}{A(s)}\right) I_d^*(s) + \left(k_p + \frac{k_i s}{s^2 + \omega^2}\right) \left(\frac{s^2}{A(s)}\right) I_q^*(s) \quad (197)$$

Being:

$$A(s) = Ls^3 + (k_p + R)s^2 + (L\omega^2 + k_i)s + (k_p + R)\omega^2 \quad (198)$$

Therefore, under the considered assumptions and specially assuming that the PLL is tuned dynamically slower than the time that the current needs to reach the steady state, it is concluded that the currents behavior to a step input reference are not different in a strong grid and in a weak grid. Note also that the \mathcal{G} phase angle in this control method, only affects to the current references $i_\alpha^*(t)$ and $i_\beta^*(t)$, what means that it does not affect to the control loops' internal behaviour, resulting thus in a quite stable or robust performance to this fact.

Obviously, it is crucial to include the voltage feedforward terms in control as in equations (192)-(193), otherwise, note that the current dynamics would be affected by the grid L_g impedance.

8.2. Control of currents in synchronous rotating reference frame (dq control) with a PLL tuned dynamically slow

In this case now, it is studied how the dq control's performance is affected by a weak grid. In Figure 52, the $\alpha\beta$ electric circuit of Figure 49 is transformed to a dq reference frame.

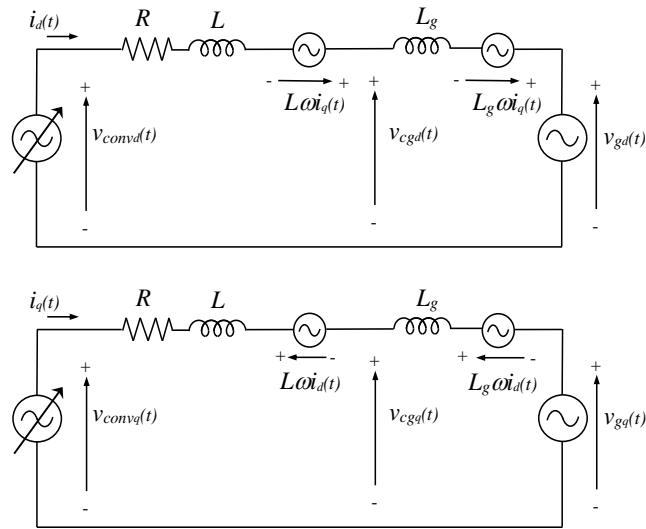


Figure 52. Equivalent electric circuit in dq , of grid-connected converter connected to a weak grid.

Again as done in previous chapter, it is assumed that the PLL is tuned in such a way that detects the phase angle after the current transient ends after a step input. In a real application for this scenario could be for instance a battery charger that is not required to actively contribute to the grid support. Then also, not filter at the measurements and neither delay is considered at the control. The control block diagram under this weak grid scenario is depicted in Figure 53.

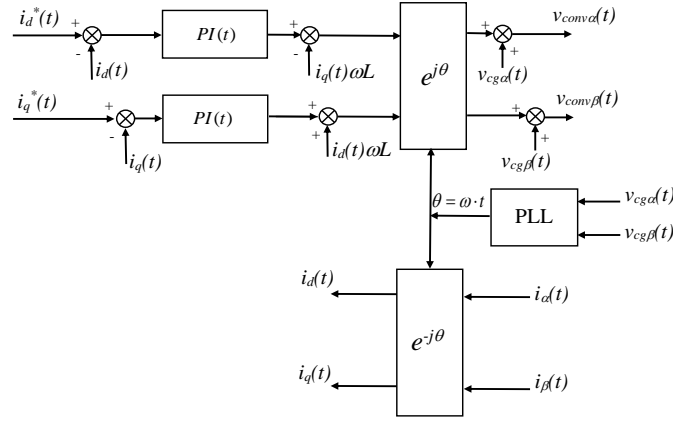


Figure 53. Current control block diagram in rotating reference frame (dq) with two PI controllers with cancellation of current coupling terms and converter connected to a weak grid.

Therefore, since we are assuming that the phase angle ϑ estimated by the PLL, does not change during the step current response, it is possible for instance to simply do the analysis in a $\alpha\beta$ reference frame. Hence, the voltage references provided by the control are equivalent to those previously derived in a strong grid:

$$\begin{aligned}
 V_{conv\alpha}(s) = & -\left(k_p + \frac{k_i s}{s^2 + \omega^2}\right) I_\alpha(s) + \left(\frac{(-\omega L)s^2 + (k_i \omega - \omega^3 L)}{s^2 + \omega^2}\right) I_\beta(s) \\
 & + \left(\frac{k_p s^2}{s^2 + \omega^2} + \frac{k_i s(s^2 - \omega^2)}{(s^2 + \omega^2)^2}\right) I_d^*(s) - \left(\frac{k_p \omega s}{s^2 + \omega^2} - \frac{2\omega k_i s^2}{(s^2 + \omega^2)^2}\right) I_q^*(s) + V_{cg\alpha}(s)
 \end{aligned} \tag{199}$$

$$\begin{aligned}
 V_{conv\beta}(s) = & -\left(\frac{(-\omega L)s^2 + (k_i \omega - \omega^3 L)}{s^2 + \omega^2}\right) I_\alpha(s) - \left(k_p + \frac{k_i s}{s^2 + \omega^2}\right) I_\beta(s) \\
 & + \left(\frac{k_p \omega s}{s^2 + \omega^2} - \frac{2\omega k_i s^2}{(s^2 + \omega^2)^2}\right) I_d^*(s) + \left(\frac{k_p s^2}{s^2 + \omega^2} + \frac{k_i s(s^2 - \omega^2)}{(s^2 + \omega^2)^2}\right) I_q^*(s) + V_{cg\beta}(s)
 \end{aligned} \tag{200}$$

On the other hand, the electric power circuit equations in $\alpha\beta$ reference frame and in Laplace domain are:

$$V_{conv\alpha}(s) = I_\alpha(s) \cdot (R + Ls) + V_{cg\alpha}(s) = I_\alpha(s) \cdot (R + Ls) + I_\alpha(s) \cdot (L_g s) + V_{g\alpha}(s) \tag{201}$$

$$V_{conv\beta}(s) = I_\beta(s) \cdot (R + Ls) + V_{cg\beta}(s) = I_\beta(s) \cdot (R + Ls) + I_\beta(s) \cdot (L_g s) + V_{g\beta}(s) \tag{202}$$

Combining all, the step current responses yield:

$$I_{\alpha}(s) = \left(k_p s + \frac{k_i(s^2 - \omega^2)}{s^2 + \omega^2} \right) \left(\frac{s}{A(s)} \right) I_d^*(s) - \left(k_p + \frac{2k_i s}{s^2 + \omega^2} \right) \left(\frac{\omega s}{A(s)} \right) I_q^*(s) + \left(\frac{(-\omega L)s^2 + (k_i \omega - \omega^3 L)}{A(s)} \right) I_{\beta}(s) \quad (203)$$

$$I_{\beta}(s) = \left(k_p + \frac{2k_i s}{s^2 + \omega^2} \right) \left(\frac{\omega s}{A(s)} \right) I_d^*(s) + \left(k_p s + \frac{k_i(s^2 - \omega^2)}{s^2 + \omega^2} \right) \left(\frac{s}{A(s)} \right) I_q^*(s) - \left(\frac{(-\omega L)s^2 + (k_i \omega - \omega^3 L)}{A(s)} \right) I_{\alpha}(s) \quad (204)$$

With:

$$A(s) = Ls^3 + (k_p + R)s^2 + (L\omega^2 + k_i)s + (k_p + R)\omega^2 \quad (205)$$

Being again these expressions only valid for a step input at both $I_d^*(s)$ and $I_q^*(s)$. Therefore, as occurred in previous chapter, it can be concluded now again that under the considered assumptions, the control performance in dq reference frame is equal in a strong or weak grid. The same conclusions can be obtained if the analysis is performed in dq reference frame.

8.3. Control of currents in stationary reference frame ($\alpha\beta$ control) with a PLL tuned dynamically fast

In this chapter, a step forward is given towards the inclusion of the Phase Locked Loop (PLL) into the model of the control loops. In general, the PLLs are included into the control loops enabling the synchronizing with the grid's phase angle. Especially when the grid in which the converter is connected is weak (it presents a considerable series equivalent impedance), it is necessary to dedicate a special attention to this fact.

Hence, in general, the PLL must be tuned considering two main issues, among other secondary factors. First of all, its synchronizing dynamics with the phase angle must be tuned as desired (functionality) or required (norms or codes). Second, it must be able to reject a certain level of perturbations such as, low amplitude ripples or noises. Thus for instance, in the specific case of a wind turbine which must meet the LVRT grid code requirements [6], the PLL should be able to quickly detect quick phase changes of the grid voltage during faults, in order to quickly provide reactive current as demanded by the grid codes [17]. At the same time, it should be also able to reject a certain level of high frequency (produced by commutations of other converter connected to the grid for instance) or low frequency voltage harmonics (flicker producing loads for instance), so they do not interfere negatively in the normal operation of the converter.

Therefore, it is very recommendable to take into consideration the effect of the phase angle estimation of the PLL and study how it interacts with the current control loops. By

considering both PLL and control loops behavior, it is possible to detect instabilities or abnormal performances of the entire control system.

However, most of the classic proposed PLLs at the literature [6] present an internal structure that is not suitable for being modelled linearly in 's' domain. The PLLs normally present an intrinsic non-linear structure that obliges to apply linearization methods [16] if 's' domain is wanted to be applied for their studies. Thus, in order to solve this modelling obstacle, by means of the block diagram of figure 54, an alternative PLL is proposed that at least in most part of its structure is linear, or in other words, it can be modelled by using the 's' operator. As can be noticed, two closed loops with resonant controllers are used in order to synchronize with the main component ω , of the grid voltages seen by the converter $V_{cg\alpha}(s)$ and $V_{cg\beta}(s)$. By an appropriate tuning of the gains of the resonant controllers, k_p^{pll} and k_i^{pll} , it is possible to obtain the desired synchronizing dynamic behavior and the ripple, oscillations or noise rejection capacity. Then, once synchronized with $V_{cg\alpha}(s)$ and $V_{cg\beta}(s)$, the $\cos(\omega t)$ and $\sin(\omega t)$ are obtained by normalizing with the voltage amplitude as graphically represented (values between -1 and +1). Note that by being strict, the left hand side of the proposed PLL can be linearly modelled in 's' domain, but the right hand side, i.e. the normalization, presents a 'smooth' or 'not severe' non-linearity.

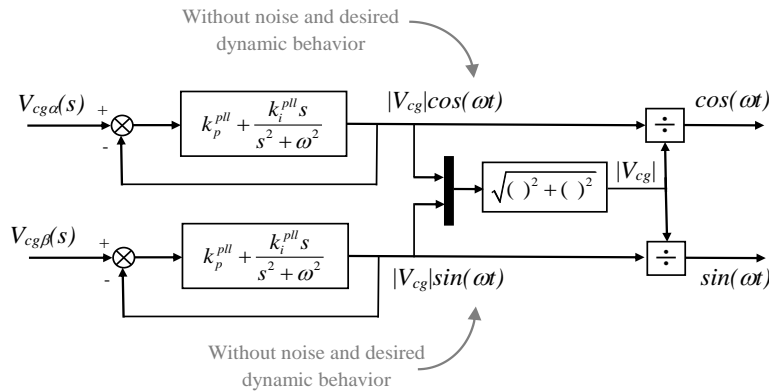


Figure 54. Proposed Phase Locked Loop.

This PLL has been tested at different operation points and different scenarios, providing a similar performance to classic PLLs. Despite the fact that the PLL of Figure 54 is used, the model of the PLL is going to be assumed as represented in Figure 55. As can be seen, the normalization is neglected (avoided), in order to obtain and therefore work with a linear model of the PLL. Note that the amplitude error that is incurred would be less than 5% in most of the realistic cases of a weak grid scenario.

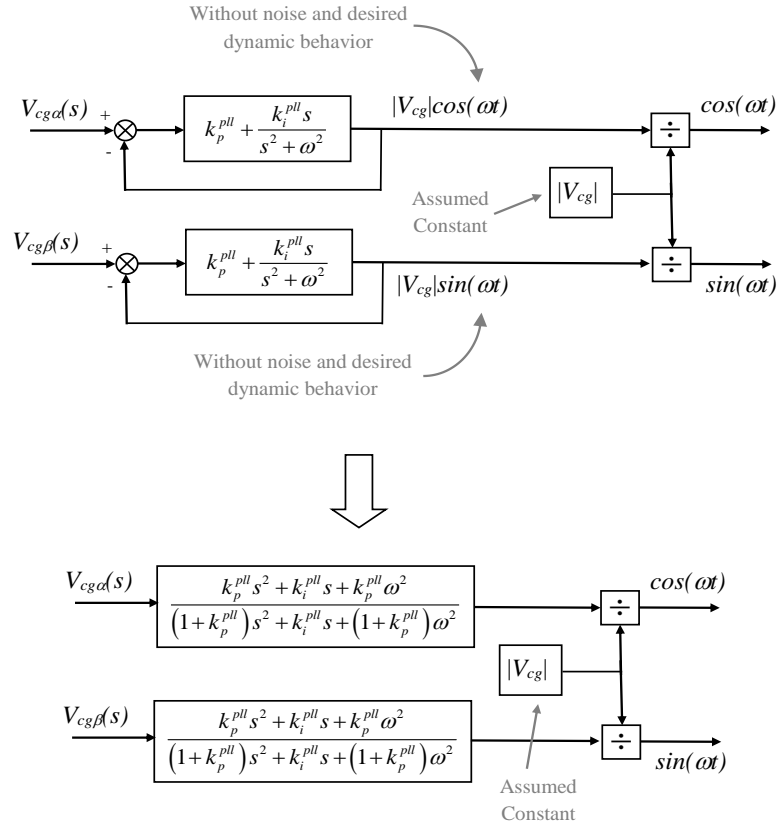


Figure 55. Proposed Phase Locked Loop model, which is an approximation of the actual PLL, but can be linearly modeled in 's' domain without a considerable error.

Therefore, the **linear model** of the PLL neglecting the variation of the grid voltage amplitude seen by the converter during the transient is given by:

$$\frac{\cos(\omega t)}{V_{cg\alpha}(s)} = \left(\frac{k_p^{pll} \cdot s^2 + k_i^{pll} \cdot s + k_p^{pll} \cdot \omega^2}{(1+k_p^{pll}) \cdot s^2 + k_i^{pll} \cdot s + (k_p^{pll} \cdot \omega^2 + \omega^2)} \right) \cdot \frac{1}{|V_{cg}|} = \left(\frac{(k_p^{pll} \cdot s^2 + k_i^{pll} \cdot s + k_p^{pll} \cdot \omega^2) / (1+k_p^{pll})}{s^2 + (k_i^{pll} / (1+k_p^{pll})) \cdot s + \omega^2} \right) \cdot \frac{1}{|V_{cg}|} \quad (206)$$

$$\frac{\sin(\omega t)}{V_{cg\beta}(s)} = \left(\frac{k_p^{pll} \cdot s^2 + k_i^{pll} \cdot s + k_p^{pll} \cdot \omega^2}{(1+k_p^{pll}) \cdot s^2 + k_i^{pll} \cdot s + (k_p^{pll} \cdot \omega^2 + \omega^2)} \right) \cdot \frac{1}{|V_{cg}|} = \left(\frac{(k_p^{pll} \cdot s^2 + k_i^{pll} \cdot s + k_p^{pll} \cdot \omega^2) / (1+k_p^{pll})}{s^2 + (k_i^{pll} / (1+k_p^{pll})) \cdot s + \omega^2} \right) \cdot \frac{1}{|V_{cg}|} \quad (207)$$

Then, by equaling the denominator to the canonic second order equation, we have:

$$\omega_n = \omega \quad 2\xi\omega_n = k_i^{pll} / (1+k_p^{pll}) \quad (208)$$

What means that a possible criterion for tuning the resonant controller (or synchronizer) could be to locate the poles, with a certain desired damping ration ξ , providing first a free value for k_p^{pll} . What means:

$$k_p^{pll} = 0.1 \quad , \quad k_i^{pll} = 2\xi\omega_n (1 + k_p^{pll}) \quad (209)$$

On the other hand, the following figure 56 shows the poles and the Bode diagram of the PLL, by using the previous two model equations, with different values of k_p^{pll} and k_i^{pll} first, and then, with different values of k_i^{pll} leaving constant k_p^{pll} .

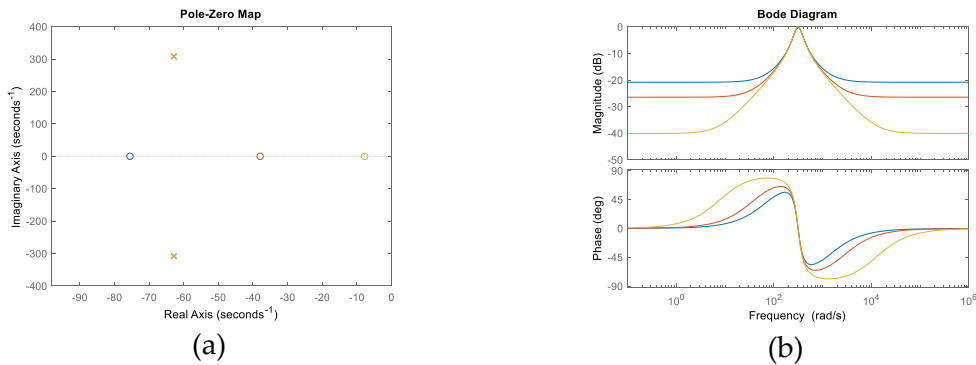


Figure 56. Poles and Bode of the simplified model of PLL with different values of k_p^{pll} and k_i^{pll} . Blue: $k_p^{pll}=0.1$, Red: $k_p^{pll}=0.05$, Orange: $k_p^{pll}=0.01$, in the three cases: $k_i^{pll} = 2 \cdot 0.2 \cdot 314.16(1 + k_p^{pll})$.

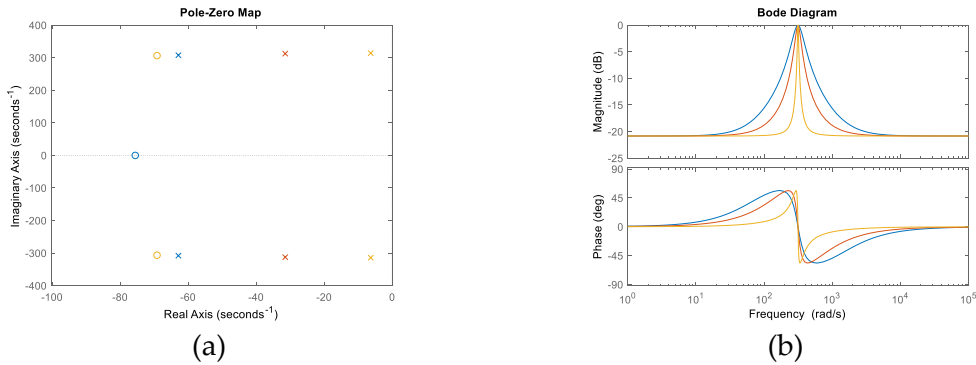


Figure 57. Poles and Bode of the model of PLL, with different values of k_i^{pll} keeping constant k_p^{pll} . $k_p^{pll}=0.01$. Blue: $k_i^{pll} = 2 \cdot 0.2 \cdot 314.16(1 + k_p^{pll})$, Red: $k_i^{pll} = 2 \cdot 0.1 \cdot 314.16(1 + k_p^{pll})$, Orange: $k_i^{pll} = 2 \cdot 0.02 \cdot 314.16(1 + k_p^{pll})$.

In first set of results, it is seen that the poles are not modified and therefore, neither the dynamic response of the synchronizing process. However, the attenuation (rejection) to different frequencies of ω can be made bigger or smaller. On the other hand, by leaving

constant k_p^{pll} and modifying k_i^{pll} , the poles can be modified as well as the rejection to frequencies near ω .

Thus, once the PLL model and its tuning method is clear, the mathematical model of the current loops including the PLL can be also obtained. The α and β components of the converter voltages, considering the grid voltage feedforward terms, are mathematically represented in time domain as follows:

$$v_{conv\alpha}(t) = \left(i_d^*(t) \cdot \cos(\omega t) - i_q^*(t) \cdot \sin(\omega t) \right) \otimes PIR(t) - i_\alpha(t) \otimes PIR(t) + v_{cg\alpha}(t) \quad (210)$$

$$v_{conv\beta}(t) = \left(i_d^*(t) \cdot \sin(\omega t) + i_q^*(t) \cdot \cos(\omega t) \right) \otimes PIR(t) - i_\beta(t) \otimes PIR(t) + v_{cg\beta}(t) \quad (211)$$

By substituting the model of the PLL:

$$v_{conv\alpha}(t) = \left(i_d^*(t) \cdot \left(PLL(t) \otimes v_{cg\alpha}(t) \right) \cdot \frac{1}{|V_{cg}|} - i_q^*(t) \cdot \left(PLL(t) \otimes v_{cg\beta}(t) \right) \cdot \frac{1}{|V_{cg}|} \right) \otimes PIR(t) - i_\alpha(t) \otimes PIR(t) + v_{cg\alpha}(t) \quad (212)$$

$$v_{conv\beta}(t) = \left(i_d^*(t) \cdot \left(PLL(t) \otimes v_{cg\beta}(t) \right) \cdot \frac{1}{|V_{cg}|} + i_q^*(t) \cdot \left(PLL(t) \otimes v_{cg\alpha}(t) \right) \cdot \frac{1}{|V_{cg}|} \right) \otimes PIR(t) - i_\beta(t) \otimes PIR(t) + v_{cg\beta}(t) \quad (213)$$

Considering a step input at both $I_d^*(s)$ and $I_q^*(s)$ and $|V_{cg}|$ constant, the previous equation in Laplace domain after substituting the PLL's transfer function yields:

$$V_{conv\alpha}(s) = \left(|I_d^*| \cdot V_{cg\alpha}(s) - |I_q^*| \cdot V_{cg\beta}(s) \right) \cdot \left(\frac{k_p^{pll} \cdot s^2 + k_i^{pll} \cdot s + k_p^{pll} \cdot \omega^2}{(1 + k_p^{pll}) \cdot s^2 + k_i^{pll} \cdot s + (k_p^{pll} \cdot \omega^2 + \omega^2)} \right) \cdot \frac{1}{|V_{cg}|} \cdot \left(k_p + \frac{k_i s}{s^2 + \omega^2} \right) - I_\alpha(s) \cdot \left(k_p + \frac{k_i s}{s^2 + \omega^2} \right) + V_{cg\alpha}(s) \quad (214)$$

$$V_{conv\beta}(s) = \left(|I_d^*| \cdot V_{cg\beta}(s) + |I_q^*| \cdot V_{cg\alpha}(s) \right) \cdot \left(\frac{k_p^{pll} \cdot s^2 + k_i^{pll} \cdot s + k_p^{pll} \cdot \omega^2}{(1 + k_p^{pll}) \cdot s^2 + k_i^{pll} \cdot s + (k_p^{pll} \cdot \omega^2 + \omega^2)} \right) \cdot \frac{1}{|V_{cg}|} \cdot \left(k_p + \frac{k_i s}{s^2 + \omega^2} \right) - I_\beta(s) \cdot \left(k_p + \frac{k_i s}{s^2 + \omega^2} \right) + V_{cg\beta}(s) \quad (215)$$

Thus, by expressing the previous two equations in transfer function form (only valid for a step input at both $I_d^*(s)$ and $I_q^*(s)$):

$$V_{conv\alpha}(s) = \left(I_d^*(s) \cdot V_{cg\alpha}(s) - I_q^*(s) \cdot V_{cg\beta}(s) \right) \cdot \left(\frac{k_p^{pll} \cdot s^2 + k_i^{pll} \cdot s + k_p^{pll} \cdot \omega^2}{(1 + k_p^{pll}) \cdot s^2 + k_i^{pll} \cdot s + (k_p^{pll} \cdot \omega^2 + \omega^2)} \right) \cdot \frac{1}{|V_{cg}|} \cdot \left(k_p + \frac{k_i s}{s^2 + \omega^2} \right) - I_\alpha(s) \cdot \left(k_p + \frac{k_i s}{s^2 + \omega^2} \right) + V_{cg\alpha}(s) \quad (216)$$

$$V_{conv\beta}(s) = \left(I_d^*(s) \cdot V_{cg\beta}(s) + I_q^*(s) \cdot V_{cg\alpha}(s) \right) \cdot \left(\frac{k_p^{pll} \cdot s^2 + k_i^{pll} \cdot s + k_p^{pll} \cdot \omega^2}{(1 + k_p^{pll}) \cdot s^2 + k_i^{pll} \cdot s + (k_p^{pll} \cdot \omega^2 + \omega^2)} \right) \cdot \frac{1}{|V_{cg}|} \cdot \left(k_p + \frac{k_i s}{s^2 + \omega^2} \right) - I_\beta(s) \cdot \left(k_p + \frac{k_i s}{s^2 + \omega^2} \right) + V_{cg\beta}(s) \quad (217)$$

Now, taking into account the power circuit equations:

$$V_{conv\alpha}(s) = I_\alpha(s) \cdot (R + Ls) + V_{cg\alpha}(s) \quad (218)$$

$$V_{conv\beta}(s) = I_\beta(s) \cdot (R + Ls) + V_{cg\beta}(s) \quad (219)$$

The closed loop current transfer function expressions yield:

$$I_\alpha(s) = \left(I_d^*(s) \cdot V_{cg\alpha}(s) - I_q^*(s) \cdot V_{cg\beta}(s) \right) \cdot \left(\frac{k_p^{pll} \cdot s^2 + k_i^{pll} \cdot s + k_p^{pll} \cdot \omega^2}{(1 + k_p^{pll}) \cdot s^2 + k_i^{pll} \cdot s + (k_p^{pll} \cdot \omega^2 + \omega^2)} \right) \cdot \frac{1}{|V_{cg}|} \cdot \left(\frac{k_p s^2 + k_i s + k_p \omega^2}{A(s)} \right) \quad (220)$$

$$I_\beta(s) = \left(I_d^*(s) \cdot V_{cg\beta}(s) + I_q^*(s) \cdot V_{cg\alpha}(s) \right) \cdot \left(\frac{k_p^{pll} \cdot s^2 + k_i^{pll} \cdot s + k_p^{pll} \cdot \omega^2}{(1 + k_p^{pll}) \cdot s^2 + k_i^{pll} \cdot s + (k_p^{pll} \cdot \omega^2 + \omega^2)} \right) \cdot \frac{1}{|V_{cg}|} \cdot \left(\frac{k_p s^2 + k_i s + k_p \omega^2}{A(s)} \right) \quad (221)$$

Or equivalently:

$$I_\alpha(s) = \left(I_d^*(s) \cdot V_{cg\alpha}(s) - I_q^*(s) \cdot V_{cg\beta}(s) \right) \cdot \left(\frac{(k_p^{pll} \cdot s^2 + k_i^{pll} \cdot s + k_p^{pll} \cdot \omega^2) / (1 + k_p^{pll})}{s^2 + (k_i^{pll} / (1 + k_p^{pll})) \cdot s + \omega^2} \right) \cdot \frac{1}{|V_{cg}|} \cdot \left(\frac{k_p s^2 + k_i s + k_p \omega^2}{A(s)} \right) \quad (222)$$

$$I_\beta(s) = \left(I_d^*(s) \cdot V_{cg\beta}(s) + I_q^*(s) \cdot V_{cg\alpha}(s) \right) \cdot \left(\frac{(k_p^{pll} \cdot s^2 + k_i^{pll} \cdot s + k_p^{pll} \cdot \omega^2) / (1 + k_p^{pll})}{s^2 + (k_i^{pll} / (1 + k_p^{pll})) \cdot s + \omega^2} \right) \cdot \frac{1}{|V_{cg}|} \cdot \left(\frac{k_p s^2 + k_i s + k_p \omega^2}{A(s)} \right) \quad (223)$$

Being as usual:

$$A(s) = Ls^3 + (k_p + R)s^2 + (L\omega^2 + k_i)s + (k_p + R)\omega^2 \quad (224)$$

Thus, in Figure 58 the poles of previous two current expressions are shown together with the Bode diagram of the PLL. It is seen that the poles corresponding to the PLL dynamics have been tuned slightly faster than the slower poles of the current dynamic, so their real part is

around 60. At the Bode plot of the PLL transfer function, it is seen that a good rejection to frequencies different from 50Hz is achieved.

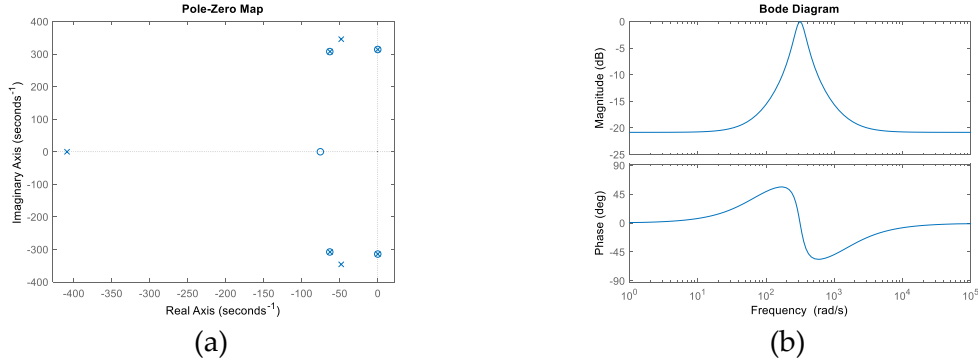
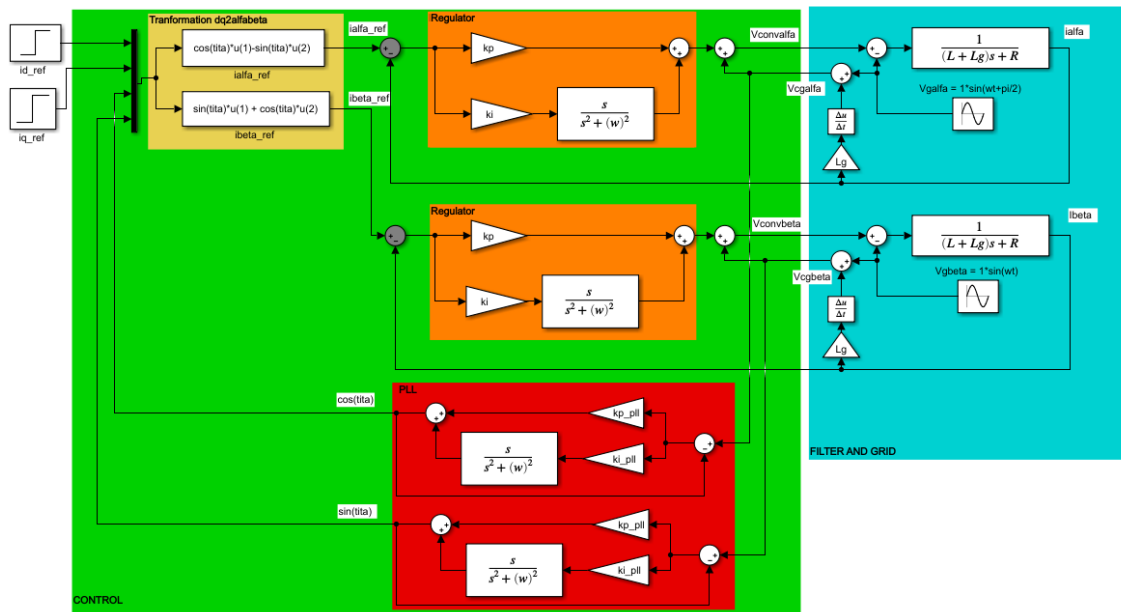
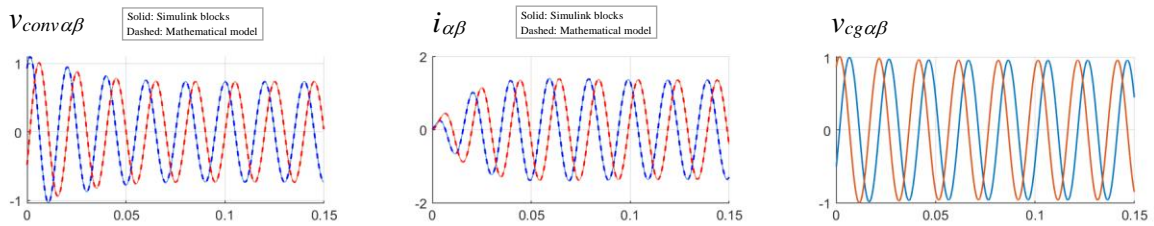


Figure 58. Poles of the closed loop currents (expressions (222) and (223)) and Bode of the model of PLL: $k_p^{pll} = 0.1$ and $k_i^{pll} = 0.2 \cdot (1 + k_p_pll) \cdot 2 \cdot w$;

Finally, the time domain responses to a step input at current i_d and i_q references is presented in Figure 59. It is seen that the Simulink based model and the mathematical model present an exact match. In this case, the grid impedance has been considered $L_g=125\mu\text{H}$. For a step input at both d and q current references, it is seen that the grid voltage seen by the converter (V_{cg}) falls approximately 4% in amplitude. Consequently, this proposed model shows that under certain assumptions, it is also possible to linearly model using the Laplace transformation, the PLL itself together with the current control loops. Further analysis and inclusion of the PLL model in dq controls, are left for future works.



(a)



(b)

Figure 59. (a) Simulink blocks based model, for evaluating the Step response of control of currents in stationary reference frame ($\alpha\beta$) and including the PLLs dynamic behavior, (b) Time domain responses comparison of mathematical model and Simulink blocks based model for a unit step input at both references. Conditions of Appendix E. $R = 0.01\Omega$; $L = 1\text{mH}$; $L_g = 0.125 \cdot L$.

Chapter 9.

Conclusions

In this book, it has been shown that it is possible to obtain useful mathematical expressions in $\alpha\beta$ frame (stationary reference frame) of controls developed in dq reference frame (synchronous rotating frame), for three phase grid-connected converters. Thanks to these mathematical expressions, it is possible to know the actual behavior of the converter's currents and voltages, i.e. the actual $\alpha\beta$ converter's currents and voltages, despite the fact that they are controlled under a dq reference frame. In addition, these mathematical equations provide a common framework that allow comparing controls conceived in different reference frames, i.e. $\alpha\beta$ controls with resonant controllers and dq controls with PI controllers.

Thanks to this analytical tool, in this book several conclusions have been derived by applying the classic control theory analysis. One remarkable fact is that the dq control with cancellation of coupling terms, provides the same current transient response (natural response) to step inputs, in $\alpha\beta$ frame or in dq frame. Being more precise, this means that the real part of the poles of the closed loop current transfer functions (damping factors), are the same in $\alpha\beta$ frame or in dq frame. Indirectly, this fact means that if in a dq control with PI controllers, if the current coupling terms are not properly cancelled by control, or simply are not considered at all, the transient response of the controlled currents will be different in $\alpha\beta$ frame and in dq frame.

Regarding to the frequency response analysis of the controlled currents, i.e. the Bode representations, it is a curious coincidence that the $\alpha\beta$ control and the dq controls without cancellation of coupling terms, provides an equivalent Bode amplitudes. Being more specific, this means that both controls obtain the same amplitude gains of the controlled currents at the evaluated frequencies.

Connected to this frequency response analysis, it is also remarkable that the dq controls with cancellation of coupling terms, is the only control evaluated that achieves equal amplitudes at both output current frequencies $\omega+\omega_1$ and $\omega-\omega_1$, when a ω_1 frequency is set at the current reference input. This fact means therefore that the other two evaluated controls, the $\alpha\beta$ control and the dq controls without cancellation of coupling terms, obtain different output current amplitudes at frequencies $\omega+\omega_1$ and $\omega-\omega_1$, when a ω_1 frequency is set at the current reference sinusoidal input.

In addition, the mathematical tool presented in this book, has shown that is possible to go further and study how the control is affected by phenomena that could be important in some specific contexts. The phenomena shortly evaluated have been: significant delays between the control and converter synthesis, significant filtering actions at currents measurements, converters connected to weak grids, PLLs tuned with particular dynamic behaviors, etc...

One more utility of some of the mathematical expressions derived in this book, could be the analysis of how different converters with their corresponding controls interact, in specific grid scenarios [14]. Connecting together the mathematical models of several grid connected converters' controls and the grid impedance models where they are connected, can also provide more analytical information about issues such as: stability, oscillations, steady-state behavior, etc...

As extension possibilities of the proposed mathematical model approach, it is remarkable that this method can also be applied to grid-connected converters that exchange currents with the grid of different frequencies, such as for instance, active filters or converters with active impedance functionalities [14]. In addition, this modelling approach can be also directly applied to control of different topologies of three phase AC motors. For instance, control of asynchronous motors, control of synchronous motors and control of doubly fed induction motors. In this context of three phase AC motors as well, the dq control with PI controllers is widely extended among researchers and manufacturers, but is not so common to study how is the performance of the actual $\alpha\beta$ currents or fluxes of the motor. As in three phase grid-connected converters, it is assumed that the behavior of the dq and $\alpha\beta$ currents is in some way similar or equivalent, but not being able to specify quantitatively how equal they are, or how much they differ.

Finally, as a future improvement of the proposed modelling approach, could be to develop discrete mathematical models (in 'z' domain) that are able to incorporate the discrete nature of the controls, when they are implemented in microcontrollers. Thanks to this, it could be also studied more powerfully how affects to the control factors such as; sample time, discretization methods, delays, etc...

Appendix A.

Step inputs in control at stationary reference frame ($\alpha\beta$)

From the control equation:

$$v_{conv\alpha}(t) = \left(i_d^*(t) \cdot \cos(\omega t) - i_q^*(t) \cdot \sin(\omega t) \right) \otimes PIR(t) - i_\alpha(t) \otimes PIR(t) + v_{g\alpha}(t) \quad (225)$$

It is equal to:

$$v_{conv\alpha}(t) = \left(i_d^*(t) \cdot \cos(\omega t) \right) \otimes PIR(t) - \left(i_q^*(t) \cdot \sin(\omega t) \right) \otimes PIR(t) - i_\alpha(t) \otimes PIR(t) + v_{g\alpha}(t) \quad (226)$$

Applying the Laplace transform to each part of this equation, and substituting a step in both inputs $i_d^*(t) = |I_d^*|$ and $i_q^*(t) = |I_q^*|$, at $t=0$:

$$\ell \left[\left(|I_d^*| \cdot \cos(\omega t) \right) \otimes (PIR(t)) \right] = \left(|I_d^*| \frac{s}{s^2 + \omega^2} \right) \left(k_p + k_i \frac{s}{s^2 + \omega^2} \right) \quad (227)$$

$$\ell \left[\left(-|I_q^*| \cdot \sin(\omega t) \right) \otimes (PIR(t)) \right] = \left(-|I_q^*| \frac{\omega}{s^2 + \omega^2} \right) \left(k_p + k_i \frac{s}{s^2 + \omega^2} \right) \quad (228)$$

$$\ell \left[\left(-i_\alpha(t) \right) \otimes (PIR(t)) \right] = \left(-I_\alpha(s) \right) \left(k_p + k_i \frac{s}{s^2 + \omega^2} \right) \quad (229)$$

$$\ell \left[v_{g\alpha}(t) \right] = V_{g\alpha}(s) \quad \text{and} \quad \ell \left[v_{conv\alpha}(t) \right] = V_{conv\alpha}(s) \quad (230)$$

Note that the convolution product in 's' domain becomes a product. Therefore, the converter voltage in 's' domain for step inputs yields:

$$V_{conv\alpha}(s) = -\left(k_p + \frac{k_i s}{s^2 + \omega^2}\right) I_\alpha(s) + \left(\frac{k_p s}{s^2 + \omega^2} + \frac{k_i s^2}{(s^2 + \omega^2)^2}\right) |I_d^*| - \left(\frac{k_p \omega}{s^2 + \omega^2} + \frac{\omega k_i s}{(s^2 + \omega^2)^2}\right) |I_q^*| + V_{g\alpha}(s) \quad (231)$$

Knowing that the step inputs in 's' domain are:

$$I_d^*(s) = \frac{|I_d^*|}{s} \quad I_q^*(s) = \frac{|I_q^*|}{s} \quad (232)$$

This last equation can be expressed in transfer function form as follows:

$$V_{conv\alpha}(s) = -\left(k_p + \frac{k_i s}{s^2 + \omega^2}\right) I_\alpha(s) + \left(\frac{k_p s^2}{s^2 + \omega^2} + \frac{k_i s^3}{(s^2 + \omega^2)^2}\right) I_d^*(s) - \left(\frac{k_p \omega s}{s^2 + \omega^2} + \frac{\omega k_i s^2}{(s^2 + \omega^2)^2}\right) I_q^*(s) + V_{g\alpha}(s) \quad (233)$$

Being this last expression only valid for step inputs. The β expression can be deduced in an equivalent manner.

Appendix B.

Sine and cosine inputs in control at stationary reference frame ($\alpha\beta$)

From the control equation:

$$v_{conv\alpha}(t) = \left(i_d^*(t) \cdot \cos(\omega t)\right) \otimes PIR(t) - \left(i_q^*(t) \cdot \sin(\omega t)\right) \otimes PIR(t) - i_\alpha(t) \otimes PIR(t) + v_{g\alpha}(t) \quad (234)$$

Taking for instance as inputs a **sine** and **cosine** at $I_d^*(s)$ and $I_q^*(s)$ respectively, at $t=0$:

$$i_d^*(t) = |I_d^*| \cdot \sin(\omega_1 t) \quad \text{and} \quad i_q^*(t) = |I_q^*| \cdot \cos(\omega_1 t) \quad (235)$$

Applying the Laplace transform to the first two elements of the right hand side of this equation:

$$\begin{aligned} \ell \left[\left(|I_d^*| \cdot \sin(\omega_1 t) \cdot \cos(\omega t) \right) \otimes (PIR(t)) \right] &= \ell \left[\left(\frac{|I_d^*|}{2} \cdot \sin((\omega_1 + \omega)t) + \frac{|I_d^*|}{2} \cdot \sin((\omega_1 - \omega)t) \right) \otimes (PIR(t)) \right] \\ &= \left(\frac{|I_d^*|}{2} \frac{(\omega_1 + \omega)}{s^2 + (\omega_1 + \omega)^2} + \frac{|I_d^*|}{2} \frac{(\omega_1 - \omega)}{s^2 + (\omega_1 - \omega)^2} \right) \left(k_p + k_i \frac{s}{s^2 + \omega^2} \right) \end{aligned} \quad (236)$$

$$\begin{aligned} \ell \left[- \left(|I_q^*| \cdot \cos(\omega_1 t) \cdot \sin(\omega t) \right) \otimes (PIR(t)) \right] &= \ell \left[- \left(\frac{|I_q^*|}{2} \cdot \sin((\omega_1 + \omega)t) - \frac{|I_q^*|}{2} \cdot \sin((\omega_1 - \omega)t) \right) \otimes (PIR(t)) \right] \\ &= - \left(\frac{|I_q^*|}{2} \frac{(\omega_1 + \omega)}{s^2 + (\omega_1 + \omega)^2} - \frac{|I_q^*|}{2} \frac{(\omega_1 - \omega)}{s^2 + (\omega_1 - \omega)^2} \right) \left(k_p + k_i \frac{s}{s^2 + \omega^2} \right) \end{aligned} \quad (237)$$

Thus, the complete 's' domain equation yields:

$$\begin{aligned}
 V_{conv\alpha}(s) = & -\left(k_p + \frac{k_i s}{s^2 + \omega^2}\right) I_\alpha(s) + \left(\frac{|I_d^*|}{2}\right) \left(\frac{\omega_1 + \omega}{s^2 + (\omega_1 + \omega)^2} + \frac{\omega_1 - \omega}{s^2 + (\omega_1 - \omega)^2}\right) \left(k_p + k_i \frac{s}{s^2 + \omega^2}\right) \\
 & - \left(\frac{|I_q^*|}{2}\right) \left(\frac{\omega_1 + \omega}{s^2 + (\omega_1 + \omega)^2} - \frac{\omega_1 - \omega}{s^2 + (\omega_1 - \omega)^2}\right) \left(k_p + k_i \frac{s}{s^2 + \omega^2}\right) + V_{g\alpha}(s)
 \end{aligned} \tag{238}$$

Knowing that the sine and cosine inputs in 's' domain are:

$$i_d^*(t) = |I_d^*| \cdot \sin(\omega_1 t) \quad \rightarrow \quad I_q^*(s) = \frac{\omega_1}{s^2 + \omega_1^2} |I_q^*| \tag{239}$$

$$i_q^*(t) = |I_q^*| \cdot \cos(\omega_1 t) \quad \rightarrow \quad I_q^*(s) = \frac{s}{s^2 + \omega_1^2} |I_q^*| \tag{240}$$

This last equation can be expressed in transfer function form as follows:

$$\begin{aligned}
 V_{conv\alpha}(s) = & \left(k_p + \frac{k_i s}{s^2 + \omega^2}\right) \left[-I_\alpha(s) + \left(\frac{1}{2}\right) \left(\frac{s^2 + \omega_1^2}{\omega_1}\right) \left(\frac{\omega_1 + \omega}{s^2 + (\omega_1 + \omega)^2} + \frac{\omega_1 - \omega}{s^2 + (\omega_1 - \omega)^2}\right) I_d^*(s)\right. \\
 & \left. - \left(\frac{1}{2}\right) \left(\frac{s^2 + \omega_1^2}{s}\right) \left(\frac{\omega_1 + \omega}{s^2 + (\omega_1 + \omega)^2} - \frac{\omega_1 - \omega}{s^2 + (\omega_1 - \omega)^2}\right) I_q^*(s)\right] + V_{g\alpha}(s)
 \end{aligned} \tag{241}$$

Being this last expression only valid for inputs sine and cosine at $I_d^*(s)$ and $I_q^*(s)$ respectively. The β expression can be deduced in an equivalent manner.

Appendix C.

Step inputs in control at synchronously rotating frame (dq) with cancellation of coupling terms

From the control equation:

$$\begin{aligned}
 v_{conv\alpha}(t) = & \left(\left[i_d^*(t) - (i_\alpha(t) \cdot \cos(\omega t) + i_\beta(t) \cdot \sin(\omega t)) \right] \otimes PI(t) \right) \cdot \cos(\omega t) \\
 & - \left(\left[i_q^*(t) - (-i_\alpha(t) \cdot \sin(\omega t) + i_\beta(t) \cdot \cos(\omega t)) \right] \otimes PI(t) \right) \cdot \sin(\omega t) \\
 & - \omega \cdot L \cdot i_q(t) \cdot \cos(\omega t) - \omega \cdot L \cdot i_d(t) \cdot \sin(\omega t) + v_{g\alpha}(t)
 \end{aligned} \tag{242}$$

It is equal to:

$$\begin{aligned}
 v_{conv\alpha}(t) = & (i_d^*(t) \otimes PI(t)) \cdot \cos(\omega t) \\
 & - ((i_\alpha(t) \cdot \cos(\omega t)) \otimes PI(t)) \cdot \cos(\omega t) \\
 & - ((i_\beta(t) \cdot \sin(\omega t)) \otimes PI(t)) \cdot \cos(\omega t) \\
 & - (i_q^*(t) \otimes PI(t)) \cdot \sin(\omega t) \\
 & - ((i_\alpha(t) \cdot \sin(\omega t)) \otimes PI(t)) \cdot \sin(\omega t) \\
 & + ((i_\beta(t) \cdot \cos(\omega t)) \otimes PI(t)) \cdot \sin(\omega t) \\
 & - \omega \cdot L \cdot i_q(t) \cdot \cos(\omega t) - \omega \cdot L \cdot i_d(t) \cdot \sin(\omega t) + v_{g\alpha}(t)
 \end{aligned} \tag{243}$$

Applying the Laplace transform to each part of this equation, and substituting a step in both inputs $i_d^*(t) = |I_d^*|$ and $i_q^*(t) = |I_q^*|$, at $t=0$, we have several terms that can be solved separately in several steps [13]. Starting from this one for instance:

$$-((i_\alpha(t) \cdot \cos(\omega t)) \otimes PI(t)) \cdot \cos(\omega t) \tag{244}$$

First, it is known that:

$$i_{\alpha}(t) \cdot \cos(\omega t) = \frac{1}{2} \cdot i_{\alpha}(t) \cdot e^{j\omega t} + \frac{1}{2} \cdot i_{\alpha}(t) \cdot e^{-j\omega t} \quad (245)$$

By using the Laplace transform property:

$$\ell[e^{-at} \cdot f(t)] = F(s+a) \quad (246)$$

The Laplace transform of expression (245) yields:

$$\ell\left[\frac{1}{2} \cdot i_{\alpha}(t) \cdot e^{j\omega t} + \frac{1}{2} \cdot i_{\alpha}(t) \cdot e^{-j\omega t}\right] = \frac{1}{2}(I_{\alpha}(s-j\omega) + I_{\alpha}(s+j\omega)) \quad (247)$$

Once we have this part solved, the following element is:

$$\ell\left[(i_{\alpha}(t) \cdot \cos(\omega t)) \otimes PI(t)\right] = \frac{1}{2}(I_{\alpha}(s-j\omega) + I_{\alpha}(s+j\omega)) \cdot \left(k_p + \frac{k_i}{s}\right) = F_1(s) \quad (248)$$

Finally, the total term is:

$$-\left((i_{\alpha}(t) \cdot \cos(\omega t)) \otimes PI(t)\right) \cdot \cos(\omega t) = -f_1(t) \cdot \cos(\omega t) = -\frac{1}{2} \cdot (f_1(t) \cdot e^{j\omega t} + f_1(t) \cdot e^{-j\omega t}) \quad (249)$$

So its Laplace transform is:

$$\ell\left[-\frac{1}{2} \cdot (f_1(t) \cdot e^{j\omega t} + f_1(t) \cdot e^{-j\omega t})\right] = -\frac{1}{2} \cdot (F_1(s-j\omega) + F_1(s+j\omega)) \quad (250)$$

And substituting in F_1 expression (248):

$$\begin{aligned} & \ell\left[-\left((i_{\alpha}(t) \cdot \cos(\omega t)) \otimes PI(t)\right) \cdot \cos(\omega t)\right] = \\ & = \ell\left[-\frac{1}{2} \cdot (f_1(t) \cdot e^{j\omega t} + f_1(t) \cdot e^{-j\omega t})\right] = -\frac{1}{2} \cdot (F_1(s-j\omega) + F_1(s+j\omega)) = \\ & = -\frac{1}{4} \cdot (I_{\alpha}(s-2j\omega) + I_{\alpha}(s)) \cdot \left(k_p + \frac{k_i}{s-j\omega}\right) - \frac{1}{4} \cdot (I_{\alpha}(s+2j\omega) + I_{\alpha}(s)) \cdot \left(k_p + \frac{k_i}{s+j\omega}\right) \end{aligned} \quad (251)$$

Then, taking the term that also depends on $i_{\alpha}(t)$ and on sinus terms:

$$-\left((i_\alpha(t) \cdot \sin(\omega t)) \otimes PI(t)\right) \cdot \sin(\omega t) \quad (252)$$

It is known that:

$$i_\alpha(t) \cdot \sin(\omega t) = \frac{1}{2j} \cdot i_\alpha(t) \cdot e^{j\omega t} - \frac{1}{2j} \cdot i_\alpha(t) \cdot e^{-j\omega t} \quad (253)$$

The Laplace transform of this term therefore yields:

$$\ell \left[i_\alpha(t) \cdot \sin(\omega t) = \frac{1}{2j} \cdot i_\alpha(t) \cdot e^{j\omega t} - \frac{1}{2j} \cdot i_\alpha(t) \cdot e^{-j\omega t} \right] = \frac{1}{2j} (I_\alpha(s - j\omega) - I_\alpha(s + j\omega)) \quad (254)$$

Once we have this part solved, the following element is:

$$\ell \left[(i_\alpha(t) \cdot \sin(\omega t)) \otimes PI(t) \right] = \frac{1}{2j} (I_\alpha(s - j\omega) - I_\alpha(s + j\omega)) \cdot \left(k_p + \frac{k_i}{s} \right) = F_2(s) \quad (255)$$

Finally, the total term is:

$$-\left((i_\alpha(t) \cdot \sin(\omega t)) \otimes PI(t)\right) \cdot \sin(\omega t) = -f_2(t) \cdot \sin(\omega t) = -\frac{1}{2j} \cdot (f_2(t) \cdot e^{j\omega t} - f_2(t) \cdot e^{-j\omega t}) \quad (256)$$

So its Laplace transform is:

$$\ell \left[-\frac{1}{2j} \cdot (f_2(t) \cdot e^{j\omega t} - f_2(t) \cdot e^{-j\omega t}) \right] = -\frac{1}{2j} \cdot (F_2(s - j\omega) - F_2(s + j\omega)) \quad (257)$$

And substituting F_2 from expression (255):

$$\begin{aligned} & \ell \left[-\left((i_\alpha(t) \cdot \sin(\omega t)) \otimes PI(t)\right) \cdot \sin(\omega t) \right] = \\ & = \ell \left[-\frac{1}{2j} \cdot (f_2(t) \cdot e^{j\omega t} - f_2(t) \cdot e^{-j\omega t}) \right] = -\frac{1}{2j} \cdot (F_2(s - j\omega) - F_2(s + j\omega)) = \\ & = \frac{1}{4} \cdot (I_\alpha(s - 2j\omega) - I_\alpha(s)) \cdot \left(k_p + \frac{k_i}{s - j\omega} \right) - \frac{1}{4} \cdot (-I_\alpha(s + 2j\omega) + I_\alpha(s)) \cdot \left(k_p + \frac{k_i}{s + j\omega} \right) \end{aligned} \quad (258)$$

Consequently, adding terms (251) and (258):

$$\begin{aligned}
 & \ell \left[- \left((i_\alpha(t) \cdot \cos(\omega t)) \otimes PI(t) \right) \cdot \cos(\omega t) - \left((i_\alpha(t) \cdot \sin(\omega t)) \otimes PI(t) \right) \cdot \sin(\omega t) \right] = \\
 & = -\frac{1}{4} \cdot (I_\alpha(s+2j\omega) + I_\alpha(s)) \cdot \left(k_p + \frac{k_i}{s+j\omega} \right) - \frac{1}{4} \cdot (I_\alpha(s-2j\omega) + I_\alpha(s)) \cdot \left(k_p + \frac{k_i}{s-j\omega} \right) + \\
 & + \frac{1}{4} \cdot (I_\alpha(s-2j\omega) - I_\alpha(s)) \cdot \left(k_p + \frac{k_i}{s-j\omega} \right) - \frac{1}{4} \cdot (-I_\alpha(s+2j\omega) + I_\alpha(s)) \cdot \left(k_p + \frac{k_i}{s+j\omega} \right) = \\
 & = -\frac{1}{2} \cdot \left(k_p + \frac{k_i}{s+j\omega} + k_p + \frac{k_i}{s-j\omega} \right) \cdot I_\alpha(s) = \\
 & = - \left(k_p + \frac{k_i s}{s^2 + \omega^2} \right) \cdot I_\alpha(s)
 \end{aligned} \tag{259}$$

Following the same procedure with terms with sine and cosine:

$$- \left((i_\beta(t) \cdot \sin(\omega t)) \otimes PI(t) \right) \cdot \cos(\omega t) \tag{260}$$

Its Laplace transform is equal to:

$$\begin{aligned}
 & \ell \left[- \left((i_\beta(t) \cdot \sin(\omega t)) \otimes PI(t) \right) \cdot \cos(\omega t) \right] = \\
 & = -\frac{1}{4j} \cdot (-I_\beta(s+2j\omega) + I_\beta(s)) \cdot \left(k_p + \frac{k_i}{s+j\omega} \right) - \frac{1}{4j} \cdot (I_\beta(s-2j\omega) - I_\beta(s)) \cdot \left(k_p + \frac{k_i}{s-j\omega} \right)
 \end{aligned} \tag{261}$$

While the other term with sine and cosine:

$$\left((i_\beta(t) \cdot \cos(\omega t)) \otimes PI(t) \right) \cdot \sin(\omega t) \tag{262}$$

Its Laplace transform is equal to:

$$\begin{aligned}
 & \ell \left[\left((i_\beta(t) \cdot \cos(\omega t)) \otimes PI(t) \right) \cdot \sin(\omega t) \right] = \\
 & = -\frac{1}{4j} \cdot (I_\beta(s+2j\omega) + I_\beta(s)) \cdot \left(k_p + \frac{k_i}{s+j\omega} \right) + \frac{1}{4j} \cdot (I_\beta(s-2j\omega) + I_\beta(s)) \cdot \left(k_p + \frac{k_i}{s-j\omega} \right)
 \end{aligned} \tag{263}$$

Consequently, adding term (261) and (263):

$$\begin{aligned}
 & \ell \left[-\left((i_\beta(t) \cdot \sin(\omega t)) \otimes PI(t) \right) \cdot \cos(\omega t) + \left((i_\beta(t) \cdot \cos(\omega t)) \otimes PI(t) \right) \cdot \sin(\omega t) \right] = \\
 & = -\frac{1}{4j} \cdot (-I_\beta(s+2j\omega) + I_\beta(s)) \cdot \left(k_p + \frac{k_i}{s+j\omega} \right) - \frac{1}{4j} \cdot (I_\beta(s-2j\omega) - I_\beta(s)) \cdot \left(k_p + \frac{k_i}{s-j\omega} \right) \\
 & - \frac{1}{4j} \cdot (I_\beta(s+2j\omega) + I_\beta(s)) \cdot \left(k_p + \frac{k_i}{s+j\omega} \right) + \frac{1}{4j} \cdot (I_\beta(s-2j\omega) + I_\beta(s)) \cdot \left(k_p + \frac{k_i}{s-j\omega} \right) \\
 & = \frac{1}{2j} \cdot \left(-k_p - \frac{k_i}{s+j\omega} + k_p + \frac{k_i}{s-j\omega} \right) \cdot I_\beta(s) = \\
 & = \left(\frac{k_i \omega}{s^2 + \omega^2} \right) \cdot I_\beta(s)
 \end{aligned} \tag{264}$$

Then, there are two terms that depend on the reference inputs that are solved as follows:

$$\begin{aligned}
 & \ell \left[(i_d^*(t) \otimes PI(t)) \cdot \cos(\omega t) \right] = \\
 & = \frac{1}{2} \cdot I_d^*(s-j\omega) \cdot \left(k_p + \frac{k_i}{s-j\omega} \right) + \frac{1}{2} \cdot I_d^*(s+j\omega) \cdot \left(k_p + \frac{k_i}{s+j\omega} \right)
 \end{aligned} \tag{265}$$

Considering a step input at both $I_d^*(s)$ and $I_q^*(s)$:

$$I_d^*(s) = \frac{|I_d^*|}{s} \qquad I_q^*(s) = \frac{|I_q^*|}{s} \tag{266}$$

The previous expression yields after substituting the step input:

$$\begin{aligned}
 & \ell \left[(i_d^*(t) \otimes PI(t)) \cdot \cos(\omega t) \right] = \\
 & = \frac{1}{2} \cdot \frac{|I_d^*|}{s-j\omega} \cdot \left(k_p + \frac{k_i}{s-j\omega} \right) + \frac{1}{2} \cdot \frac{|I_d^*|}{s+j\omega} \cdot \left(k_p + \frac{k_i}{s+j\omega} \right)
 \end{aligned} \tag{267}$$

And after several developments seeking to eliminate the imaginary operator 'j':

$$\begin{aligned}
 & \ell \left[(i_d^*(t) \otimes PI(t)) \cdot \cos(\omega t) \right] = \\
 & = \left(\frac{k_p s}{s^2 + \omega^2} + \frac{k_i (s^2 - \omega^2)}{(s^2 + \omega^2)^2} \right) \cdot |I_d^*|
 \end{aligned} \tag{268}$$

Doing the same with the following term:

$$\begin{aligned} & \ell \left[-\left(i_q^*(t) \otimes PI(t) \right) \cdot \sin(\omega t) \right] = \\ & = -\frac{1}{2j} \cdot I_q^*(s-j\omega) \cdot \left(k_p + \frac{k_i}{s-j\omega} \right) + \frac{1}{2j} \cdot I_q^*(s+j\omega) \cdot \left(k_p + \frac{k_i}{s+j\omega} \right) \end{aligned} \quad (269)$$

Substituting the step input:

$$\begin{aligned} & \ell \left[-\left(i_q^*(t) \otimes PI(t) \right) \cdot \sin(\omega t) \right] = \\ & = -\frac{1}{2j} \cdot \frac{|I_q^*|}{s-j\omega} \cdot \left(k_p + \frac{k_i}{s-j\omega} \right) + \frac{1}{2j} \cdot \frac{|I_q^*|}{s+j\omega} \cdot \left(k_p + \frac{k_i}{s+j\omega} \right) \end{aligned} \quad (270)$$

And after several developments:

$$\begin{aligned} & \ell \left[-\left(i_q^*(t) \otimes PI(t) \right) \cdot \sin(\omega t) \right] = \\ & = -\left(\frac{k_p \omega}{s^2 + \omega^2} - \frac{2\omega k_i s}{(s^2 + \omega^2)^2} \right) \cdot |I_q^*| \end{aligned} \quad (271)$$

Finally, the remaining terms are:

$$-\omega \cdot L \cdot i_q(t) \cdot \cos(\omega t) - \omega \cdot L \cdot i_d(t) \cdot \sin(\omega t) + v_{g\alpha}(t) \quad (272)$$

Substituting their equivalent currents in $\alpha\beta$ representation:

$$-\omega \cdot L \cdot \left(-i_\alpha(t) \cdot \sin(\omega t) + i_\beta(t) \cdot \cos(\omega t) \right) \cdot \cos(\omega t) - \omega \cdot L \cdot \left(i_\alpha(t) \cdot \cos(\omega t) + i_\beta(t) \cdot \sin(\omega t) \right) \cdot \sin(\omega t) + v_{g\alpha}(t) \quad (273)$$

Rearranging terms and applying trigonometric equalities, it is obtained:

$$-\omega \cdot L \cdot i_\beta(t) + v_{g\alpha}(t) \quad (274)$$

So its Laplace transform:

$$\ell \left[-\omega \cdot L \cdot i_\beta(t) + v_{g\alpha}(t) \right] = -\omega \cdot L \cdot I_\beta(s) + V_{g\alpha}(s) \quad (275)$$

Hence, adding all the resulting terms, the Laplace transform of the complete expression (242) is:

$$\begin{aligned} V_{conv\alpha}(s) = & -\left(k_p + \frac{k_i s}{s^2 + \omega^2}\right) I_\alpha(s) + \left(\frac{(-\omega L)s^2 + (k_i \omega - \omega^3 L)}{s^2 + \omega^2}\right) I_\beta(s) \\ & + \left(\frac{k_p s}{s^2 + \omega^2} + \frac{k_i (s^2 - \omega^2)}{(s^2 + \omega^2)^2}\right) \cdot |I_d^*| - \left(\frac{k_p \omega}{s^2 + \omega^2} - \frac{2\omega k_i s}{(s^2 + \omega^2)^2}\right) \cdot |I_q^*| \end{aligned} \quad (276)$$

Knowing that these expressions are only valid for a step input at both $I_d^*(s)$ and $I_q^*(s)$, we can represent them in transfer function form:

$$\begin{aligned} V_{conv\alpha}(s) = & -\left(k_p + \frac{k_i s}{s^2 + \omega^2}\right) I_\alpha(s) + \left(\frac{(-\omega L)s^2 + (k_i \omega - \omega^3 L)}{s^2 + \omega^2}\right) I_\beta(s) \\ & + \left(\frac{k_p s^2}{s^2 + \omega^2} + \frac{k_i s(s^2 - \omega^2)}{(s^2 + \omega^2)^2}\right) I_d^*(s) - \left(\frac{k_p \omega s}{s^2 + \omega^2} - \frac{2\omega k_i s^2}{(s^2 + \omega^2)^2}\right) I_q^*(s) \end{aligned} \quad (277)$$

Appendix D.

Sine and cosine inputs in control at synchronously rotating frame (dq) with cancellation of coupling terms

From the control equation that has been solved in previous chapter:

$$\begin{aligned}
 v_{conv\alpha}(t) = & \left(i_d^*(t) \otimes PI(t) \right) \cdot \cos(\omega t) \\
 & - \left(\left(i_\alpha(t) \cdot \cos(\omega t) \right) \otimes PI(t) \right) \cdot \cos(\omega t) \\
 & - \left(\left(i_\beta(t) \cdot \sin(\omega t) \right) \otimes PI(t) \right) \cdot \cos(\omega t) \\
 & - \left(i_q^*(t) \otimes PI(t) \right) \cdot \sin(\omega t) \\
 & - \left(\left(i_\alpha(t) \cdot \sin(\omega t) \right) \otimes PI(t) \right) \cdot \sin(\omega t) \\
 & + \left(\left(i_\beta(t) \cdot \cos(\omega t) \right) \otimes PI(t) \right) \cdot \sin(\omega t) \\
 & - \omega \cdot L \cdot i_q(t) \cdot \cos(\omega t) - \omega \cdot L \cdot i_d(t) \cdot \sin(\omega t) + v_{g\alpha}(t)
 \end{aligned} \tag{278}$$

Only two terms that depend on new inputs must be recalculated. Assuming as inputs a **sine** and **cosine** at $I_d^*(s)$ and $I_q^*(s)$ respectively, at $t=0$:

$$i_d^*(t) = |I_d^*| \cdot \sin(\omega t) \quad \text{and} \quad i_q^*(t) = |I_q^*| \cdot \cos(\omega t) \tag{279}$$

These terms are:

$$\left(i_d^*(t) \otimes PI(t) \right) \cdot \cos(\omega t) \quad \text{and} \quad - \left(i_q^*(t) \otimes PI(t) \right) \cdot \sin(\omega t) \tag{280}$$

In this case, we will solve the problem by following an alternative method. First of all taking the Laplace transform of the input reference and the $PI(t)$:

$$\ell[i_d^*(t) \otimes PI(t)] = \left(|I_d^*| \frac{\omega_1}{s^2 + \omega_1^2} \right) \left(k_p + \frac{k_i}{s} \right) = |I_d^*| \left(\frac{k_p \cdot \omega_1}{s^2 + \omega_1^2} + \frac{k_i \cdot \omega_1}{s(s^2 + \omega_1^2)} \right) \quad (281)$$

Now taking the inverse Laplace transform:

$$i_d^*(t) \otimes PI(t) = \ell^{-1} \left[|I_d^*| \left(\frac{k_p \cdot \omega_1}{s^2 + \omega_1^2} + \frac{k_i \cdot \omega_1}{s(s^2 + \omega_1^2)} \right) \right] = |I_d^*| \left(k_p \sin(\omega_1 t) + \frac{k_i}{\omega_1} (1 - \cos(\omega_1 t)) \right) \quad (282)$$

Multiplying this last expression by $\cos(\omega t)$:

$$\begin{aligned} (i_d^*(t) \otimes PI(t)) \cdot \cos(\omega t) &= |I_d^*| \left(k_p \sin(\omega_1 t) \cos(\omega t) + \frac{k_i}{\omega_1} (\cos(\omega t) - \cos(\omega_1 t) \cos(\omega t)) \right) \\ &= |I_d^*| \left(\frac{k_i}{\omega_1} \cos(\omega t) + \frac{k_p}{2} (\sin((\omega_1 + \omega)t) + \sin((\omega_1 - \omega)t)) - \frac{k_i}{2\omega_1} (\cos((\omega_1 + \omega)t) + \cos((\omega_1 - \omega)t)) \right) \end{aligned} \quad (283)$$

And its Laplace transform is calculated directly:

$$\begin{aligned} \ell[(i_d^*(t) \otimes PI(t)) \cdot \cos(\omega t)] &= \\ &= |I_d^*| \left(\frac{k_i}{\omega_1} \left(\frac{s}{s^2 + \omega_1^2} \right) + \frac{k_p}{2} \left(\frac{\omega_1 + \omega}{s^2 + (\omega_1 + \omega)^2} + \frac{\omega_1 - \omega}{s^2 + (\omega_1 - \omega)^2} \right) - \frac{k_i}{2\omega_1} \left(\frac{s}{s^2 + (\omega_1 + \omega)^2} + \frac{s}{s^2 + (\omega_1 - \omega)^2} \right) \right) \end{aligned} \quad (284)$$

Being this expression only valid for a sine input at d component current:

Following the same procedure the remaining term and considering a cosine input at q component of current reference:

$$\ell[i_q^*(t) \otimes PI(t)] = \left(|I_q^*| \frac{s}{s^2 + \omega_1^2} \right) \left(k_p + \frac{k_i}{s} \right) = |I_q^*| \left(\frac{k_p s}{s^2 + \omega_1^2} + \frac{k_i}{s^2 + \omega_1^2} \right) \quad (285)$$

Now taking the inverse Laplace transform:

$$i_q^*(t) \otimes PI(t) = \ell^{-1} \left[|I_q^*| \left(\frac{k_p \cdot s}{s^2 + \omega_1^2} + \frac{k_i}{s^2 + \omega_1^2} \right) \right] = |I_q^*| \left(k_p \cos(\omega_1 t) + \frac{k_i}{\omega_1} \sin(\omega_1 t) \right) \quad (286)$$

Multiplying this last expression by $\sin(\omega t)$:

$$\begin{aligned} -(i_q^*(t) \otimes PI(t)) \cdot \sin(\omega t) &= -|I_q^*| \left(k_p \cos(\omega_1 t) \sin(\omega t) + \frac{k_i}{\omega_1} \sin(\omega_1 t) \sin(\omega t) \right) = \\ &= -|I_q^*| \left(\frac{k_p}{2} (\sin((\omega_1 + \omega)t) - \sin((\omega_1 - \omega)t)) + \frac{k_i}{2\omega_1} (-\cos((\omega_1 + \omega)t) + \cos((\omega_1 - \omega)t)) \right) \end{aligned} \quad (287)$$

And its Laplace transform is calculated directly:

$$\begin{aligned} \ell[-(i_q^*(t) \otimes PI(t)) \cdot \sin(\omega t)] &= \\ &= -|I_q^*| \left(\frac{k_p}{2} \left(\frac{\omega_1 + \omega}{s^2 + (\omega_1 + \omega)^2} - \frac{\omega_1 - \omega}{s^2 + (\omega_1 - \omega)^2} \right) + \frac{k_i}{2\omega_1} \left(-\frac{s}{s^2 + (\omega_1 + \omega)^2} + \frac{s}{s^2 + (\omega_1 - \omega)^2} \right) \right) \end{aligned} \quad (288)$$

Hence, adding all the resulting terms, the Laplace transform of the complete expression (278) is:

$$\begin{aligned} V_{convz}(s) &= - \left(k_p + \frac{k_i s}{s^2 + \omega^2} \right) I_\alpha(s) + \left(\frac{(-\omega L)s^2 + (k_i \omega - \omega^3 L)}{s^2 + \omega^2} \right) I_\beta(s) \\ &+ \left(\frac{k_p}{2} \right) \left(\frac{\omega_1 + \omega}{s^2 + (\omega_1 + \omega)^2} + \frac{\omega_1 - \omega}{s^2 + (\omega_1 - \omega)^2} \right) |I_d^*| \\ &- \left(\frac{k_i}{2} \right) \left(\frac{s}{s^2 + (\omega_1 + \omega)^2} + \frac{s}{s^2 + (\omega_1 - \omega)^2} + \frac{2s}{s^2 + \omega^2} \right) |I_d^*| \\ &- \left(\frac{k_p}{2} \right) \left(\frac{\omega_1 + \omega}{s^2 + (\omega_1 + \omega)^2} - \frac{\omega_1 - \omega}{s^2 + (\omega_1 - \omega)^2} \right) |I_q^*| \\ &- \left(\frac{k_i}{2\omega_1} \right) \left(\frac{s}{s^2 + (\omega_1 + \omega)^2} - \frac{s}{s^2 + (\omega_1 - \omega)^2} \right) |I_q^*| + V_{ga}(s) \end{aligned} \quad (289)$$

Knowing that these expressions are only valid for a sine and cosine input at both $I_d^*(s)$ and $I_q^*(s)$ respectively, we can represent them in transfer function form:

$$\begin{aligned}
V_{conv\alpha}(s) = & -\left(k_p + \frac{k_i s}{s^2 + \omega^2}\right) I_\alpha(s) + \left(\frac{(-\omega L)s^2 + (k_i \omega - \omega^3 L)}{s^2 + \omega^2}\right) I_\beta(s) \\
& + \left(\frac{k_p}{2}\right) \left(\frac{s^2 + \omega_1^2}{\omega_1}\right) \left(\frac{\omega_1 + \omega}{s^2 + (\omega_1 + \omega)^2} + \frac{\omega_1 - \omega}{s^2 + (\omega_1 - \omega)^2}\right) I_d^*(s) \\
& - \left(\frac{k_i}{2}\right) \left(\frac{s^2 + \omega_1^2}{\omega_1^2}\right) \left(\frac{s}{s^2 + (\omega_1 + \omega)^2} + \frac{s}{s^2 + (\omega_1 - \omega)^2} + \frac{2s}{s^2 + \omega^2}\right) I_d^*(s) \\
& - \left(\frac{k_p}{2}\right) \left(\frac{s^2 + \omega_1^2}{s}\right) \left(\frac{\omega_1 + \omega}{s^2 + (\omega_1 + \omega)^2} - \frac{\omega_1 - \omega}{s^2 + (\omega_1 - \omega)^2}\right) I_q^*(s) \\
& - \left(\frac{k_i}{2\omega_1}\right) \left(\frac{s^2 + \omega_1^2}{s}\right) \left(\frac{s}{s^2 + (\omega_1 + \omega)^2} - \frac{s}{s^2 + (\omega_1 - \omega)^2}\right) I_q^*(s) \\
& + V_{g\alpha}(s)
\end{aligned} \tag{290}$$

Appendix E.

Numerical conditions for simulations

AC grid:

$$L_g = 0\text{mH},$$

$$\omega = 2 \cdot \pi \cdot 50 \text{ rad/s}$$

$$|V_g| = 1\text{V}$$

Filter:

$$R = 10\text{m}\Omega$$

$$L = 1\text{mH}$$

Control:

$$\omega_1 = 11 \cdot \omega \text{ rad/s}$$

$$\omega_n = (R/L) \cdot 25 \text{ rad/s}$$

$$\xi = 1.01$$

$$k_p = s_i \cdot L \cdot 2 \cdot \omega_n - R = 0.495$$

$$k_i = L \cdot \omega_n^2 = 62.5$$

Appendix F.

Experimental platform

AC grid:

$$L_g = 0\text{mH},$$

$$\omega = 2 \cdot \pi \cdot 50 \text{ rad/s}$$

$$|V_g| = 25\text{V}$$

Filter:

$$R = 32\text{m}\Omega$$

$$L = 4\text{mH}$$

Converter:

2L - VSC – with IGBTs, commutating at $f_{sw} = 8\text{kHz}$.

Appendix G.

Space Vectors

Next figure graphically shows the two reference frames in which the space vectors can be represented:

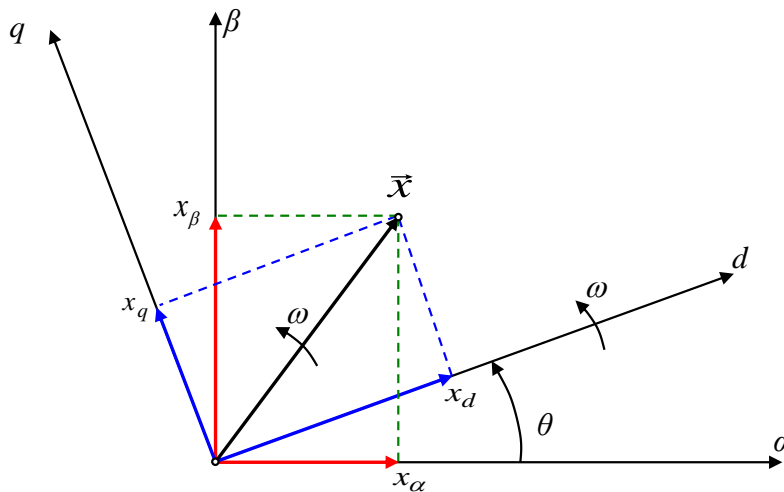


Figure 60. Transformation between stationary and synchronous reference frames.

Transformations between reference frames are made according to the following matrix equations:

$$\begin{bmatrix} v_d \\ v_q \end{bmatrix} = \begin{bmatrix} \cos \theta & \sin \theta \\ -\sin \theta & \cos \theta \end{bmatrix} \begin{bmatrix} v_\alpha \\ v_\beta \end{bmatrix} \quad (291)$$

$$\begin{bmatrix} v_\alpha \\ v_\beta \end{bmatrix} = \begin{bmatrix} \cos \theta & -\sin \theta \\ \sin \theta & \cos \theta \end{bmatrix} \begin{bmatrix} v_d \\ v_q \end{bmatrix} \quad (292)$$

Finally, to transform into a three phase system:

$$\begin{bmatrix} x_a \\ x_b \\ x_c \end{bmatrix} = \begin{bmatrix} 1 & 0 \\ -\frac{1}{2} & \frac{\sqrt{3}}{2} \\ -\frac{1}{2} & -\frac{\sqrt{3}}{2} \end{bmatrix} \cdot \begin{bmatrix} x_\alpha \\ x_\beta \end{bmatrix} \quad (293)$$

$$\begin{bmatrix} x_\alpha \\ x_\beta \end{bmatrix} = \frac{2}{3} \begin{bmatrix} 1 & -\frac{1}{2} & -\frac{1}{2} \\ 0 & \frac{\sqrt{3}}{2} & -\frac{\sqrt{3}}{2} \end{bmatrix} \cdot \begin{bmatrix} x_a \\ x_b \\ x_c \end{bmatrix} \quad (294)$$

References

1. G. Abad, A. Milikua, I. Baraia, Electric Technology in Wind Turbines from a Dialectic Perspective, in *Techné: Research in Philosophy and Technology*. **2019**. 174-203. 23:2.
2. B. K. Bose, *Power Electronics and Motor Drives. Advances and Trends*; Elsevier: Burlington, USA, **2006**.
3. M. P. Kazmierkowski, F. Blaabjerg, R. Krishnan, *Control in Power Electronics. Selected Problems*. Academic Press: San Diego, California, USA, **2002**.
4. Mattavelli, P.; Buso, S. *Digital Control in Power Electronics*; Morgan & Claypool: San Rafael, CA, USA, **2006**.
5. Sul, K., *Control of electric machine drive systems*; John Wiley & Sons. Inc., **2011**.
6. Teodorescu, R.; Liserre, M.; Rodriguez, P. *Grid Converters for Photovoltaic and Wind Power Systems*; John Wiley and Sons: Hoboken, NJ, USA, **2011**.
7. Abad, G. *Power electronics and electric drives for traction applications*; John Wiley and Sons: Chichester, UK, **2016**.
8. Ruan, X.; Wnag, X.; Pan, D.; Yang, D.; Li, W.; Bao, C. *Control techniques for LCL grid connected inverters*; Springer: Singapore, Singapore, **2018**.
9. Miller, T. J. E. *Reactive power control in electric systems*; John Wiley and Sons: New York, USA, **1982**.
10. Hingorani, N. G.; Gyugyi, L. *Understanding FACTS: Concepts and Technology of Flexible AC Transmission Systems*; John Wiley and Sons: Hoboken, NJ, USA, **2000**.
11. Schauder, C. D. and Mehta, H. Vector Analysis and Control of Advanced Static Var Compensators. In *IEE 5th International Conference on AC and DC Transmission*. **1991**. 266-272.
12. Sato Y.; Ishizuka, T. Nezu, K., Kataota, T. A New Control Strategy for Voltage-Type PWM Rectifiers to Realize Zero Steady-State Control Error in Input Current. In *IEEE Transaction on Industry Applications*. **1998**. Vol 34. 3. 480-486.
13. Zmood, D. N., and Holmes, D. G. Stationary Frame Current Regulation of PWM Inverters with Zero Steady State Error. In *Conference Proceedings PESC'99*. **1999**.
14. Abad, G.; Laka, A.; Saavedra, G.; J.A. Barrena. Analytical Modeling Approach to Study Harmonic Mitigation in AC Grids with Active Impedance at Selective Frequencies. *Energies* **2018**, 11, 1337-1368.
15. Etxeberria-Otadui, I.; Viscarret, U.; Caballero, M.; Rufer, A.; Bacha, S. New Optimized control structures and strategies under unbalanced voltage transients. In *IEEE Transactions on Industrial Electronics*; **2007**, 2902-2914, 54 (5).
16. Ogata, K. *Modern Control Engineering*; Prentice Hall. **1970**.
Abad, G.; López, J., Rodríguez, M. A. , Marroyo, L., Iwanski, G. "Doubly Fed Induction Machine: Modeling and Control for Wind Energy Generation"; John Wiley and Sons: Hoboken, NJ, **2011**.

Gonzalo Abad received his degree in Electrical Engineering from Mondragon University in 2000, his M.Sc. degree in Advanced Control from the University of Manchester (UK) in 2001 and his Ph.D. degree in Electrical Engineering from the Mondragon University in 2008. He joined the Electronics and Computing Department of Mondragon University in 2001. His main research interests include renewable energies, power conversion and motor drives. He has co-authored several papers, patents and books in the areas of wind power generation, multilevel power converters and control of electric drives.

Ander de Marcos received his degree in Industrial Electronics and Automation Engineering, from the University of the Basque Country, Spain, in 2015. Currently, he is pursuing his final year project in the master of Energy and Power Electronics at Mondragon University. He is mostly interested in power electronics and electromagnetic compatibility.